3 8006 10137 7540

CRANFIELD INSTITUTE OF TECHNOLOGY

DEPARTMENT OF AIRCRAFT DESIGN

M.Sc THESIS

Academic Year 1974-1975

E. J. BUCHANAN

Design Study of a Tailless Glider.

Supervisor: R.E. WARD

September, 1975

SUMMARY

The important theoretical parameters in the design of a high performance tailless sailplane have been determined. Inter-relationships between these parameters have been discovered and are shown on a work study flow chart.

The design specification demanded,

a. equal, or better, achieved cross-country performance, than a conventional sailplane of equal span, and,

b. satisfactory stability and control.

The 15 metre, standard class, Standard Cirrus sailplane, was used as a basis for comparison of performance, stability and control. The design study revealed a tailless sailplane with a calculated 10% performance gain. The rigid aircraft, longitudinal stability and control analysis showed the aircraft to be more dependent on centre of gravity location but capable of simulating the Standard Cirrus. Yaw control posed a problem, but the severest encounter involved the longitudinal dynamics of the flexible wing. Wing structural layout will hopefully eliminate this problem.

During the course of the study the 15 metre class was widened to allow the use of flaps. This became a necessary feature of the tailless design and the performance increment is likely to be similar.

ACKNOWLEDGEMENTS

It would be selfish not to record the heartfelt thanks I give to Pam. As a wife, mother and cook she cared for Brett, Kyla and me during two years of study at Cranfield. She not only enabled me to further satisfy my deep compassion for gliding by encouraging my study of the subject during this thesis, the second in twelve months, but also gave invaluable assistance with the numerous graphs, compilation and proof reading of the final product.

My appreciation is also expressed to the staff members of the Cranfield Institute of Technology, Aircraft Design Department, for their help and guidance in preparing this work. Particular credit is due to my supervisor, Mr. Bob Ward, for preserving a realistic outlook and providing the best of advice.

Thanks are also extended to Mrs. K. Hayward for so ably typing this project.

CONTENTS

		Page No.
NOTATION		
1.	INTRODUCTION	1
2.	SCOPE	4
3.	DESIGN PERSPECTIVE	6
4.	REDUCING THE DESIGN VARIABLES	7
	4.1 Stick Fixed Static Longitudinal Stability	
	4.2 The Layout of Stable Wings	
	4.3 Aerofoil Requirements	
	4.4 Control Effectiveness	
	4.5 Centre of Gravity Range	
	4.6 Selection of Wing Sweep	
5.	SAILPLANE PERFORMANCE	18
	5.1 The Computerized Optimization of a 15 m Tailless Sailplane	
	5.2 Conventional and Tailless Performance Comparison	
6.	SHAPING THE WING	26
	6.1 Selection Proceedure for the Unflapped Planform	
	6.2 Analysis of Flap Effects	
7.	LONGITUDINAL DYNAMIC STABILITY AND CONTROL	43
	7.1 Modifications to the Program	
	7.2 Short Period Oscillation	
	7.3 Phugoid Motion	
	7.4 Response to Instantaneous Application of Pitch Control	
	7.5 Response to Exponential Application of Pitch Control	
8.	LATERAL DYNAMIC STABILITY AND CONTROL	54
	8.1 Modifications to the Program	
	8.2 The Lateral Oscillation	
	8.3 Spiral Stability	
	8.4 Lateral Control	
9.	SUMMARY ANALYSIS OF THE RICOCHET SAILPLANE	68
	9.1 Ricochet Particulars	
	9.2 Gliding and Turning Performance	
	9.3 Aerodynamic Stability and Control Derivatives	

Page No.

10. THE NON RIGID STRUCTURE 74

10.1 Variation of Wing Twist with Speed
10.2 Symmetric Gust and Manoeuvre Stability
10.3 Coupling of Longitudinal Dynamic Oscillations and Wing Distortions
10.4 Flutter, Divergence and Elevon Reversal

11. CONCLUSIONS. 88

REFERENCES.

CONTENTS

LIST OF FIGURES

1. Preliminary Layout.

2. The Layout of Stable Wings.

3. Elevon Angles to Trim.

4. Aerofoil Section Data.

5. Effect of Sweep, Aspect Ratio and Taper on Control Effectiveness Parameter ($h_c - h_o$)

6. Centre of Gravity Shift due to Change in Inclination of the Pilot's Back.

7. Typical Flight Cross Section.

8. Straight Flight Polar of a Given Sailplane.

9. Glide Comparison of Standard Cirrus and Unflapped Ricochet at Wing Loadings for equal, Unflapped Stalling Speeds.

10. A Comparison of the M^{ac}Ready Cross-Country Performance.

11. Example of Planform Induced Drag Efficiency.

12. Example of Planform Induced Drag Efficiency.

13. Example of Spanwise Lift Distributions.

14. Spanwise Aerodynamic Wing Twist Distribution.

15. Elevon Trim Curves for Unflapped Ricochet.

16. Spanwise Distribution of Lift Coefficient with Control Deflections.

17. Comparison of Ricochet and Standard Cirrus Induced Drag Efficiencies.

18. Spanwise Distribution of Lift Coefficient for Unflapped Wing and Representative Control Deflections.

19. Example Layout of a Flapped Tailless Sailplane.

20. Two dimensional Pitching Moment Coefficient per Degree Control Deflection.

21. Nett Pitching Moment Coefficients Due to Flap Deflections.

22. Spanwise Lift Coefficient Distributions for Flapped Planform.

LIST OF FIGURES (contd.)

23. Pitching Moment Derivative due to Pitch, for Wing Alone.

24. Short Period Oscillation Parametric Study.

25. Comparison of Short Period Oscillation Characteristics of Standard Cirrus and Ricochet Sailplanes, Without Water Ballast.

26. Phugoid Characteristics.

27. Comparison of Response to Instantaneous Application of Pitch Control (No Ballast).

28. Comparison of Response to Instantaneous Application of Pitch Control (No Ballast).

29. Comparison of Response to Exponential Application of Pitch Control.

30. Comparison of Response to Exponential Application of Pitch Control.

31. Comparison of Ricochet and Standard Cirrus Dutch Roll Pilot Opinion Ratings.

32. Response Due to Instantaneous Application of Full Spoiler at Sea Level, Without Ballast.

33. Response Due to Instantaneous Application of Full Aileron at Sea Level, Without Ballast.

34. Response Due to Instantaneous Application of Full Spoiler and Part Deflection of Opposite Aileron, No Water Ballast.

35. Response due to Instantaneous Application of Full Spoiler and Full Aileron at Sea Level, No Water Ballast.

36. Ricochet Response due to Application of Full Spoiler at two Speeds, 4.57 Km altitude and Full Water Ballast.

37. Ricochet Glide Performance.

38. Ricochet Turn Performance.

39. Aerodynamic Wing Twist at C_L = 1.0 and 0.2.

40. Change in Aerodynamic Twist per Unit Change in Load Factor.

CONTENTS

LIST OF TABLES

1. Spanwise Distributions of Flap Deflections.

2. A Comparison of the Standard Cirrus and Ricochet Cycles to Halve Amplitude for the Lateral Oscillation Mode.

3. A Comparison of the Standard Cirrus and Ricochet Times to Double or Halve Amplitude for the Spiral Stability Mode.

4. Aerodynamic Twist due to Torque at $C_L = 1.0$, $n = 1$, $W = 277.3$ Kg.

5. Aerodynamic Twist due to Torque at $C_L = 0.2$, $n = 1$, $W = 277.3$ Kg.

6. Aerodynamic Twist due to Bending at $C_L = 1.0$, and $C_L = 0.2$, $n = 1$, $W = 277.3$ Kg.

7. Natural Frequencies of Vibration for Wings of Different Uniform Stiffnesses and Mass.

LIST OF APPENDICES

A. Analysis of the Standard Cirrus Sailplane.

B. The Theory of Longitudinal Static Stability and Manoeuvrability for the Tailless Aircraft.

C. Optimization of the Cross Country Performance of a 15 m Tailless Sailplane.

D. Wing Planform Optimization.

E. Derivation of Equations for Aircraft Response in Pitch.

F. Spanwise Load Distributions.

G. Preliminary Stressing.

H. Aircraft Natural (Structural) Frequencies of Vibration.

NOTATION

a	Aircraft lift curve slope.
a_1	Wing body lift curve slope.
a_2	Control surface lift curve slope.
a_3	Tab lift-curve slope.
a.c.	Aerodynamic centre.
a_o	Wing section 2-dimensional wing curve slope.
a_e	Effective wing-lift curve slope.
a_z	$\dfrac{a_o}{1 + \dfrac{2a_o}{\pi A}}$.
a_{1T}	Tailplane lift curve slope (due to incidence).
A	Aspect ratio
A'	Semi height of body cross-section opposite wing.
A_a	Aspect ratio of an analogous wing.
b	Span.
$\overline{b}$	Span of an analogous wing.
$b_{\nu\nu}$	Multhopp coefficient.
b_0, b_1, b_2, b_3	Control hinge moment constants.
B'	Semi width of body cross-section opposite wing.
$c(y)$	Chord distribution.
c.g	Centre of gravity.
$\overline{c}$	Standard Mean chord.
$\overline{\overline{c}}$	Mean aerodynamic chord.
c_{mac}	Section pitching moment coefficient.
$\overline{c}_{mac}$	Total aerofoil section contribution to wing pitching moment coefficient.
$\overline{\overline{c}}_\eta$	Mean aerodynamic chord of control.
c_m	Wing crank chord.

c_r	Wing root chord.
c_t	Wing tip chord.
$\overline{c}_T$	Mean tailplane chord.
C_D	Drag coefficient.
C_{D_o}	Zero lift profile drag.
$\triangle C_{D_i}$	Induced drag coefficient increment.
$\overline{C}_{D_I}$	Total induced drag coefficient.
C_H	Control hinge moment coefficient.
C_{H_S}	Total hinge moment due to springs.
C_{m_o}	Aircraft pitching moment coefficient about the aerodynamic centre.
C_{M_o}	Wing planform and twist contribution to C_{m_o}.
C_M	Pitching moment coefficient about the wing vertex due to planform sweep and twist.
C_m	Aircraft pitching moment coefficient about a.c. centre of gravity.
C_{m_q}	Pitching moment coefficient for unit pitching velocity of wing about aircraft centre of gravity.
C_L	Lift coefficient.
$\overline{C}_L$	Total lift coefficient.
d	Distance between fuselage centre of gravity and wing root elastic axis.
g	Gravitational constant.
$h\overline{\overline{c}}$	Distance aft of leading edge of mean aerodynamic chord to aircraft centre of gravity.
$h_c\overline{\overline{c}}$	Distance aft of leading edge of mean aerodynamic chord to control centre of pressure.
h_m	Stick fixed manoeuvre point.
h_m'	Stick free manoeuvre point.
$h_n\overline{\overline{c}}$	Distance of the stick fixed neutral point aft of the leading edge of the mean aerodynamic chord of the wing.
$h_n'\overline{\overline{c}}$	Distance of the stick free neutral point aft of the leading edge of the mean aerodynamic chord of the wing.

$h_o \bar{\bar{c}}$	Distance from leading edge of mean aerodynamic chord to aerodynamic centre of aircraft.
h_q	is given by $h_m = h_o + h_q$.
h_q'	is given by $h_m' = h_o + h_q'$.
$-\Delta h$	Forward shift in aerodynamic centre, due to fuselage.
H	Total moment.
H_m	Manoeurve margin with stick fixed.
H_m'	Manoeuvre margin with stick free.
i_y, i_x, i_z, i_{xz}	Non dimensional moments of inertia.
I_X	Rolling moment of inertia about centre of gravity.
I_Y	Pitching moment of inertia about the centre of gravity.
I_Z	Yawing moment of inertia about the centre of gravity.
J	is the natural damped frequency of the short period motion.
J^2	The undamped natural frequency of motion.
K	Span efficiency factor.
K_B	Pitching radius of gyration.
$\frac{k}{2p}$	Spring stiffness.
K_n	The static margin, stick fixed.
l_p	Non dimensional rolling moment due to rolling.
l_r	Non dimensional rolling moment derivative due to yawing.
l_v	Non dimensional rolling moment derivative due to sideslip.
l_ξ'	Non dimensional rolling moment derivative due to elevon.
l_T'	Distance between control centre of pressure and aircraft centre of gravity.
L	Total lift on aircraft.
L_C	Additional lift due to control deflection.
L_F	Vertical tail arm.
L_T	Horizontal tail arm.

L_W	Wing and body lift.
m_e	Gear ratio between control stick and control surface.
m_o	Increment in section moment coefficient with unit control deflection.
m_q	Non dimensional pitching moment derivative due to rate of pitch.
m_u	Non dimensional pitching moment derivative due to velocity increment along O_X.
m_W	Non dimensional pitching moment derivative due to velocity increment along the O_Z.
$m_{\dot{W}}$	Non dimensional pitching moment derivative due to rate of change of W.
M	Total moment.
M_o	Zero lift pitching moment.
M_T	is moment arising when elevator is deflected due to the centre of pressure of elevator load not coinciding with the aerodynamic centre of tailplane.
$M_{\dot{\theta}}$	is the pitching damping moment of aircraft, less tail.
n	Load factor.
n_p	Non dimensional yawing moment derivative due to rolling.
n_r	Non dimensional yawing moment derivative due to yawing.
n_v	Non dimensional yawing moment due to sideslip.
n_ξ	Non dimensional elevon yawing derivative.
P	Stick force to hold aircraft in a steady pull out from an initially trimmed stick free glide.
P_e	Stick force to hold aircraft in a glide.
$q = \dot{\theta}$	Angular velocity in pitch.
Q	Stick force per 'g'.
Q_1	Stick travel per 'g'.
r	is the instantaneous radius of motion.
R	Damping coefficient of the short period motion.
R^2	The undamped natural frequency of motion.

S	Wing area.
S_F	Area of fin and rudder.
S.M.C.	Standard mean chord.
S_T	Horizontal tail area.
S_{wet}	Fuselage wetted surface area.
S_η	Total control surface area behind the hinge line.
t	Time (in seconds).
$\hat{t}$	Unit of aerodynamic time.
t	Wing root maximum thickness.
T.A.S.	True air speed.
v_C	Achieved climb rate.
v_S	Glider sinking speed.
v_e	Equivalent sideslip velocity.
V	Airspeed.
V_1	Optimum speed through stationary air.
$\overline{V}$	Tail volume ratio.
Va	Average cross-country speed.
V_C	Achieved cross-country speed.
V_S	Stalling speed.
V_{CC}	M^{ac}Ready achieved cross-country speed.
V_{CR}	Cruising speed.
W	Maximum all-up weight.
W_b	Maximum water ballast.
W_E	Equipped Weight.
W_P	Maximum pilot weight.
x	Distance of leading edge of the mean aerodynamic chord aft of the wing vertex.
$\overline{x}$	Aerodynamic centre of wing alone.

x'	is the longitudinal distance from wing aerodynamic centre to wing quarter chord line at any spanwise station.
x_q	Non dimensional symmetric force - rotary derivative.
x_u	Non dimensional symmetric force - velocity derivative.
x_w	Non dimensional symmetric force - velocity derivative.
x_β	Spring lever arm.
$\bar{x}_\beta$	Trimmer movement to trim with stick free.
X_{AC}	Local aerodynamic centre.
x_S	Control stick movement.
y	Spanwise coordinate, spanwise axis.
z_q	Non-dimensional symmetric force - rotary derivative.
z_u	Non-dimensional symmetric force - velocity derivative.
z_w	Non-dimensional symmetric force - velocity derivative.
Z_q	is the rate of change of aerodynamic load on the main wing with respect to pitching velocity.
ZQ	$= \frac{a_1}{4}\left(\frac{1}{2} + 2(h_o - h)\right)\frac{\bar{c}}{\mu l_T}$.
μ_1	Aircraft longitudinal density parameter.
$\bar{\beta}$	Tab angle to trim
$\beta - \frac{v}{V}$	Side slip angle.
ϵ	Aerodynamic twist (positive for washout).
$\frac{1}{2}\rho V^2$	Dynamic pressure.
ρ	The local air density.
ω	Frequency of vibration.
δ	Control deflection measured normal to the sweep.
α	Angle of incidence.
α_B	Angle between refernce axis, in the body, and the flight direction.
α_e	Local effective incidence.
α_i	Local induced angle of attack.

α_T	Tailplane-body setting angle.
Λ	$\frac{1}{4}$ Chord sweep.
Γ	Dihedral.
λ	Taper Ratio.
Ψ	Angle of yaw.
η	Control angles.
$\eta_o + \eta_i$	are the non-dimensional semispan location of outboard and inboard aileron ends.
$\bar{\eta}_\nu$	Spanwise positions as given by Thwaites.
η_S	Control angle due to spring.
$\bar{\eta}$	Control angle to trim.
τ	Aerodynamic time.
ϕ	Sweepback angle at mid chord.
ϕ_a	Mid chord sweep of the analogous wing.
ϕ	Roll angle.
ϕ_e	Effective sweep of the analogous wing allowing for finite aspect ratio effects.
ϕ_{STR}	Sweep of a straight constant chord line.
$\bar{\gamma}$	Wing spanwise loading.
$\bar{\gamma}'$	Additional loading due to body upwash.
θ_a	Aerodynamic twist root/tip.

1. INTRODUCTION

In 1949 John K. Northrops' all wing YB-49 lost a United States Air Force contract to Convairs' B-36. Both of these aircraft were designed to bomb Germany from America, if Britain should be defeated. The loss of this contract was the final blow to Northrops' tailless aeroplane program. Whether it was dealt through the unfortunate economical and political lobbying, which besets many an abandoned aircraft project, or whether it was a suspicion that the all wing margin of superiority would turn into an elusive will-o'-the-wisp that might vanish when put into practice was unknown. "There was instantly a babble of comment across the nation, which was suddenly raised to fever-heat" and further fueled by the news media's conversion of technical jargon to the layman's terminology. An unfounded suspicion, because the YB-49 later made headlines by demonstrating greater range capabilities, at higher cruise speeds, than the B-36 was capable of producing.

The history of tailless sailplanes images the typical fate of tailless powered aircraft. A concept is flown, its faults analysed, and the project abandoned due to lack of finance or effort. In the case of sailplanes it is usually the personal finance and effort of a homebuilder. Several homebuilders have persevered, notably the Horten brothers, Charles Fauvel, Jim Marske and Al Backstrom. The war interrupted the development of the Horten sailplanes. However, a flight test performance and drag analysis, of the 20 metre span, Horten IV sailplane, was conducted by the Mississippi State University in 1959. This demonstrated many shortcomings of the aircraft, none of which could not be solved, and illustrated the likely performance after redesign. Jim Marske gained knowledge and experience through practical experimentation on a series of tailless sailplanes. His efforts have been aimed at stability and control and he claims the formula for success lies in a wing with an unswept leading edge. His Pioneer sailplane is sold in kit form in America, and although it is basically a sport class sailplane, the performance claims are quite controversial, being substantiated by some and contested by most. In any case the aspect ratio of existing tailless gliders is about half that of current conventional designs and the aerofoil sections are grossly inferior.

The modern high performance sailplane is a sophisticated machine, incorporating aerodynamic refinements unmatched by powered aircraft. This performance increase has primarily been achieved by the progressive reduction of the three major components of drag, ie induced, profile and parasite drag. To begin with, the parasite drag was reduced by the elimination of struts, bracing wires, open cockpits, external control runs, skids and fixed undercarriages. Induced drag was decreased by the use of higher aspect ratios whilst the profile drag was reduced by the use of low Reynolds' number, low drag aerofoils. This has been especially apparent with the aerofoils designed by Professor F.X. Wortmann and Dr. R. Eppler which, when combined with materials like moulded fibre reinforced plastics, achieved profile drag reductions as high as 25% over their NACA counterparts with considerable widening of the drag bucket. The

reduction of profile drag continues by the use of narrow chord, speed and lift flaps, but renowned aerodynamicists claim that, a plateau has seemingly been reached. For a given span the performance has not greatly improved over the last 10 years, when fibre reinforced plastic sailplanes were first produced, whereas the costs have soared dramatically.

Reductions in profile drag, by reducing the wetted surface area, with a corresponding reduction in material, labour and maintenace costs are the aims of tailless designers. These have not been achieved. In fact, by comparison with current conventional designs the reverse is true. Tailless wing areas are double, induced drag 30% higher, multiple, ill-placed, or mere large fin and rudders claim their penalties, whilst the interference and trim drag could hardly be worse.

An update of the tailless sailplane is required. All the refinements of existing competition sailplanes have to be incorporated. The aerofoils have to be redesigned, the ideals of reduced cost, weight, labour, and inceased performance have to be realized. The weight range and aspect ratio have to be optimized to achieved cross country performance rather than stability and control. Compatibility here still would not be enough. The tailless sailplane will have to win, in major flying competitions against its conventional counterpart, before it is accepted.

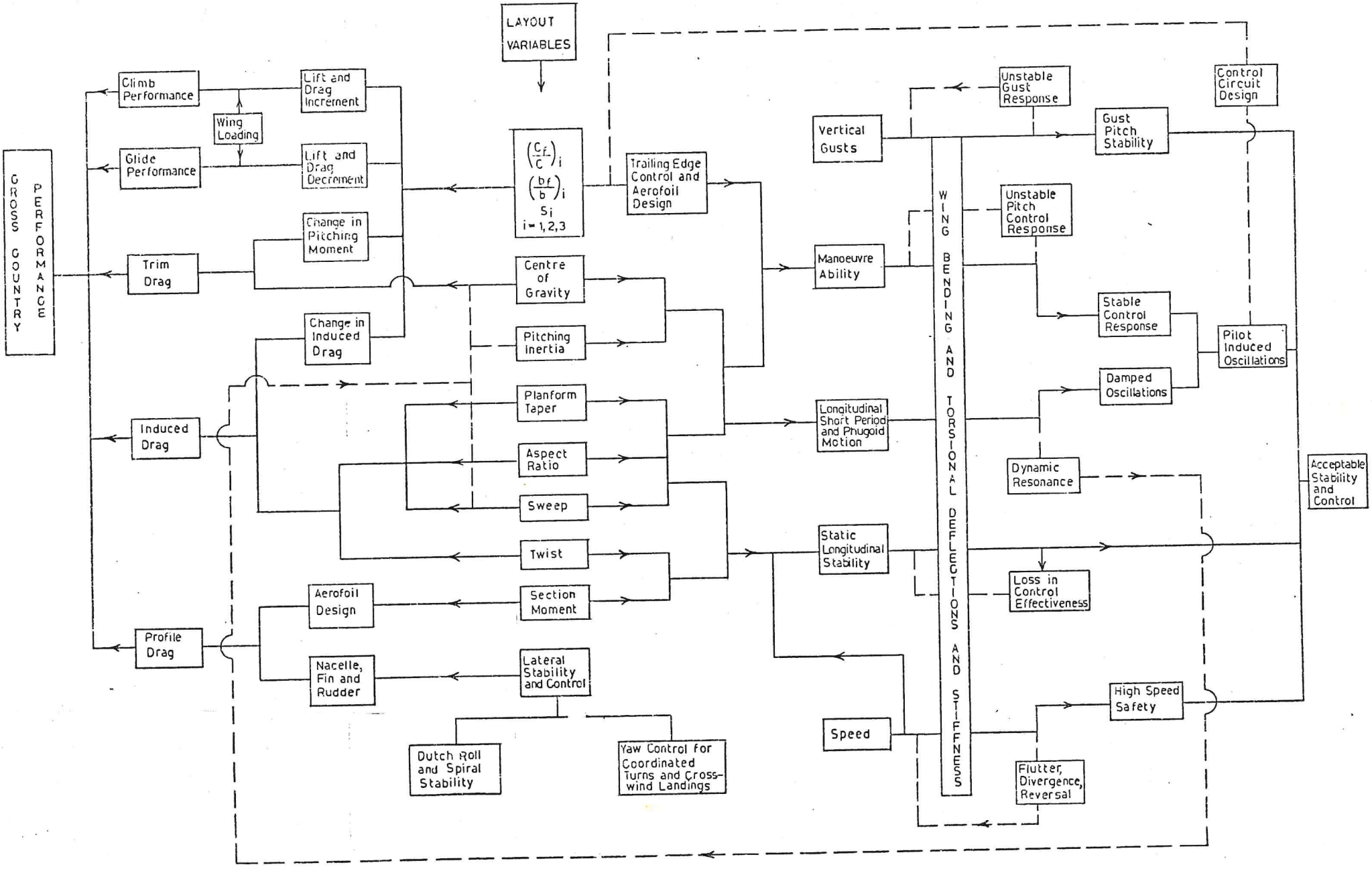
LAYOUT VARIABLES
GROSS COUNTRY PERFORMANCE
Climb Performance
Glide Performance
Trim Drag
Induced Drag
Profile Drag
Wing Loading
Lift and Drag Increment
Lift and Drag Decrement
Change in Pitching Moment
Change in Induced Drag
$\left(\frac{C_f}{C}\right)_i$ $\left(\frac{bf}{b}\right)_i$ S_i $i = 1,2,3$
Centre of Gravity
Pitching Inertia
Planform Taper
Aspect Ratio
Sweep
Twist
Section Moment
Aerofoil Design
Nacelle, Fin and Rudder
Lateral Stability and Control
Dutch Roll and Spiral Stability
Yaw Control for Coordinated Turns and Cross-wind Landings
Trailing Edge Control and Aerofoil Design
Vertical Gusts
Manoeuvre Ability
Longitudinal Short Period and Phugoid Motion
Static Longitudinal Stability
Speed
WING BENDING AND TORSIONAL DEFLECTIONS AND STIFFNESS
Unstable Gust Response
Gust Pitch Stability
Control Circuit Design
Unstable Pitch Control Response
Stable Control Response
Pilot Induced Oscillations
Damped Oscillations
Dynamic Resonance
Loss in Control Effectiveness
High Speed Safety
Flutter, Divergence, Reversal
Acceptable Stability and Control

2. SCOPE

The work study flow chart is intended to show some of the more basic design interactions and indicate the more desirable methods of problem solving. The chart is reasonably complex and merits some explanations.

We begin with the aircraft layout variables, such as aspect ratio, sweep and twist for example, near the chart centre. Initial considerations were aimed at reducing the range of these design variables to within acceptable working limits. This was first done by examining the requirements of static longitudinal stability and manoeuvrability. No severe constraints arose from this investigation, although the sailplane layout must favour a limited centre of gravity range. Since high aspect ratios did not appear problematic the next logical step was the optimization of the sailplane performance. The most restrictive coupling between sailplane cross-country performance and longitudinal static stability occurred through the aerofoil section characteristics.

The section of flow chart to the left of the design layout variables is concerned with the cross-country performance of the sailplane. There is very little likelihood of the sailplane winning appeal unless the performance is better than an equivalent conventional sailplane. The performance analysis of the sailplane must be fairly rigorous. At a speed of 50 kts something like a mere 7.5 kg of total drag is invisaged, implying that only small amounts of, say, trim or induced drag, can give a percentage performance decrement outweighing any advantages in performance the tailless sailplane might show. The interrelationship of parameters such as trim drag and induced drag with the wing planform shape can be seen from the chart. The layout should preferrably allow the use of flaps to enhance the performance.

Some of the variables affecting the longitudinal dynamic stability, such as aspect ratio, sweep and pitching inertia can be altered with a minimum effect on performance or static stability. All indications so far were for a high aspect ratio wing. It was therefore possible at this stage to design a sailplane with optimum cross-country performance and satisfactory longitudinal stability and control, the major variables being aspect ratio sweep and twist. The aspect ratio was finally chosen as high as the performance would allow, such that sweep and twist could be minimized. Minimum twist was particularly important for high speed performance but the demands of static stability had to be satisfied.

The effect of lateral stability and control on performance is important and should be integrated with considerations of fuselage layout and wing sweep.

The right hand side of the flow chart considers the effects of wing flexibility. It is illustrated, that where possible, problems should be solved by altering the wing torsional and flexural stiffenesses and the location of the flexural axis, and section twist centre

locii. Minimizing the sweep is the best way of allowing for these problems in the early design stages. Flutter, divergence and control reversal should not pose any significantly different problems to conventional sailplanes (whose solution is possible with fibre reinforced plastics). Bending of a swept back wing will introduce twisting and hence a pitching moment about the aircraft centre of gravity. This can manifest itself in an unstable pitch control response, an unstable gust response, or an unstable (or unacceptable) coupling of wing bending vibration and the short period pitching oscillation. Either this latter oscillation or a pilot induced oscillation may demand a preliminary design change for a satisfactory solution.

3. DESIGN PERSPECTIVE

We require a guide with which to compare the ideals of the tailless sailplane. For example, we wish to determine the degree of stick fixed stability required. The stability of a bomber may be restrictive on design whilst the lack of stability of a competitive aerobatic aircraft may tire the pilot on a long soaring flight.

The best method of placing the tailless design in perspective is to compare it with a conventional sailplane of the type it is intended to outmode. The Standard Cirrus Sailplane has been chosen as a basis for comparison because its cross-country performance and stability and control are equal to, or better than, any other "Standard Class" (15 m. wing span) sailplane. A review of the standard class rules and an analysis of the Standard Cirrus Sailplane is contained in appendix A. Where possible, theoretical results have been compared with experimental values to justify the methods of ananlysis. Although these tools of analysis have to be modified in the case of the tailless sailplane, we may now feel more satisfied with their use.

In particular, we may look at the glide performance of the sailplane and note that the computerized performance, given by,

$$C_D = 0.0108 + C_L^2 \left(0.00225 + \frac{1.05}{\pi A}\right),$$

is in good agreement with the flight test results of 3 independent workers. C_D, C_L and A are the drag coefficient, lift coefficient and aspect ratio respectively. The factor 0.00225 gives the component of lift dependent drag arising from the aerofoil characteristics and 1.05 is the induced drag factor, K. Checks on the longitudinal phugoid mode, spiral, and dutch roll lateral modes, give satisfactory agreement. Similarly the times to roll and yaw through given angles were predicted quite well. The Cirrus was also useful in determining exponential elevator application rates to simulate soaring "pull up" manoeuvres.

4. REDUCING THE DESIGN VARIABLES

The derivation of the theory of longitudinal static stability and manoeuvrability, stick fixed and free, for tailless aircraft is given in appendix B. The example sailplane, figure 1, has also been used in appendix B to illustrate the analysis and provide a comparison with a conventional sailplane. To avoid distracting the reader from the main argument presented here only the basic conclusions from the appendix will be given. Many peculiarities of the tailless sailplane are discovered in the appendix and the use of springs and weights to provide solutions is investigated.

4.1 Stick Fixed Static Longitudinal Stability

For stability we require,

a. the centre of gravity forward of the sailplane aerodynamic centre, and

b. a positive sailplane pitching moment coefficient, C_{M_o}, if elevator angles to trim are going to be zero at some C_L values, for a sensible centre of gravity range.

4.2 The Layout of Stable Wings

Figure 2 presents the wing contribution to the pitching moment coefficient, C_{M_o}, for wings of various twist ϵ, sweep, Λ, and mean values of section pitching moment coefficient, c_{mac}. A wing of aspect ratio 12 requires twice the twist that a wing of aspect ratio 20 requires to achieve a given C_{M_o}, for the same sweep. The values of 0.03 and 0.04 chosen for C_{M_o} are representative of the wing stability required to produce reasonable control trim angles for sensible control dimensions. Trim curves for the sailplane of figure 1 are provided in figure 3.

4.3 Aerofoil Requirements

From figure 2, an unswept wing requires the use of reflexed aerofoil sections for stability whilst less stable, or unstable sections, can be used, if sweep and twist are used to provide a positive C_{M_o}. Washin is compatible with forward sweep and washout with sweepback. It will be shown later that a high, maximum wing lift coefficient improves considerably the cross-country performance.

Tailless sailplanes of the past have had aspect ratios of 9 to 15 (see reference 9). Even the swept wing designs have had to use full span reflexed aerofoils to avoid the adverse effects of large amounts of wing twist at low C_L.

The modern, conventional sailplanes of today have achieved their performances through the success of their low drag, low Reynolds number aerofoil sections. These successes are due to the works of Professor F.X. Wortmann and Dr. R. Eppler, examples of which are contained in references 10 to 15. Only minor improvements

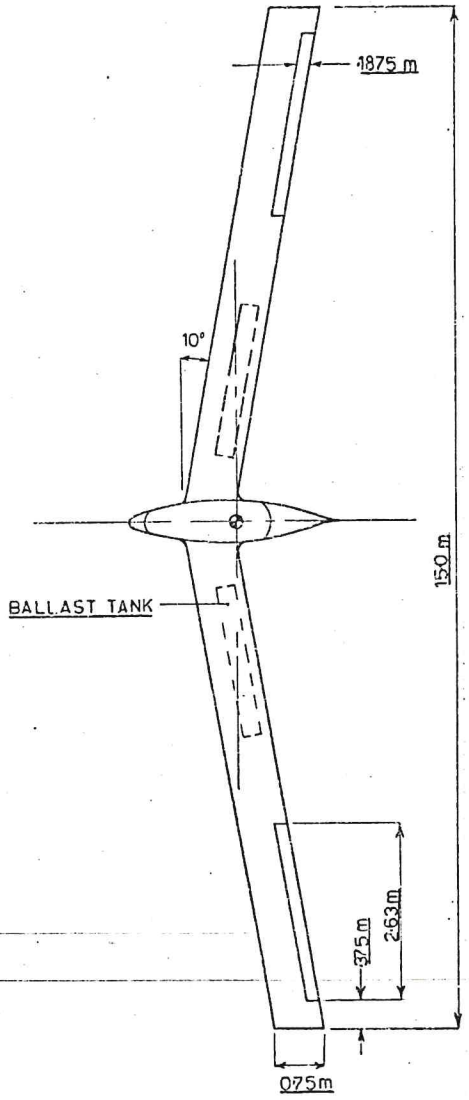

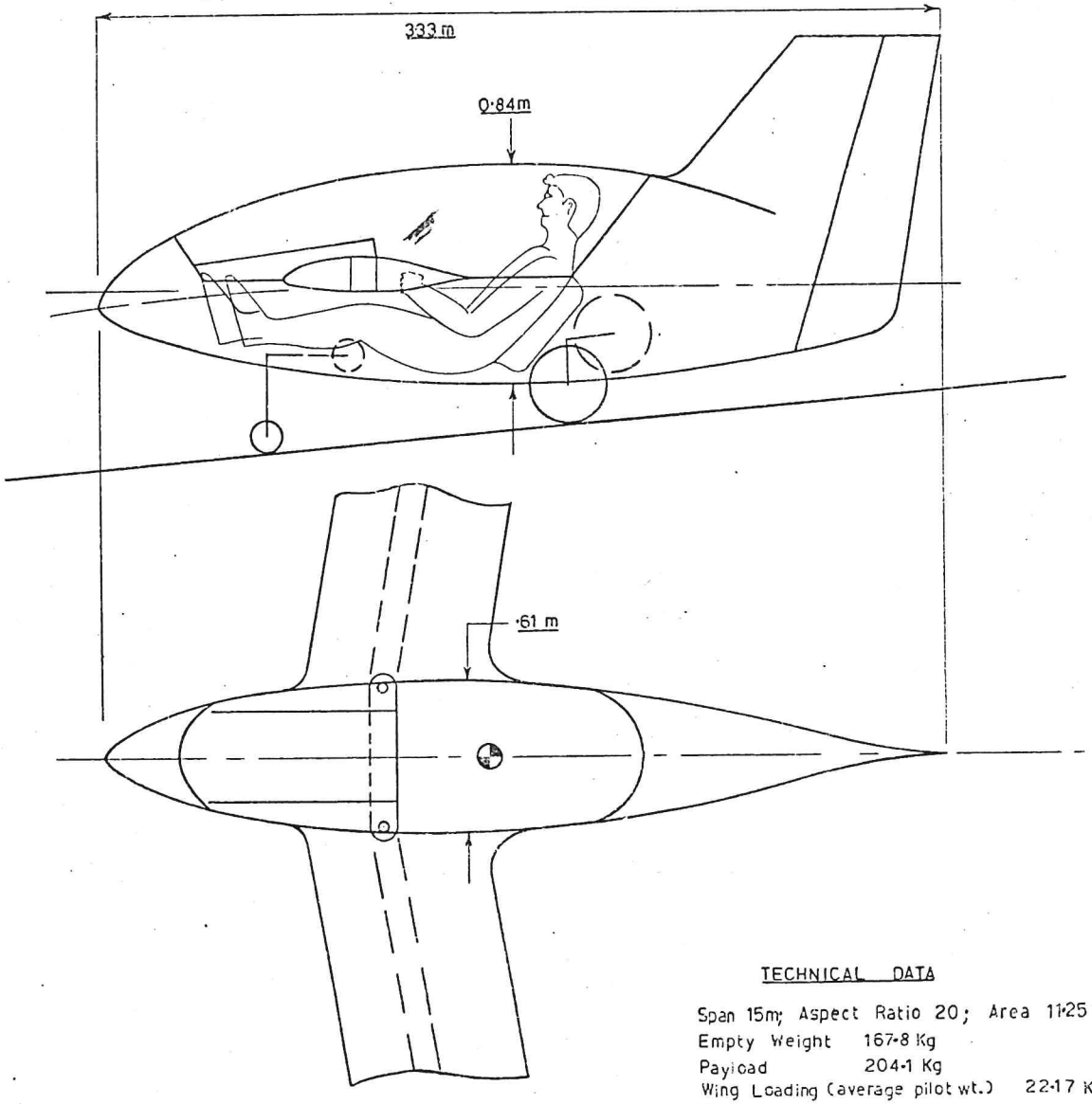

FIG 1

8

TECHNICAL DATA

Span 15m; Aspect Ratio 20; Area 11·25 m²

Empty Weight	167·8 Kg
Payload	204·1 Kg
Wing Loading (average pilot wt.)	22·17 Kg.m⁻²
Wing Loading (maximum)	39·06 Kg.m⁻²
Stall Speeds (corres.)	64·36 and 85·43 kph

DRAWN	CHKD	APPD	SCALE	TITLE:-
E.T. BUCHANAN			1/10	PRELIMINARY LAYOUT

COLLEGE OF AERONAUTICS
CRANFIELD INSTITUTE OF TECHNOLOGY
CRANFIELD.

DRAWING No.

SHT 1 OF 1 SHEETS

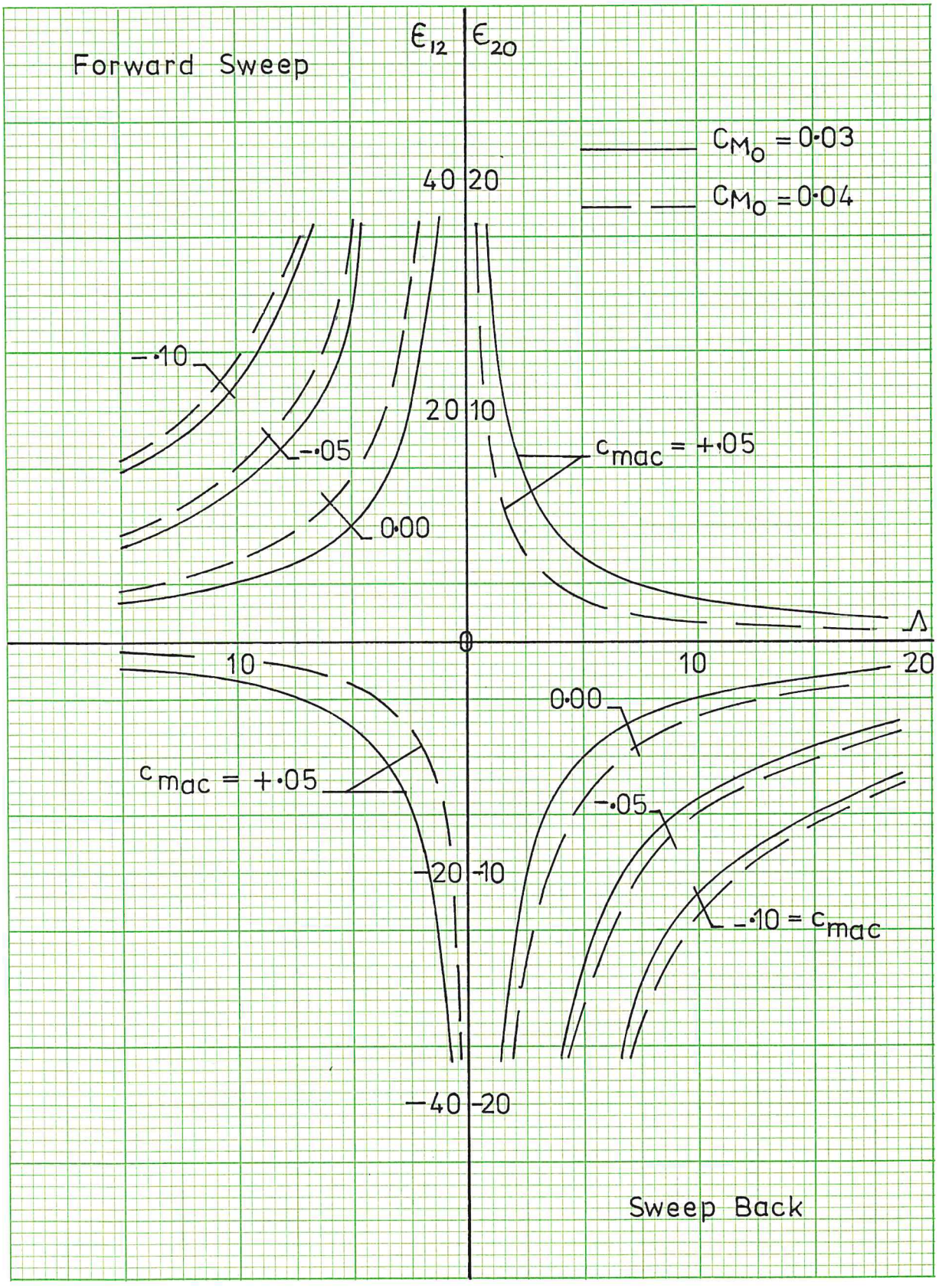

FIG 2. THE LAYOUT OF STABLE WINGS.

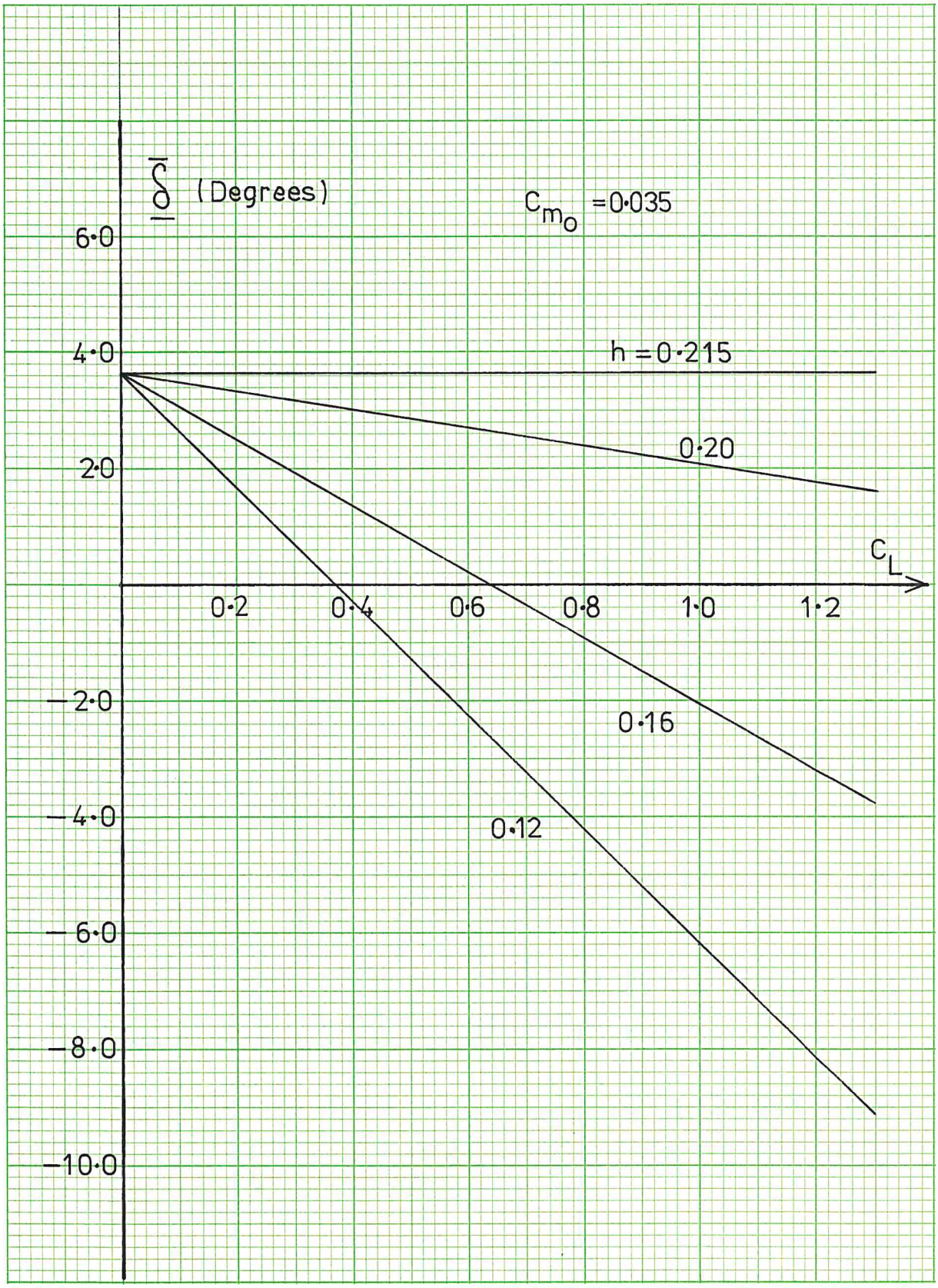

FIG 3. ELEVON ANGLES TO TRIM

have been made to these aerofoils in the last 10 years and Professor Wortmann states in reference 16, that a plateau in the design of low drag aerofoils for sailplanes, has seemingly been reached, and that further performance gains are most likely to be achieved through other aerodynamic refinements.

Consideration is given to the suitability of the following aerofoil types for a high performance tailless sailplane.

a. Conventional

Modern, conventional sailplane aerofoil sections have a $c_{mac} \approx -0.1$. From figure 2 these would require 8 degrees wing twist for an aspect ratio of 20 and 15 degrees of sweep. Such an arrangement provides only a very small operating C_L range to avoid either wing root or tip stalling, or to keep the sections within their low drag range. Tailless sailplanes, have in the past, made use of the limited range of reflexed airfoils or have reflexed some of the earlier NACA sections. This latter method cannot be applied to the current low drag sailplane aerofoils, because, as shown in references 11 and 15, the upper and lower surfaces of the aerofoil are designed separately by prescribing a desired velocity distribution for a given range of angles of attack. The shape of the velocity distribution over the rear portion of the aerofoil, where reflexing may have to be carried out, is critical in the formation of the various stages in laminar boundary layer transition.

b. Reflexed

Reflexed aerofoils have been used in the past for swept and unswept wings due to the low aspect ratios used. Such an aerofoil section will never be satisfactory for the production of high maximum lift coefficients. As a consequence the sailplanes' climb performance, or the wing loading range is reduced. Combined with a narrower low drag bucket this means the sailplanes' flexibility and cross-country performance is impaired.

c. Spanwise Variation of Section Camber

If, on an untapered planform, we used a conventional aerofoil with $c_{mac} = -0.1$ at the root and a symmetrical, or reflexed section, with $c_{mac} = 0.0$ at the tip, our nett section c_{mac} is $\simeq -0.05$. From figure 2 a 15 degree swept-back wing of aspect ratio 20 now only requires 5 degrees washout. Hence we can combine the properties of a conventional low drag, positive cambered aerofoil section, and high maximum lift coefficient at the wing root, where it is needed, with a stable tip aerofoil section, having a lower maximum lift coefficient, where it is more acceptable. The gradual introduction of reflex along the span introduces an effective wing twist, due to the change in section zero lift coefficients, even when the wing leading and trailing edges are kept

in the same untwisted plane. Consequently, not only is the mean section pitching moment, c_{mac}, reduced but it is likely that all sections are able to fly at the same relative positions in their drag buckets ensuring each is always flying at its optimum best for all required angles of attack. Dr. Eppler provided the author with a copy of the computer programme used for the design of sailplane aerofoil sections and a dissertation from Dr. Miley (reference 17) provided some theoretical consolidation and practical design hints. Although the program is running, insufficient time was available to ensure adequate familiarity. However, Dr. Eppler was able to provide two possible aerofoil series (one of which is reproduced in figure 4) along with the advice that the optimization of wings of the type considered is very difficult. As a guide to the possibilities, the sailplane of figure 1 uses 3.5 degrees of washout, 10 degrees of sweep and a relatively low performance aerofoil section whose mean spanwise pitching moment is 0.0.

To summarize so far, a wing of lower stability, C_{M_o}, is likely to provide a higher maximum lift coefficient especially if sweep is used. The lower limit on C_{M_o} is determined by the stability required at aft centre of gravity (figure 3), and the control effectiveness.

4.4 Control Effectiveness

To examine the longitudinal problem, a plain-flap, fixed hinge control surface has been considered. The effect of sweep, aspect ratio and taper ratio for a control surface whose area is 8.75% of the total wing area is shown in figure 5. The difference between control centre of pressure and wing aerodynamic centre, $h_c - h_o$, is shown in appendix B to behave similarly to the conventional tail volume ratio $\overline{V}$. The increase in control effectiveness with sweep or aspect ratio should allow smaller control surfaces or smaller deflections than has been possible in the past and hence lower the trim drag. This presupposes the same percentage chord centre of gravity range which implies a reduction in absolute shift for the high aspect ratio wing. It should also be pointed out that 5 to 7 degrees sweep can double the control effectiveness of an unswept wing.

4.5 Centre of Gravity Range

For a conventional sailplane the greatest change in centre of gravity is occasioned by catering for pilots of different weight, seated on a substantial moment arm from the empty aircraft centre of gravity. If, for a tailless, we seat pilots of different weight on the empty aircraft centre of gravity we have eliminated the major need for an allowable centre of gravity range.

The two lesser factors in establishing the centre of gravity range for a conventional, are the shift due to the pilot moving from the nominal seating position, and the shift, with attitude changes, due to water ballast movement.

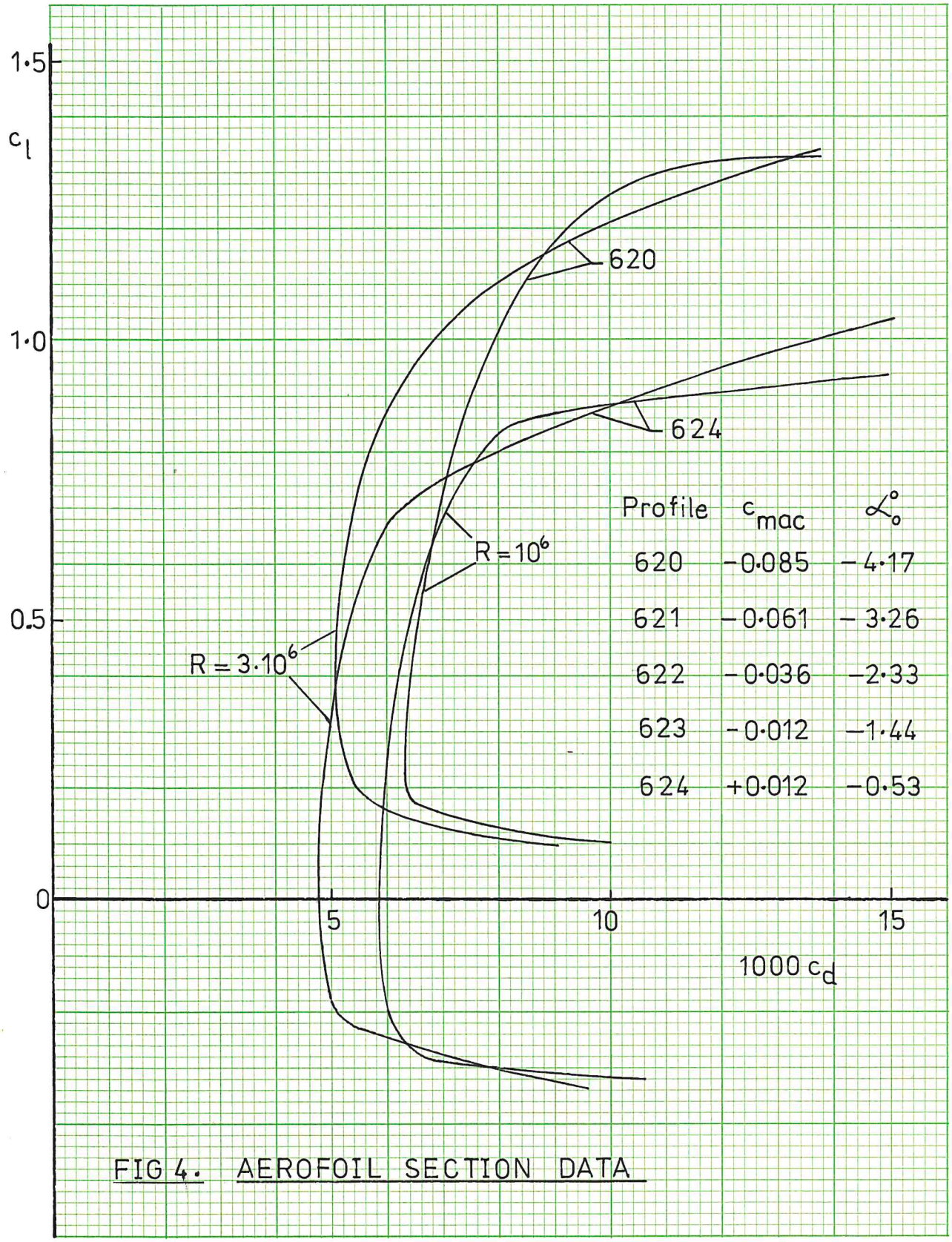

FIG 4. AEROFOIL SECTION DATA

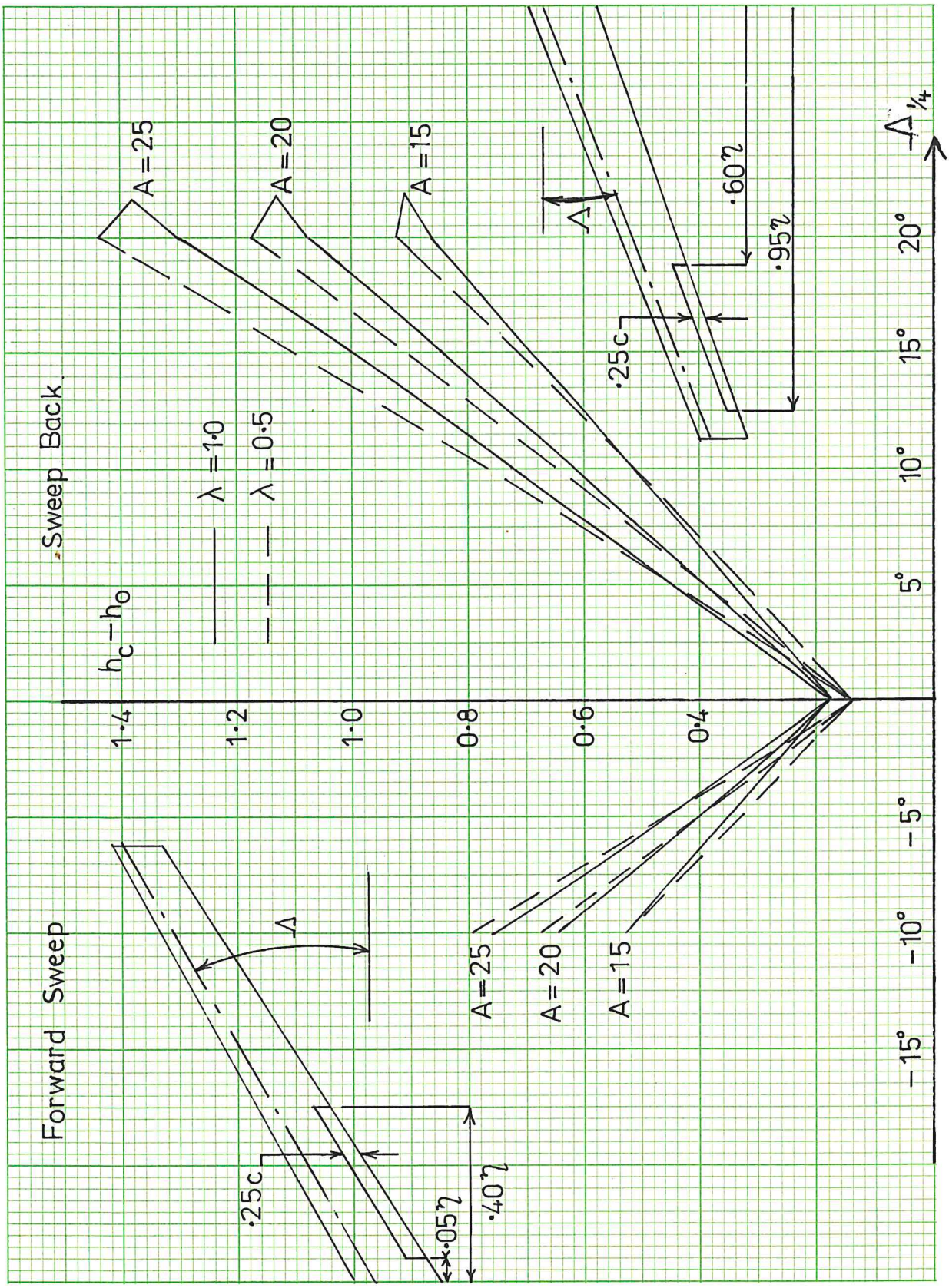

FIG 5. EFFECT OF SWEEP, ASPECT RATIO AND TAPER ON CONTROL EFFECTIVENESS PARAMETER $(h_c - h_o)$

Figure 6 shows the results of a simple experiment, conducted to determine the change in pilots' centre of gravity due to a change in the pilots' back angle.

Modern sailplanes, with low cockpit cross-sectional areas, use a semi-reclining back angle of approximately 45 degrees. Using this value for a fixed back rest, and a value of 75 degrees for the pilot reaching forward to the instrument panel, gives a change in pilot centre of gravity of 7.0 cms. The difference in personal centres of gravity from pilot to pilot is negligibly small and so a value of 7.0 cms shift from a known seating position will be catered for. For comfort the rudder pedals will adjust relative to the seat. For figure 1 the corresponding shift in aircraft centre of gravity is 2.2 cms.

For unpartitioned water ballast tanks in the spar of figure 1, half full tanks give a change in centre of gravity of 3.5 cm between nose vertically up and nose vertically down.

It is pessimistically assumed that the sum of these centre of gravity shifts gives a resultant shift of 5.7 cm or 7.6 percent of mean aerodynamic chord.

4.6 Selection of Wing Sweep

A swept back wing offers the following advantages.

a. A higher maximum wing lift coefficient with favourable spanwise airload distribution.

b. The optimum use of full span trailing edge flaps by programming inboard deflections to be greater than outboard. From figure 2 the effective increase in washout can compensate for the increase in unstable pitching moments associated with positive flap deflections.

c. Increased control effectiveness compared to an unswept wing.

d. Allows the use of high aspect ratios with only moderate twist to avoid unfavourable lift distributions at low C_L.

e. Incorporates sufficient washout to prevent unstable tip stalling tendencies.

f. The use of high aspect ratios require sweep to provide longitudinal manoeuvre damping. An unswept wing requires a much lower aspect ratio to avoid the large changes in stick travel, or force, per g for a given centre of gravity range (see appendix B).

g. The same pitch damping is required for improved longitudinal dynamic oscillations (see later).

h. Provides a degree of directional stability, partially compensating for the reduced fin arm.

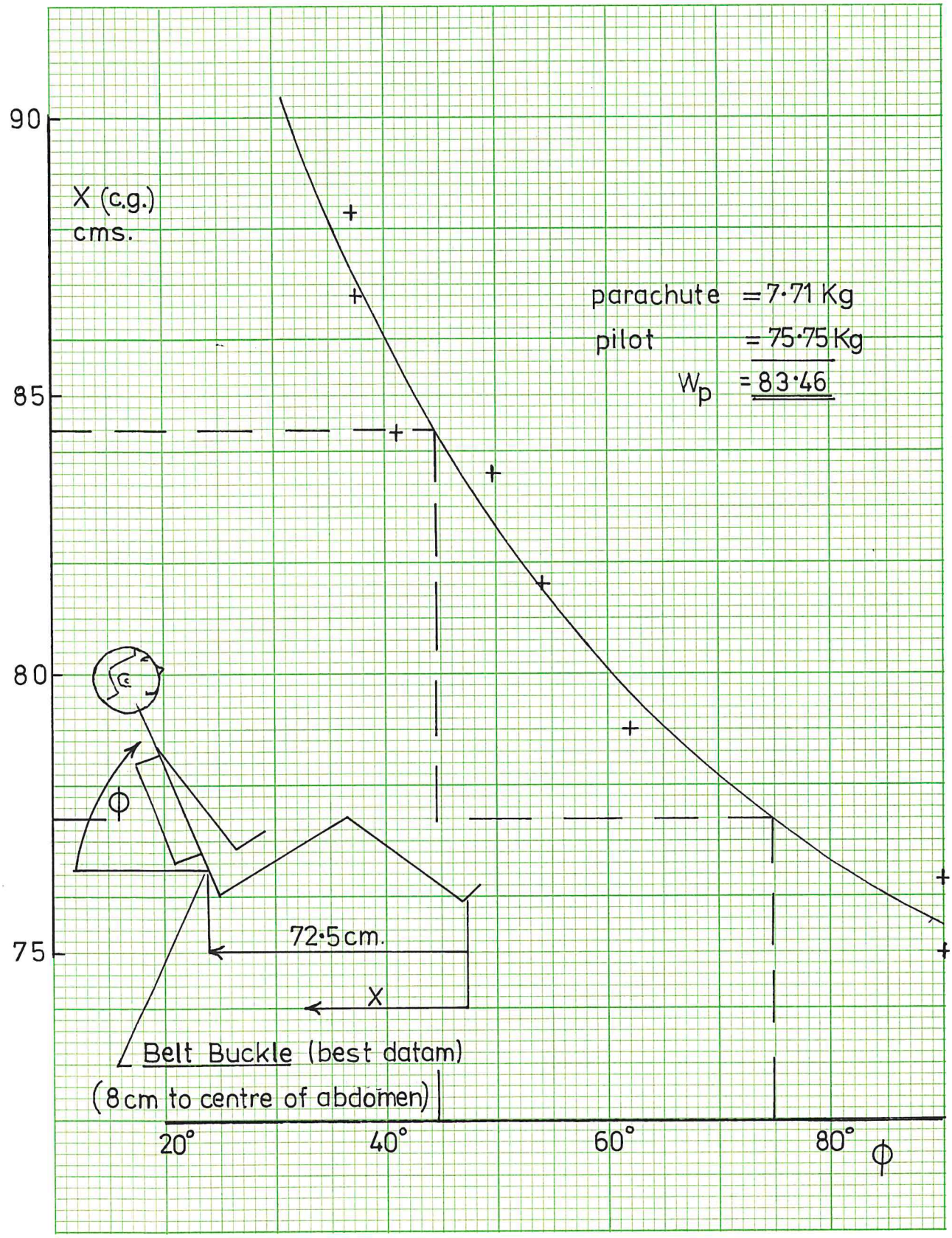

FIG 6 CENTRE OF GRAVITY SHIFT DUE TO CHANGE IN INCLINATION OF THE PILOTS' BACK.

i. Reduces the tendency to high speed wing divergence associated with forward sweep.

j. Allows combination of ailerons and elevators to reduce interference drag, (or conversely the use of flaps for pitch control).

Swept forward and unswept wings provide a layout simplification by allowing the pilot to sit forward of the main spar. To avoid large centre of gravity ranges, and extra wetted surface areas with a swept back wing, the wing has to be located ahead of the pilot as in figure 1. The resultant loss of visibility and increased cockpit layout difficulty is reduced as the wing chord is reduced. A rough mock up of the figure 1 layout was possible with an existing sailplane and the only disadvantage is thought to occur when photographing turn points during competition tasks. This is not a real handicap. A low wing would have provided an ideal layout from the points of view of visibility and undercarriage load paths, but the wing would be unfavourably low to the ground during the inadvertent outlanding.

The layout in figure 1 has been devised to show that the minimum angle of sweepback for this configuration is 10 degrees. Reduction of this angle will cause the wing spar to restict the pilot movement.

5. SAILPLANE PERFORMANCE

Sailplane performance is best determined by the speed at which a specified cross-country task can be completed, by an idealpilot, under a given set of meteorological conditions. National and international gliding competitions primarily consist of closed circuit races. Even when weather precludes the completion of a task, making it one of distance rather than speed, the higher achieved cross-country speed generally allows the greater distance to be covered prior to landing.

Two necessary phases of cross-country flying are climbing and gliding. Height is generally gained by circling in rising, "thermal", air currents. The achieved rate of climb will therefore be dependent on the thermal strength (vertical velocity), the distribution of this velocity over the thermal cross section, the sinking velocity of the glider in the turn, and the radius of turn. An aerodynamically clean glider with a low wing loading or good slow speed capability is likely to execute efficient, tight turns in the stronger thermal core. If assumptions are made about the shape, size, strength and strength distribution of a given thermal it is a simple matter to determine the speed and bank required of a given glider, at a particular weight, to optimize the rate of climb. A sailplane could be designed to achieve the highest rate of climb in particular thermals. It would be a very light sailplane whose best straight gliding performance is achieved at quite slow speeds. Therefore, whilst such a vehicle might climb quite rapidly, the time it takes to fly a given distance after the climb will inevitably be long, resulting in a poor, achieved cross-country speed.

On the other hand a vehicle could be designed to glide flatter and faster than any other glider. To design for an optimum glide ratio at high speed would result in a very heavy glider with an extreme aspect ratio, making it incapable of circling within the confines of a rising air current.

Almost to date, the design of sailplanes for optimum cross-country performance has been affected by aiming for the best flight polar attainable, whilst providing satisfactory climb rates in thermaling flight. The design art has therefore been in determining the latter. Armed with experience, the manufactures of the current generation of 15 metre-span sailplanes, have converged on aspect ratios of 21 to 23 and wing loadings of 30 to 40 kg/m^2. With such vehicles pilots are achieving cross-country speeds up to 120 $km/hr.$ for closed circuit races of 200 to 500 km; or distances, in one solar day, in excess of 1000 kms.

Height can be achieved on a cross-country flight not only by circling in thermals but also by gliding in rising air masses associated with "wave" phenomena, hill lift, sea breeze fronts etc. Competition flying, generally uses the more common thermal air currents. Each successful flight will involve the attainment of height by circling in thermals. Equally certain is the fact that height will be gained by flying straight and level, through lift,

attributable to these thermals. For example, on a given day, thermals may line up with the prevailing wind to form "thermal streets", in which case the pilot flies, slowly along the street and climbs in the general direction of desired course. At the "top", or end of the street, the pilot will turn onto a heading which will make good his desired track, and fly fast across the intervening "sinking" air to the next thermal street. In this way he may fly a complete leg of a given triangular task, thereby, covering a distance in excess of 100 kms without losing height. This soaring technique is quite new and made possible by the high glide ratios of modern sailplanes. It is known as "Dolphin" soaring, because the pilot executes abrupt pull ups on encountering rising air, so he can fly slow and feel out the path of strongest lift, to be followed by a dive through sinking air, to minimize the latters' effect. Theories have suddenly appeared for the optimization of cross-country speeds under conditions of hypothetical distributions of rising and sinking air masses of varying intensities along a given section of flight. It can readily be appreciated that under such conditions more emphasis is placed on the straight flight polar curve of the aircraft. A sailplane has not yet been designed specifically for these conditions because,

a. the concept and theories are new, and

b. the micro-meteorological conditions, which favour the technique, are not available all the time.

In fact sailplane designs are only now being optimized to the classical MacReady theory of cross-country soaring. This theory of soaring has been used for the last ten years by competition pilots and has been used for the "next" generation (all manufacturers have distributed sales pamphlets, and one or two prototypes have been built) of 15 metre sailplanes.

The MacReady theory of soaring assumes a height gain by circling in an isolated thermal, followed by a glide through "smooth" air, to the next thermal, where the process is repeated. Figure 7 is a typical flight cross section.

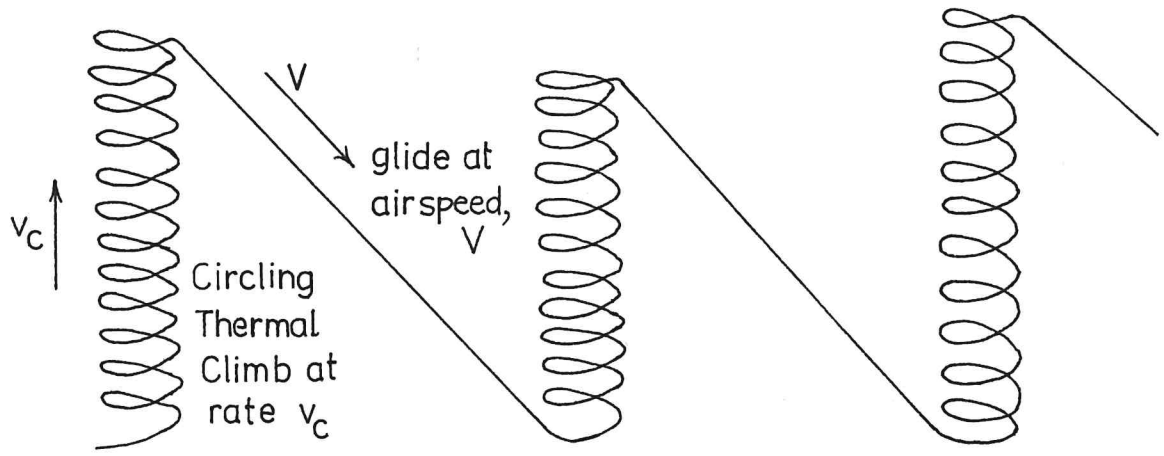

Figure 7

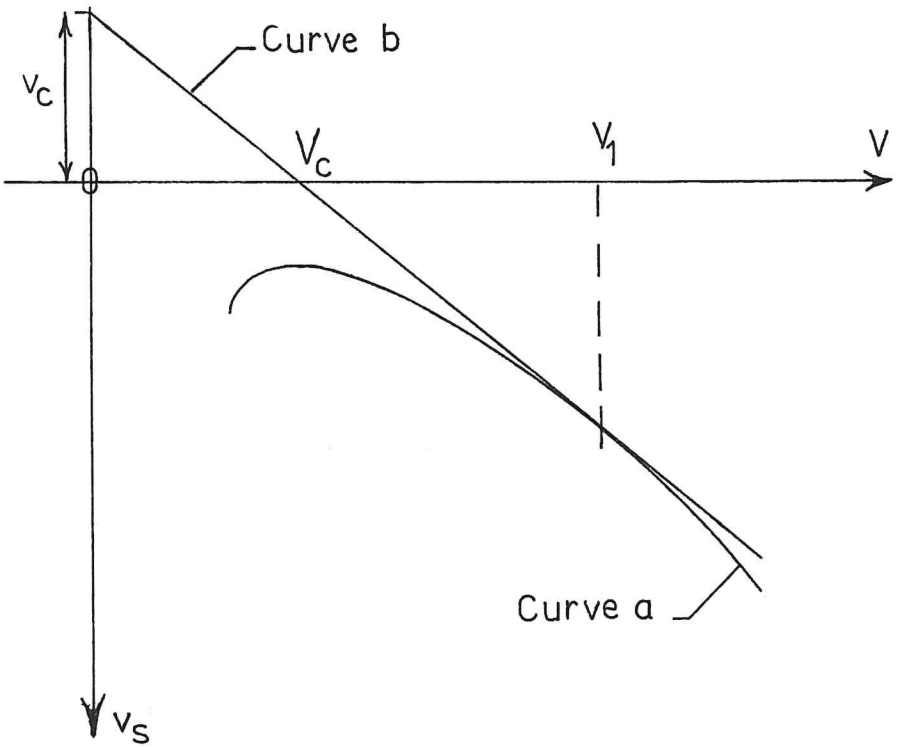

Figure 8

Curve 'a', figure 8 is the straight flight polar of a given sailplane. The equivalent glider sinking speed, v_s, is plotted against equivalent airspeed V. If a pilot expects to climb at an equivalent rate, v_c, in the next thermal he encounters, then the optimum speed through stationary air to the next thermal is given by V_1, where line 'b' is tangent to curve 'a' and bisects the ordinate at v_c. The achieved cross-country speed is V_c. The mathematics of the optimization is simple and is covered in any basic text book on gliding. The effect of wind and sinking air can be superimposed on the construction and the effect of water ballast (aircraft weight) can be studied by the effects on achieved climb rate, v_c and by the shift of the polar curve within the axes. It is apparent that,

a. a pilot must fly faster than the speed corresponding to best lift to drag speed of the aircraft for any climb rate greater than zero,

b. the expected climb rate in the next thermal can only be estimated by the calculated climb rate in the last thermal,

c. the pilot requires an instrumented presentation to give him the speed he should be flying at, corresponding to the sink rate he is actually flying through, assuming the expected rate

of climb in the next thermal, and

d. the pilot must carry the correct amount of water ballast to optimize his cross-country speed; too much water will give good glide penetration but poor climb rate, whilst too little ballast will give a high climb rate but insufficient penetration.

The foregoing has been intended to give the reader a very brief encounter of glider cross-country flying. As such, a necessary injustice, to the art of soaring flight has been committed. References 18 to 30 inclusive, may be helpful, but answers to all the questions have not yet been written. Answers to questions on thermalling technique, on pullups, or final glides, on height bands to be worked, on pilot comfort aircraft stability and control, are as important as those concerning which thermals should be used, and which ones should be passed up on a given day, are available in the minds of individuals. The following design work will tend to eliminate the individual, but factors such as wing loading range and cockpit visibility for example may tend, or appear, to be personal decisions. The lift coefficient at which the author tends to use in thermals, to provide a margin over gust stall or incompetence, is used for optimum thermal climbs, for example. In general our ideal pilot will fly a given sailplane under the hypothetical meteorological conditions with computerized precision. In so doing the sailplane performance can be optimized with respect to aspect ratio and weight for a given span, assuming adequate layout for stability and control.

5.1 The Computerized Optimization of a 15 m Tailless Sailplane.

In reference 31, F.G. Irving discusses the use of a computer program with which he determined the optimum aspect ratio and weight range for a 15 m conventional sailplane. He found that, for thermals having a parabolic velocity distribution, and strengths between 4 and 12 knots, and radii from 91.5 metres to 305 metres, that the optimum aspect ratio was about 16. He later reinterpreted the results (reference 32) and decided on an aspect ratio of 18 for British thermals of either parabolic or fourth power distributions. His analysis assumed a given Wortmann aerofoil section and the MacReady theory of cross-country soaring. It is likely that the MacReady theory is representative of 50% of the soaring tasks set in competitions and that it places a lower limit on the desired aspect ratio. The analysis showed that sailplane performance was more critical with weight than aspect ratio. The ballasted weight range of the Irvings' ideal sailplane should vary from as light as possible to something over 1.5 times the unballasted AUW. Eppler undertook a similar study (reference 33) for a 15 m sailplane in European type conditions and obtained similar results, calling for an aspect ratios of 16.7 to 18.

Appendix C gives the results and discusses a similar analysis for a 15 m tailless sailplane. The optimum aspect ratio is between 20 and 22 for Australian thermal conditions (same shape and size of thermal but 8 kts strength instead of the 6 kts assumed for British

thermals). In contrast to Irving and Eppler the analysis in appendix C contains the effects of "final gliding". A competition flight starts at 1000 metres and finishes at ground level. The MacReady theory optimizes for no nett height change. Therefore we can add the "final glide effect", of gliding down from 1000 metres height, at the optimum speed prescribed by the meteorological conditions, to the MacReady achieved cross-country speed. The results show that an aspect ratio of about 2 points higher than the optimum predicted by MacReady gave better performances for cross-country tasks under 500 kms length.

So far, the sailplane optimizations discussed, have not considered the use of flaps. At slow speed flaps enable smaller turn radii and therefore higher achieved rates of climb compared to an unflapped aircraft of the same aspect ratio and wing loading. Appendix C shows that an increment in the climbing lift coefficient of 0.1 gives a 3 to 11 percent improvement in cross-country performance. It is also shown that an increment in profile drag coefficient during the climb has only a tenth of the effect on cross-country performance that the same profile drag coefficient increment, during gliding, has on performance. The optimum aspect ratio of a flapped sailplane is higher than for an unflapped one because the improved climb rate allows a higher wing loading, which in this case is best achieved by an increase in aspect ratio since the straight flight, glide performance is also improved. Flaps also improve the glide performance by the use of negative deflections which shift the low drag bucket and align the parasite surfaces along the airflow direction.

As explained in appendix A the allowance of flaps in the 15 m class has resulted in the recent display of "next generation" 15 m sailplanes. The aspect ratios of these flapped aircraft varies from 20 to 22 which is lower than the current generation of unflapped aircraft, illustrating the more sophisticated trend in designing for optimum achieved cross-country speed. The design of flapped aerofoil sections for conventional sailplanes is now a well established art. The work of Wortmann and Eppler illustrate that an ordered transition from laminar to turbulent flow, for the aerofoil with deflected flap, can prevent flow separation over the flap, for a wide range of lift coefficients and flap deflections. The resultant aerofoil exhibits a shift in the C_L range of the low drag bucket without increasing the drag. The characteristics of a typical flapped aerofoil section are presented in reference 7. A family of suitable flapped aerofoils is not yet available for the tailless sailplane.

5.2 Conventional and Tailless Performance Comparison

Drawing No. TG-GA-01 is a general layout drawing of the proposed tailless glider "Ricochet". This layout is as much influenced by static and dynamic stability and control as it is by performance. It represents the final rigid body solution obtained in this thesis.

A comparison of the unflapped "Ricochet", and Standard Cirrus glide performance is given in figure 9. Glide performances of sailplanes are usually compared at equal wing loadings. This gives

them a similar climb performance. A tailless sailplane will have a lower unflapped, wing lift coefficient than a conventional sailplane and will therefore require a lower wing loading to perform the same radius of turn at the same angle of bank. Since the stalling speed combines available lift coefficient and wing loading it is used as a basis of comparison in figure 9 .

A comparison of the MacReady cross-country performance is given in figure 10. This gives a pessimistic view of the practical cross-country advantage of the tailless sailplane because firstly, it neglects the effect of the final glide and secondly, it neglects the fact that a pilot, by Dolphin flying, spends much more of his task distance in gliding than is assumed by the MacReady theory. Both these effects give an additional performance increment proportional to the difference in glide performances given in figure 9. Not too much emphasis should be placed on the performance increment, shown in figure 10, for the narrow (91.4 m. radius) thermals. The cross-country speeds can be quite low in narrow thermals and, as shown in appendix B, the effect of increasing the climbing lift coefficient by 0.1 in 91.4 m. radius, 8 kt thermals can give a 30% performance increase. Thereby indicating the sensitivity, or importance of the available lift coefficient in calculating performances for narrow thermals. The performance increment in the more common, wider thermals is thought to be realistic.

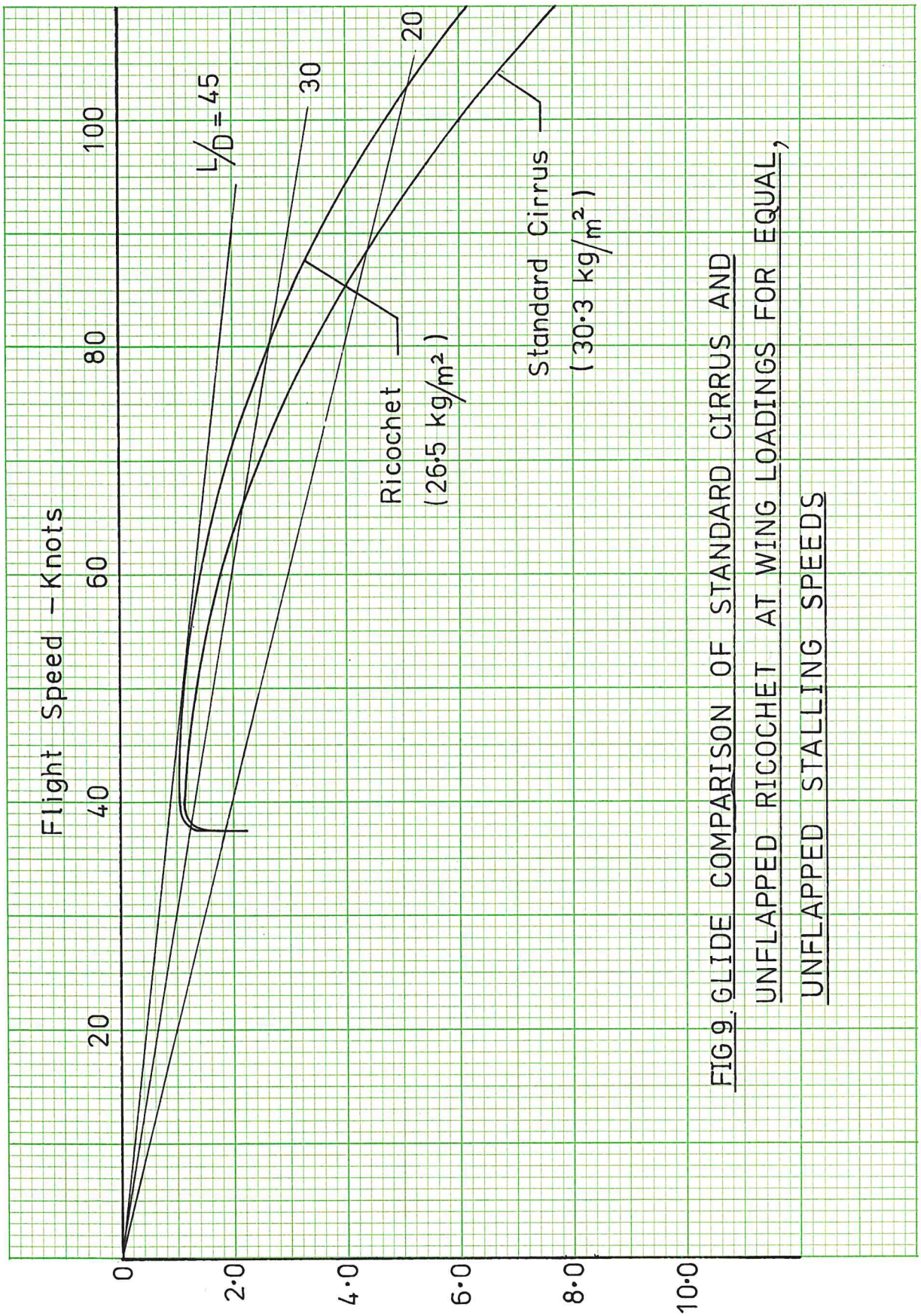

FIG 9. GLIDE COMPARISON OF STANDARD CIRRUS AND UNFLAPPED RICOCHET AT WING LOADINGS FOR EQUAL, UNFLAPPED STALLING SPEEDS

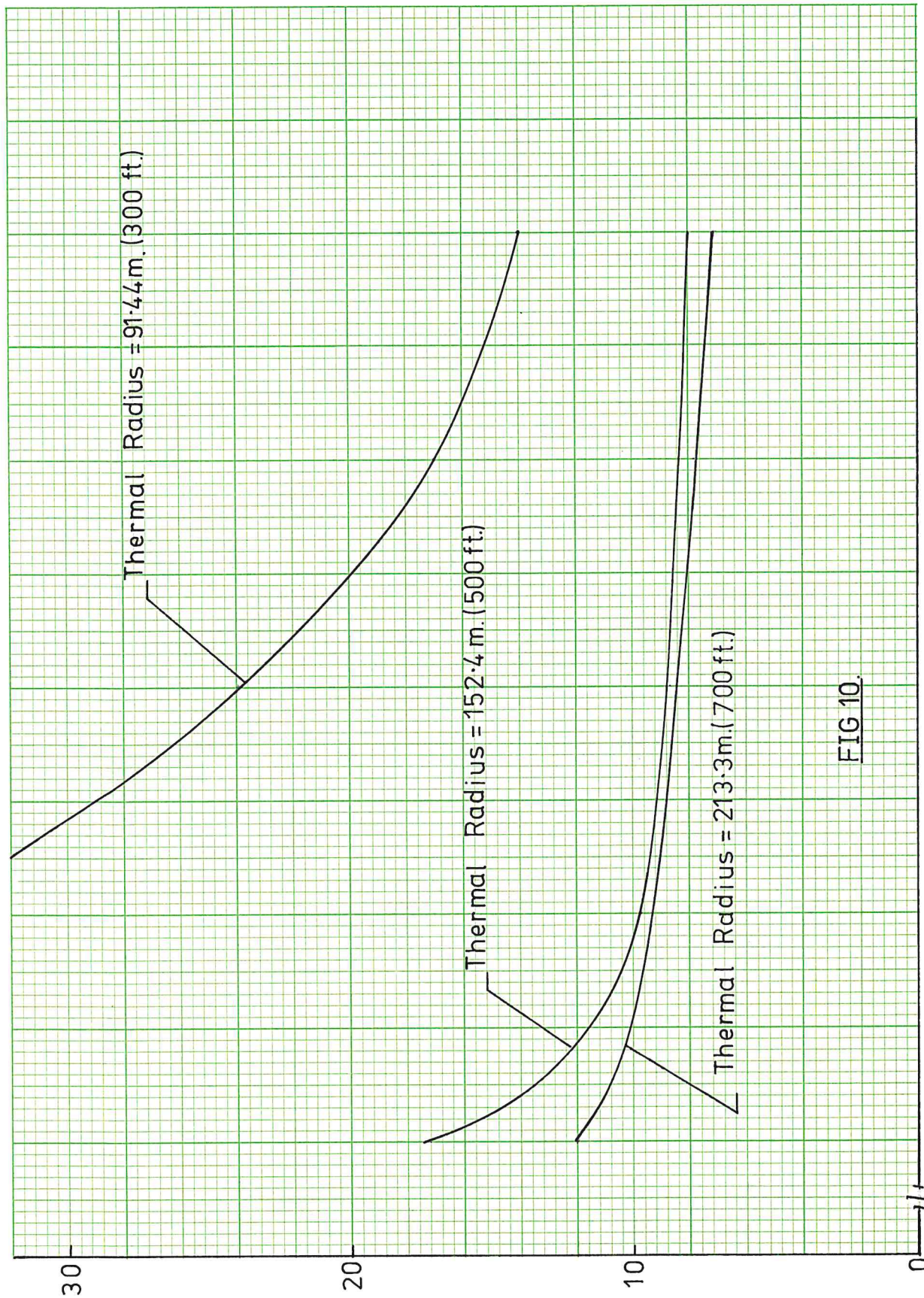
Thermal Radius = 91·44m. (300 ft.)
Thermal Radius = 152·4 m. (500 ft.)
Thermal Raddius = 213·3m. (700 ft.)
30
20
10
0
4
6
8
10
12
THERMAL STRENGTH KNOTS.
M∞ READY CROSS COUNTRY SPEED INCREMENT %

FIG 10.

6. SHAPING THE WING

The optimization of the wing planform has been very difficult, particularly when flaps are used. The selection of a suitable layout is dependent on the wing aerofoil section characteristics, and again, whether the aerofoil has flaps or not. The converse is also true as the planform can assist in determining an aerofoil specification. As pointed out previously only one, unflapped, aerofoil is at present available.

Performance considerations require us to maximize our climbing lift coefficient. It is also necessary to ensure that the wing tip does not stall first. Appendix C shows that an increase in induced drag coefficient of 1.0×10^{-3} during the climb reduces the cross-country performance by 0.5 percent but the same increase, whilst gliding, reduces the cross-country speed by 4.5 percent. To achieve the calculated performances it is still necessary to show that the assumed climbing lift coefficient of 0.95 can be obtained, and that the planform induced drag is acceptable during the glide.

A parametric investigation of the wing planform shape is contained in appendix D. Since the computer program used can only calculate fuselage effects for a mid-wing arrangement the optimization was conducted with no body at all. The use of flaps also changes the effective wing body incidence and would only confuse the optimization at this stage. In-flight spanwise airload measurements for a high aspect ratio sailplane are given in reference 42 and can be used to confirm the theoretical trends given by the computer program.

Figures 11, 12, and 13 are reproduced from the results in appendix D. It is apparent that the tapered planform, F, has much lower induced drag than the parallel wing of planform B but the latter gives a stable inboard stall, whilst the former gives an unstable tip stall. The stability contribution, C_{M_o}, from the planforms B, and F, in figures 11 and 12 is seen to be similar.

The results of appendix D can generally be summarized as;

a. Sweep between 10 and 15 degrees had a minimal effect on the C_L distribution for a given twist.

b. Twist had the greatest effect on C_L distribution.

c. Taper had an important effect on C_L distribution as well as widening the C_L range over which induced drag, for a given twist, was minimum.

d. The double tapered planforms showed no aerodynamic advantage over the rectangular tapered planforms, although in practice they allow a greater spar depth at the wing root.

e. The single straight tapered wings gave the worst aerodynamic compromise (but perhaps the best structurally).

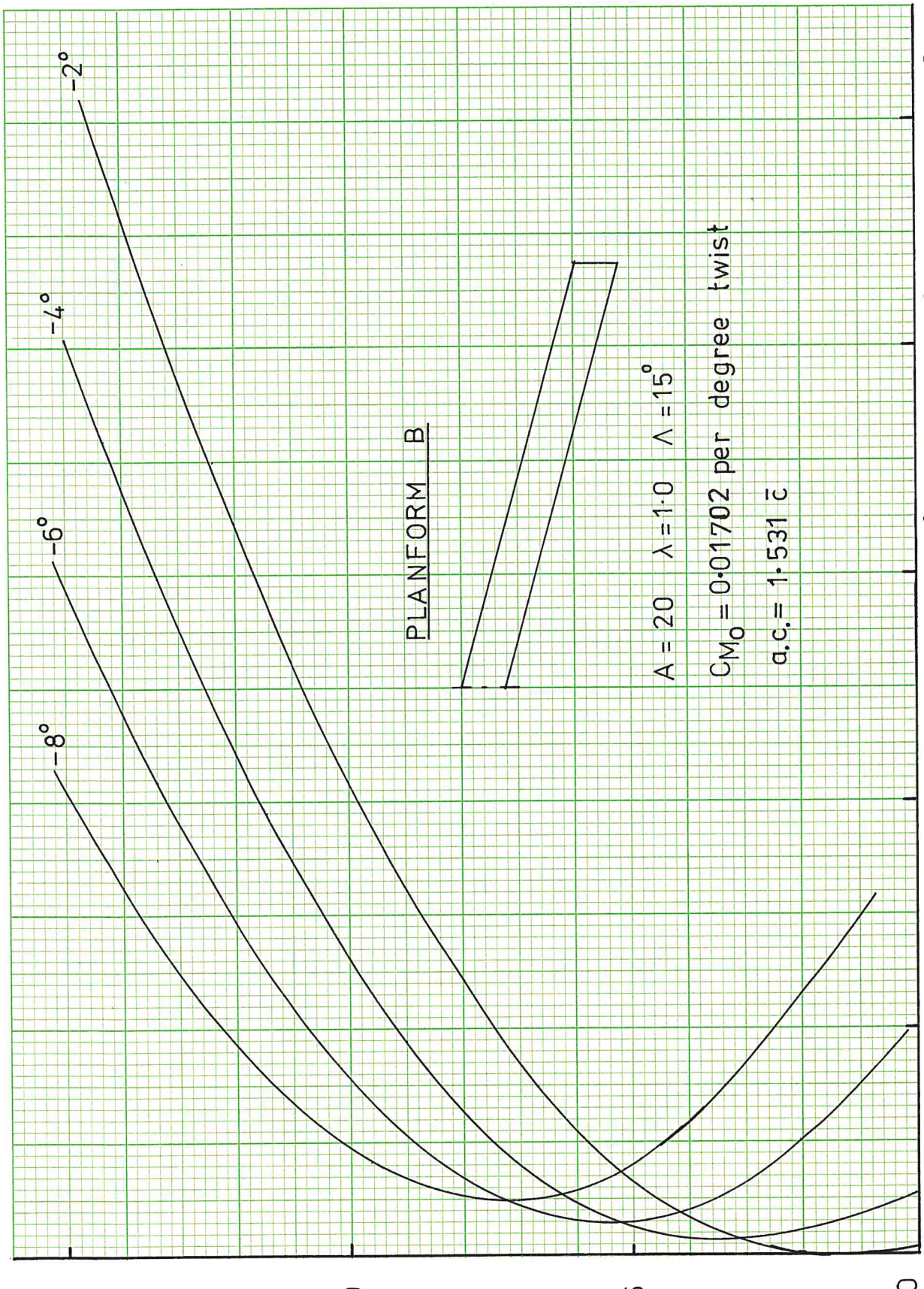
-2°
-4°
-6°
-8°
PLANFORM B
A = 20 λ = 1·0 Λ = 15°
C_{M_0} = 0·01702 per degree twist
a.c. = 1·531 c̄
C_L
1·5
1·0
0·5
0·0
0·0
1.10⁻³
2.10⁻³
3.10⁻³
4.10⁻³
5.10⁻³
ΔCD_i

FIG 11.

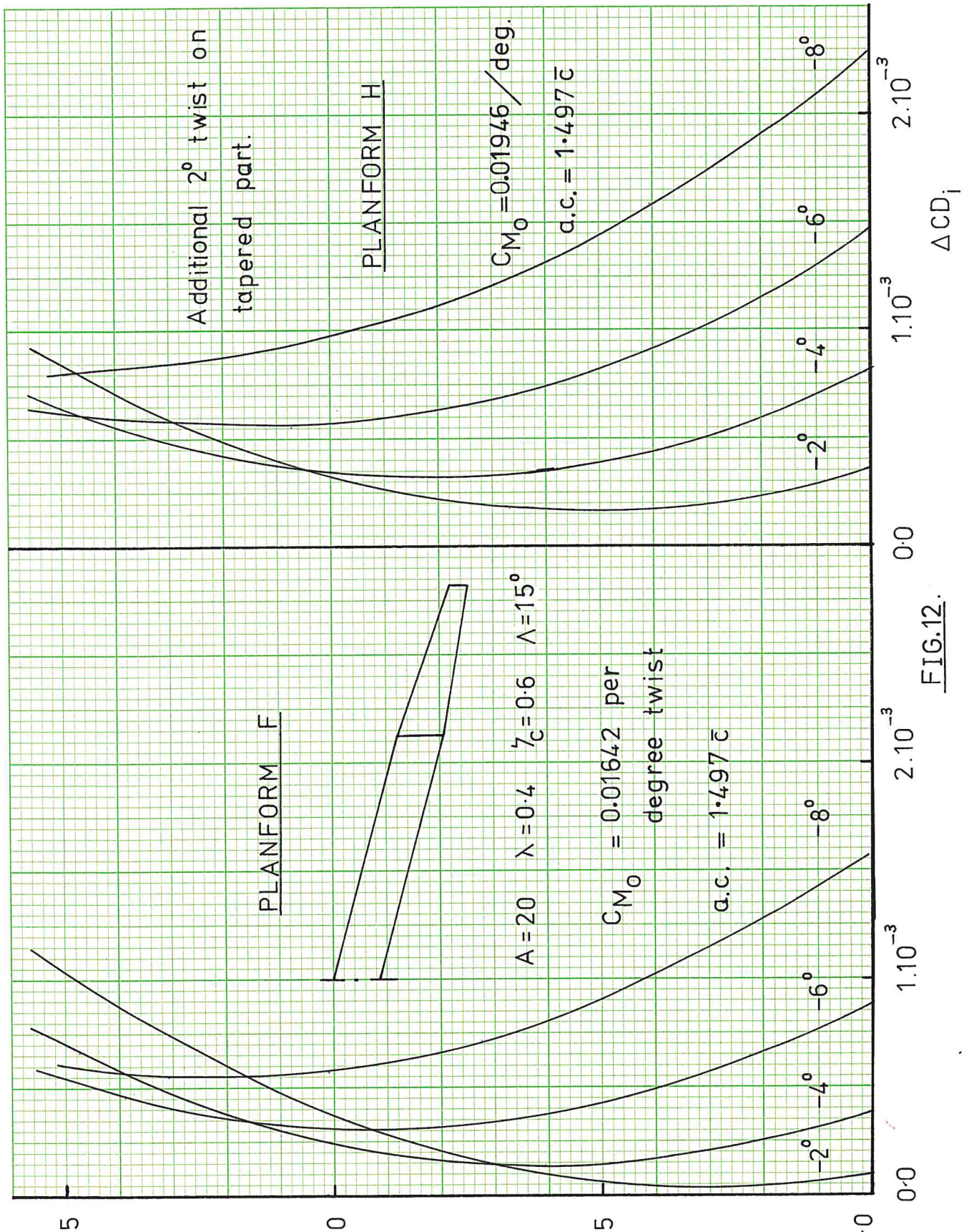
Additional 2° twist on tapered part.
PLANFORM H
C_{M_0} =0.01946/deg.
a.c. = 1·497 $\bar{c}$
-2°
-4°
-6°
-8°
PLANFORM F
A=20 λ=0·4 η_c=0·6 Λ=15°
C_{M_0} = 0.01642 per degree twist
a.c. = 1·497 $\bar{c}$
C_L
1·5
1·0
0·5
0·0
0·0
1.10^{-3}
2.10^{-3}
ΔCD_i

FIG.12.

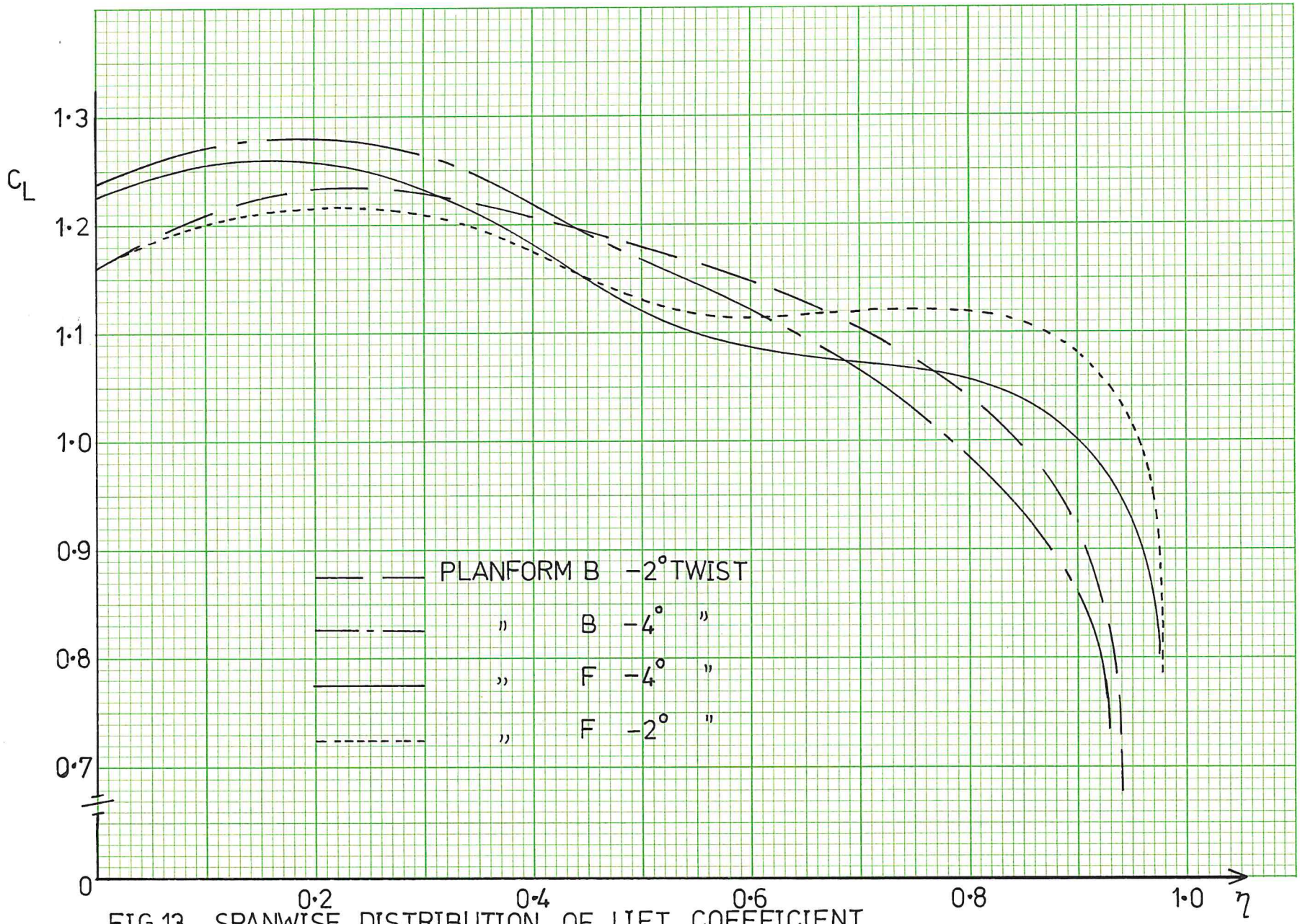

FIG 13 SPANWISE DISTRIBUTION OF LIFT COEFFICIENT

f. Although twist gave the greatest contribution to stability the effect of increasing the sweep from 10 degrees to 15 degrees was equivalent to an increase of one half of a degree in twist.

The effect of aspect ratios between 15 and 30 has little effect on the results.

6.1 Selection Procedure for the Unflapped Planform

It is best to consider the unflapped planform (DWG. TG-GA-01) in some detail because we can make considerable use of the aerofoil data in figure 4. The distribution of aerofoil sections, and total effective twist across the span is given in figure 14. The structural twist is obtained without twisting the spar, giving a total aerodynamic twist of 5 degrees. This is perhaps nearly 1 degree of (structural) twist too much for an unflapped aircraft but was chosen as a conservative initial design, allowing a good aft centre of gravity margin, whilst obtaining improved estimates of aerodynamic coefficients.

a. Wing pitching stability.

The contribution to the wing pitching moment coefficient from the aerofoil sections is,

$$\bar{c}_{mac} = -0.038$$

Although an aspect ratio of 20 was aimed for it was found that the 10 percent increase was justified by the reduction of twist allowed. The rigid wing contribution is therefore,

$$= 0.0775$$

A likely pessimistic fuselage contribution is

$$= -0.008$$

Giving, for the complete rigid aircraft,

$$C_{M_o} = 0.0315$$

From Section 10, the wing twist due to bending and torsion, at $C_L = 1.0$ and 0.2, is negligible. Its effect on stability and elevon trim curves is insignificant.

b. Elevon trim curves

The elevon angles to trim, given in figure 15, show that at the maximum C_L of 1.1 and centre of gravity aft, at 0.21 $\bar{c}$, a downward elevon deflection is obtained, giving an increase in available lift. This is unnecessary and would not have occured with the original 4 degrees washout. Since climbing at maximum lift coefficient is normally restricted to turning in thermals the elevon deflection is also a function of the aircraft spiral stability and bank angle. It is likely that

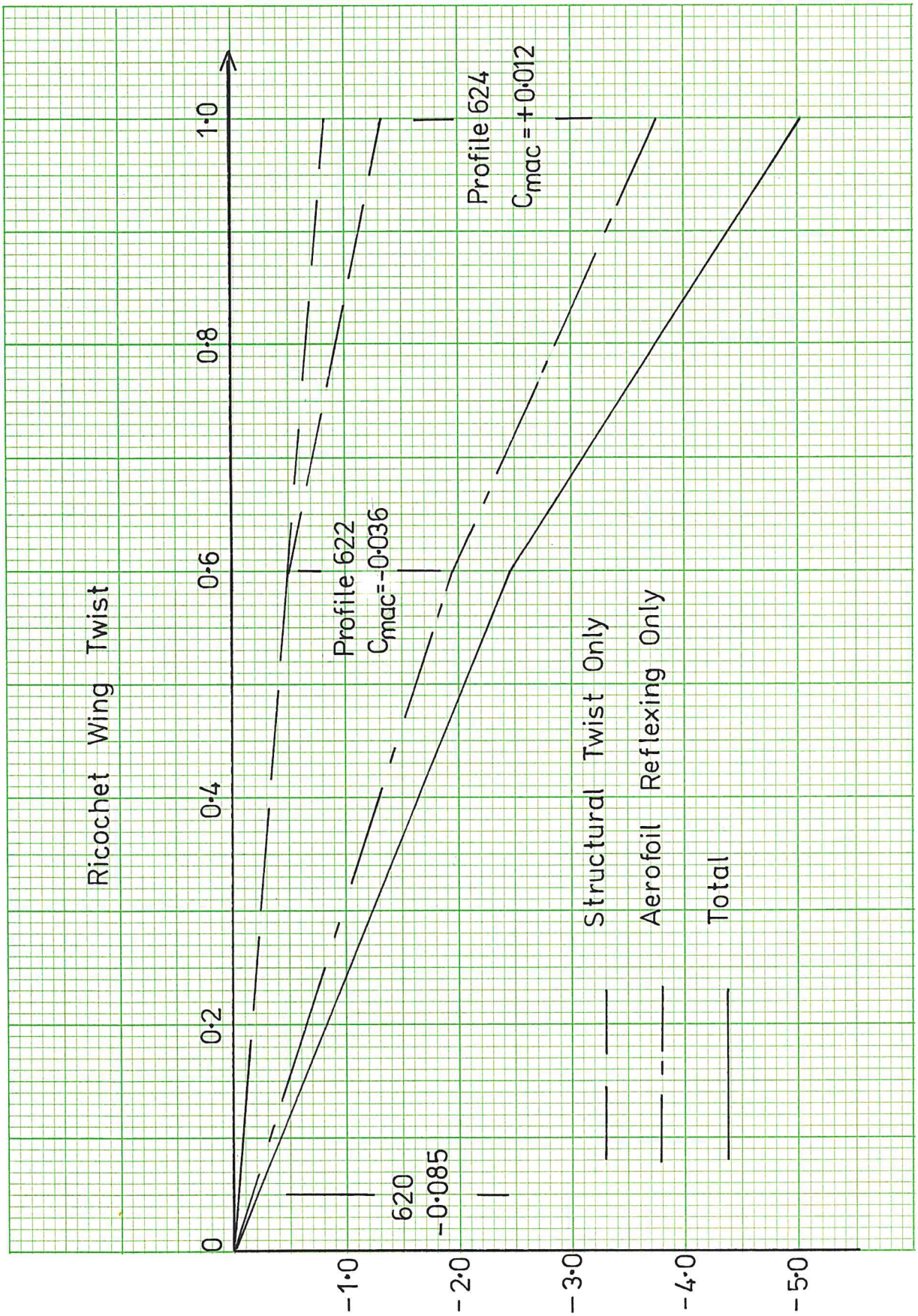

FIG 14 SPANWISE AERODYNAMIC WING TWIST DISTRIBUTION

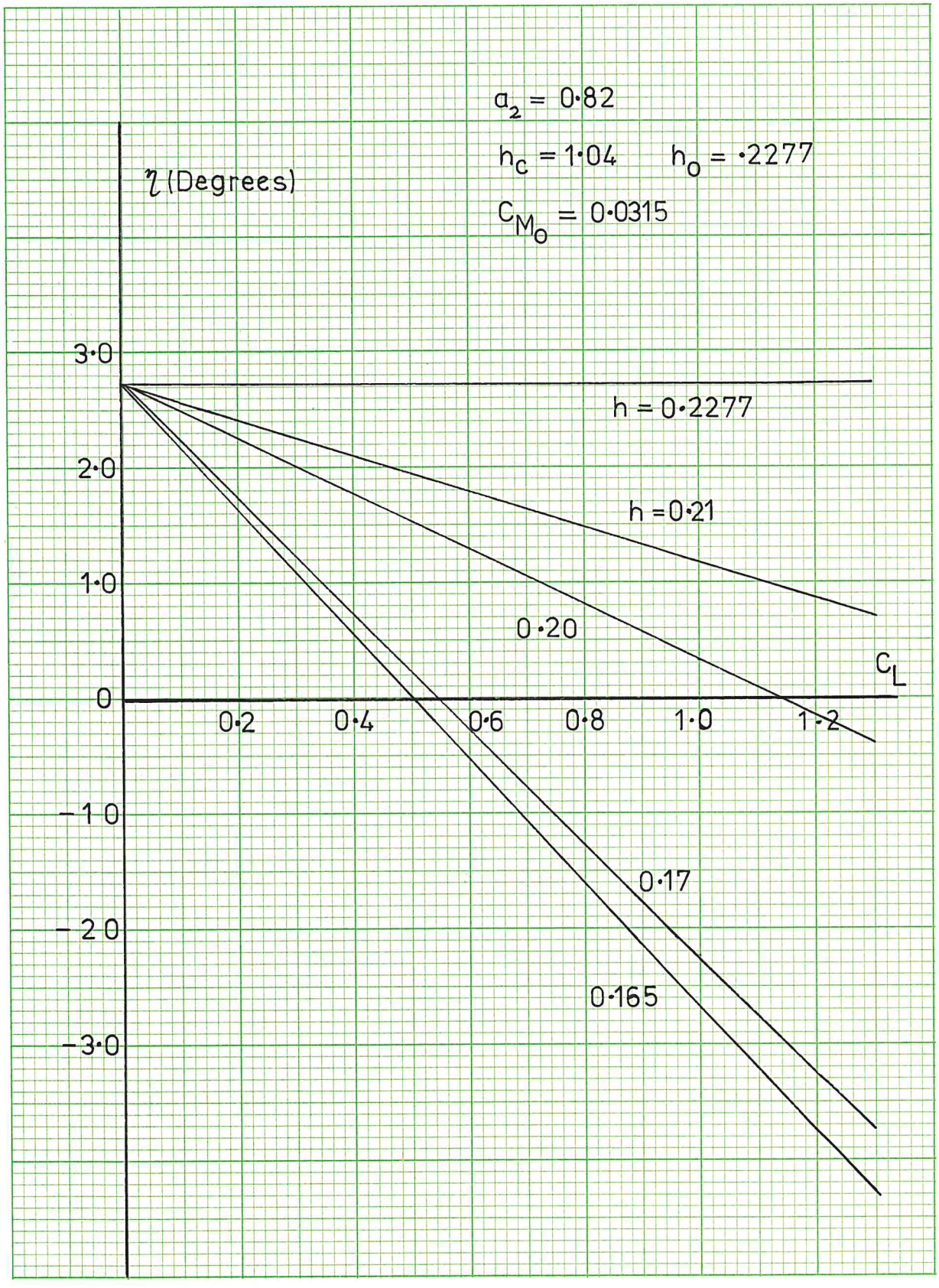

FIG 15 ELEVON TRIM CURVES FOR UNFLAPPED RICOCHET

"holding off" bank will give a downward deflection of the inboard elevon, but a further upwards deflection is required to trim the aircraft in circling flight. It is considered desirable to have a small, downward deflection of the inboard elevon during circling flight. This can be achieved with a wing twist of 4 degrees and low spiral instability. Adding one degree of up (negative) elevon deflection to the trim curves of figure 15 gives the resultant trim curves for a wing with 4 degrees twist. For example the elevon deflection at $C_L = 1.1$ and centre of gravity at 0.21 $\bar{c}$ is then zero. In both cases the aircraft should be flown at aft centre of gravity for high C_L. Inflight centre of gravity variation was originally envisaged by mounting the pilots seat on irreversable tracks, giving the pilot the capability of flying by shifting his weight. A favourable, automatic shift in centre of gravity is also obtainable from the swept wing water ballast tanks. An additional method incorporated fore-and-aft fuselage tanks, containing half a cubic foot of water which would go to the nose at high speed and to the rear at low speed. Irrespective of how a pilot shifts his position in flight it inevitably amounts to an increased workload during competition flying. That this is unacceptable is demonstrated by recent manufacturers' decisions to interconnect flap and elevator circuits on conventional sailplanes, for all flying except landing and take off. Also, from figure 15, the reduction in trim angles at low C_L is very small. It is shown later that the control deflections to trim produce favourable span-load distributions, reducing the induced drag during cruise. Also, since the design of modern flapped aerofoil sections, for sailplanes, (references 7 and 8) allows control deflections of $\pm$ 8 degrees with little or no drag increment, the small deflections calculated for the unflapped sailplane will result in no profile drag increment. Thus the elevon angles to trim are an advantage involving no trim drag. Slight modification to the outer aerofoil sections is required. The use of an inflight variable centre of gravity would therefore be more of a handicap rather than an advantage. The aircraft should be flown at aft centre of gravity for maximum performance.

c. Wing lift coefficient distributions

The wing lift coefficient distributions given in figure 16 show that all the aerofoil sections remain within their low drag range for the whole spectrum of nett lift coefficients. This is also true for the wing tips at negative lift coefficients.

The tendency for inboard stall is noticed, particularly with the body effects added. Being too conservative here can effect the cross-country performance. If the whole wing were to stall simultaneously a stable recovery is likely. The centre of gravity is forward of the aerocentre, providing the nose down pitch, and simultaneous unstalling of the whole wing when no controls are deflected, and possible tip recovery

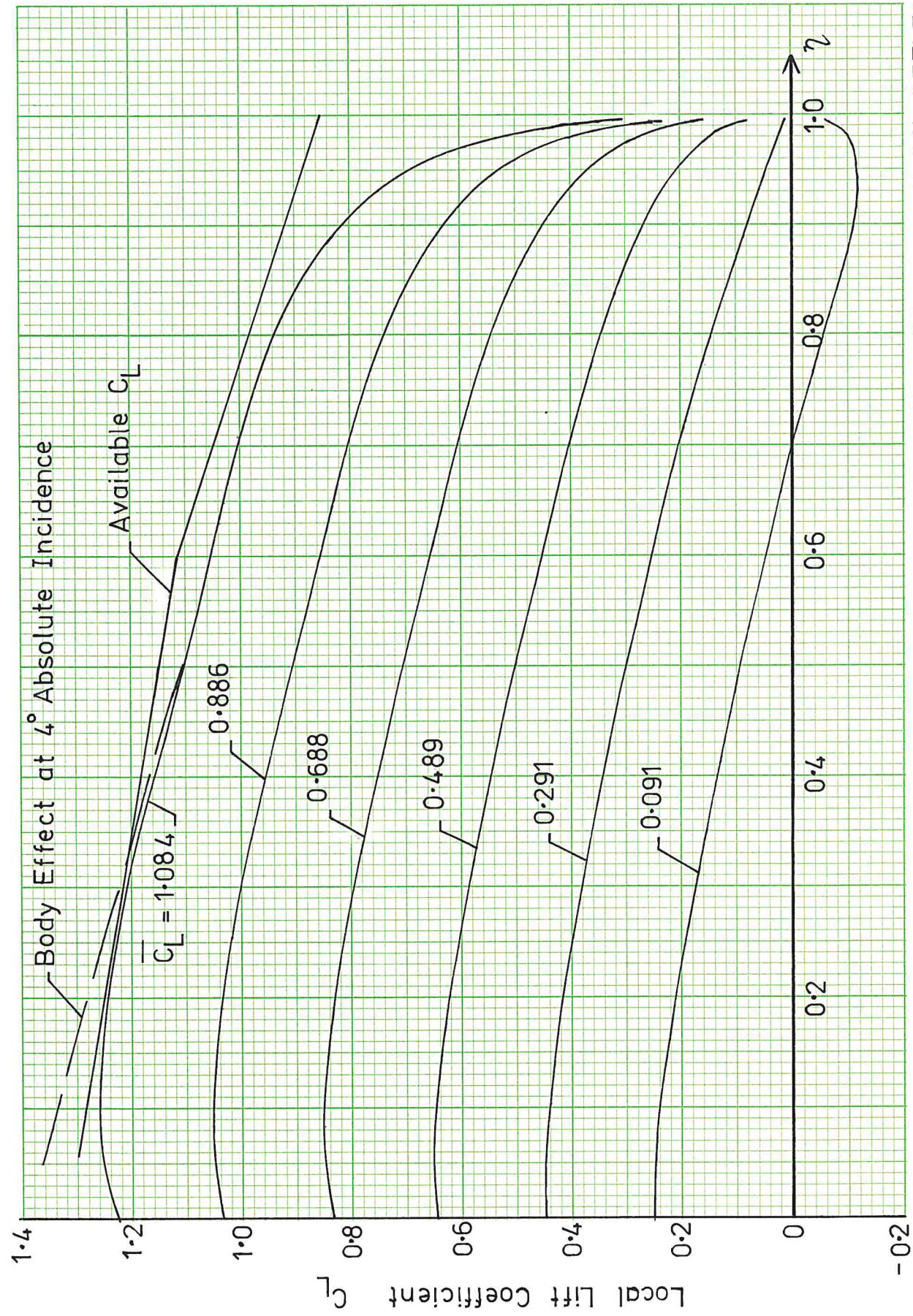

FIG 16. SPANWISE DISTRIBUTION OF LIFT COEFFICIENT WITH NO CONTROL DEFLECTIONS.

first, if down elevon, (forward stick) is applied.

The wing with only 4 degrees washout still gives stable stalling characteristics since most of the lift is due to incidence.

To reduce the tendency for boundary layer thickening the sweep has been kept to the minimum possible for the given aerofoil sections. The tip chord is higher than the optimum for induced drag at low C_L values to ease the tip stall. The same is true of the additional twist given to the tapered section of wing.

d. The induced drag

At zero lift a twisted wing has an induced drag factor of infinity. Thus, consideration of the induced drag coefficient increment, ΔC_{Di}, compared to the ideal elliptic is more useful. Figure 17 compares the Ricochet induced drag coefficient increments with the Standard Cirrus increments. The effect of elevon deflections is akin to reducing the washout at low C_L. This is illustrated by the spanwise lift coefficient distribution curves for the Ricochet, with control deflections, in figure 18. Comparisons between figures 18 and 15 show that the elevon deflections used are not associated with extreme centre of gravity locations. Aft centre of gravity appears favourable in attaining reduced induced drag at low C_L and a higher climbing C_L. Since the aircraft will be more sensitive to pitch control at aft C_L provision is made for more conventional flying qualities (see appendix B) at forward centre of gravity. The wing twist is certainly capable of reduction if the centre of gravity range is restricted to aft values.

The increments in induced drag coefficients at low C_L, given in figure 17, are much less than the consistent value of 1×10^{-3} required for a cross-country performance reduction of 4.5 percent.

6.2 Analysis of Flap Effects

The trailing edge controls shown in figure 19 are divided into three sections. The inboard flap extends from 5 to 35 percent semispan, the outboard flap from 35 to 60 percent semispan, and the elevon from 60 to 95 percent semispan. The flaps and elevon are 17.5 percent of the local chords. Downward deflection of the inboard flap gives a nose-up pitching moment, whilst downward deflection of the outboard flap gives a weaker, nose-down, pitching moment. A downwards deflection of the elevon is required to balance the aircraft and complete the full span, stepped flap effect. These effects have been estimated from the existing available data.

Reference 5 gives the increment in section pitching moment coefficient with control deflection, m_o, for aerofoils at zero degrees

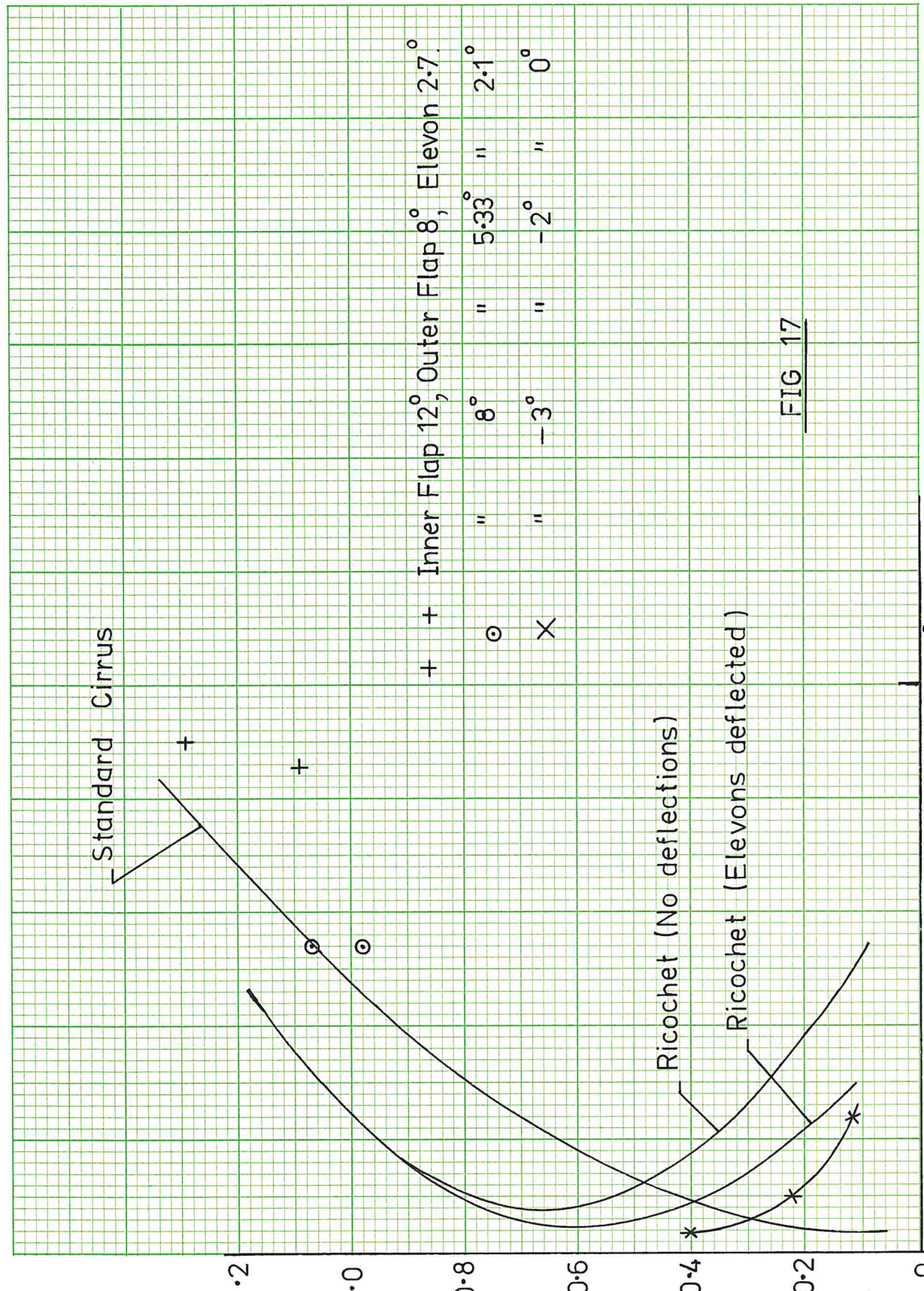
Standard Cirrus
+ + Inner Flap 12°, Outer Flap 8°, Elevon 2·7°
+ " 8° " 5·33° " 2·1°
⊙ " 3° " −2° " 0°
× " −3° " −2° " 0°
Ricochet (No deflections)
Ricochet (Elevons deflected)
C_L
1·2
1·0
0·8
0·6
0·4
0·2
0
1
1×10^{-3}
ΔC_{D_i}

FIG 17

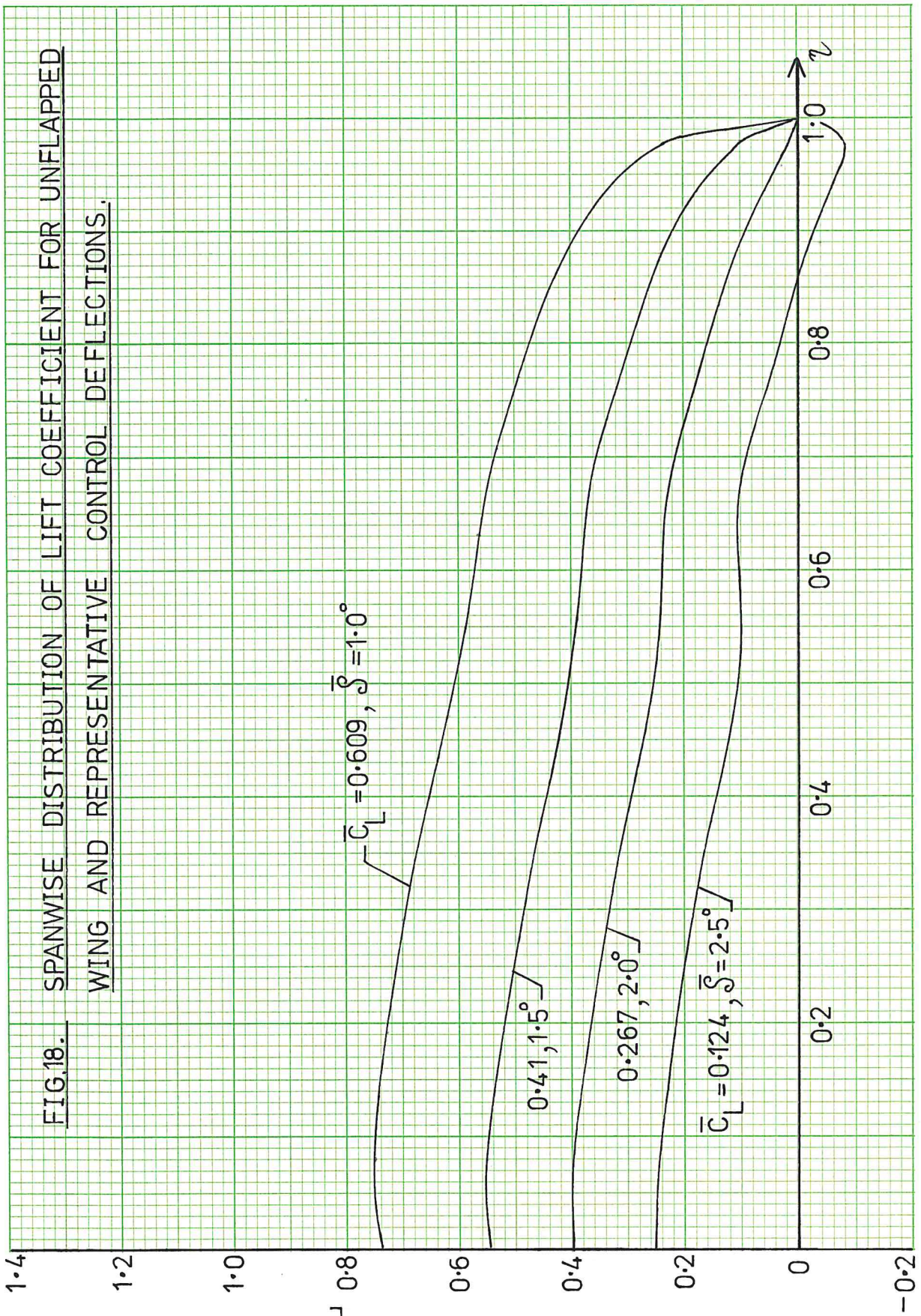

FIG.18. SPANWISE DISTRIBUTION OF LIFT COEFFICIENT FOR UNFLAPPED WING AND REPRESENTATIVE CONTROL DEFLECTIONS.

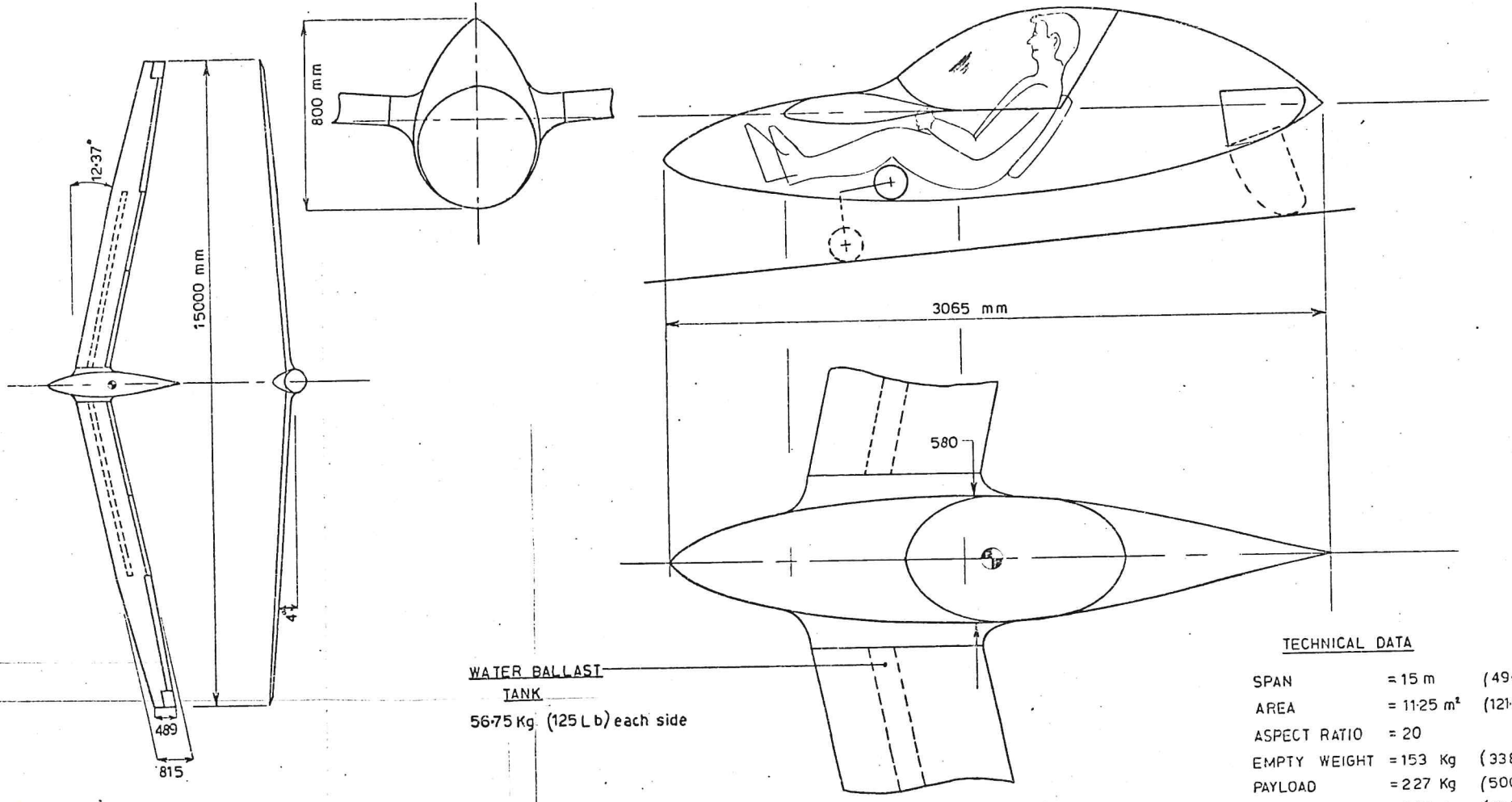

TECHNICAL DATA

SPAN	= 15 m	(49·2 ft)
AREA	= 11·25 m²	(121·1 ft²)
ASPECT RATIO	= 20	
EMPTY WEIGHT	= 153 Kg	(338 Lb)
PAYLOAD	= 227 Kg	(500 Lb)
ALL UP WEIGHT	= 380 Kg	(838 Lb)

FIG 19

DRAWN	CHK	APP'D	SCALE	TITLE:-
E.J. BUCHANAN			1/10	PRELIMINARY LAYOUT

COLLEGE OF AERONAUTICS
CRANFIELD INSTITUTE OF TECHNOLOGY
CRANFIELD.

DRAWING No.

SHT 1 OF 1 SHEETS

incidence. This is plotted in figure 20a. for representative controls, and compared with actual aerofoil data from two cambered sections.

In using the computer program (appendix D) to determine the span-wise lift distribution and wing pitching moment contribution due to a control deflection it is necssary to use an effective local angle of attack over the control span. This is given by,

$$\alpha_{eff} = \left(\frac{a_2}{a_1}\right) \delta \quad ,$$

where, a_2 and a_1 are two-dimensional lift curve slopes for control and wing respectively. The lift contribution due to control deflection (section rotation) is therefore assumed to act at the local aerodynamic centre. The pitching moment coefficient per unit control deflection, about the wing aerodynamic centre can therefore be determined. This is given in figure 20b. for the planform and flaps given in figure 19, for various flap chords. A combination of the values of figure 20a. and 20b. give the nett piting moment about the wing aero-centre due to a control deflection. This is presented in figure 21 for various flap chords and for the Ricochet 17.5 percent flap chord. The difference in values assumed for flap effectiveness at high and low lift coefficients is due to the difference in $\frac{a_2}{a_1}$ and m_o for different lift coefficients and direction of control rotation. This can be verified from typical section data. At low C_L the flap deflections are negative and vice versa. It is considered pessimistic to use

$$\frac{a_2}{a_1} = 0.34 \quad , \quad \text{for positive deflections}$$

at high C_L, and

$$\frac{a_2}{a_1} = 0.45 \quad , \quad \text{for negative deflections}$$

at low C_L.

By programing the outboard flap deflection to be half the inboard deflection we can obtain the nett elevon deflections, required for trim, given in table 1, for the centre of gravity at 0.21 $\bar{c}$.

C_L	Inboard Deflection	Outboard Deflection	ΔC_m	Elevon Deflection
1.2	12°	8°	0.0415 - 0.0206 = 0.0209	2.7°
1.2	8°	5.33°	0.0276 - 0.0137 = 0.014	2.1°
0.2	-3°	-2°	-0.0167 + 0.0052 = -0.0115	1°

Table 1

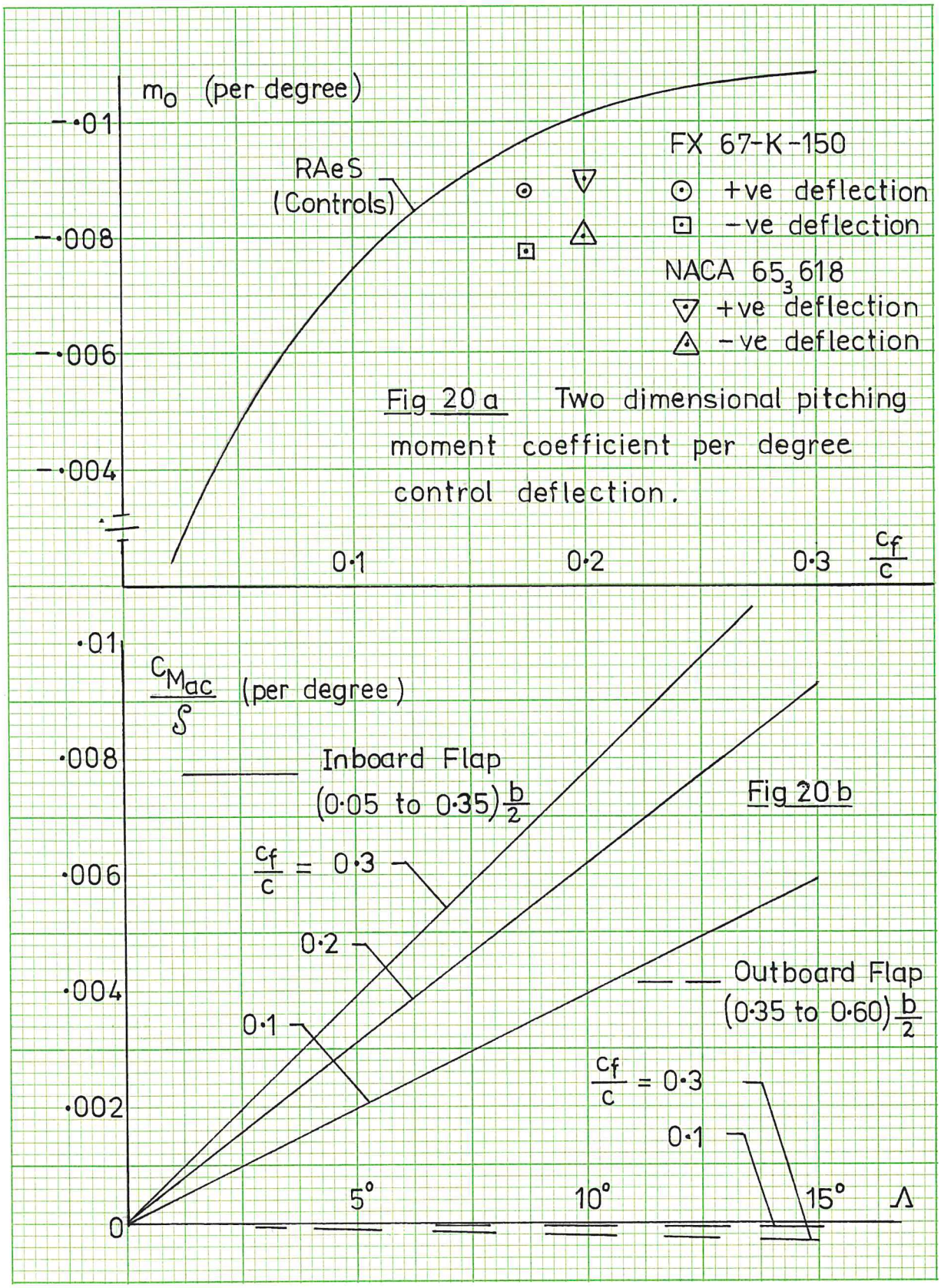
m_o (per degree)
-·01
-·008
-·006
-·004
RAeS
(Controls)
FX 67-K-150
+ve deflection
-ve deflection
NACA 65$_3$ 618
+ve deflection
-ve deflection
Fig 20 a Two dimensional pitching moment coefficient per degree control deflection.
0·1
0·2
0·3
$\frac{c_f}{c}$
·01
$\frac{C_{Mac}}{S}$ (per degree)
·008
·006
·004
·002
0
Inboard Flap
(0·05 to 0·35) $\frac{b}{2}$
$\frac{c_f}{c}$ = 0·3
0·2
0·1
Fig 20 b
Outboard Flap
(0·35 to 0·60) $\frac{b}{2}$
$\frac{c_f}{c}$ = 0·3
0·1
5°
10°
15°
Λ

FIG 20.

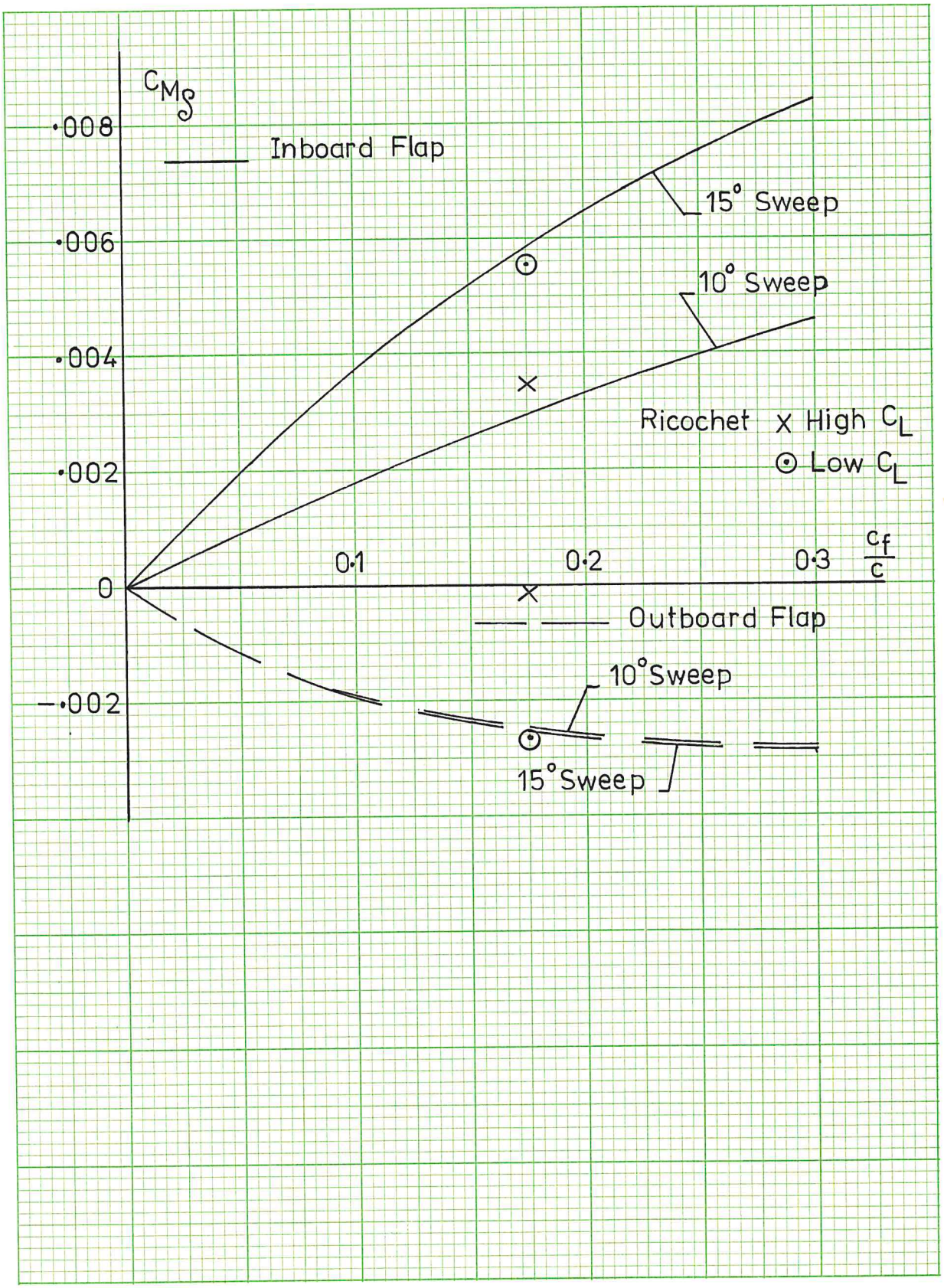

FIG 21. NETT PITCHING MOMENT COEFFICIENTS DUE TO FLAP DEFLECTIONS.

The corresponding distributions of lift coefficient are given in figure 22 and the effect on induced drag is given on figure 17.

The increment in maximum lift coefficient is perhaps not as great as is possible for a conventional sailplane but still gives us an increase in performance. The true value of flaps is to allow an aerofoil design of much narrower drag bucket and correspondingly reduced minimum drag. The flaps shift this drag bucket to the desired operating C_L range, without increasing the minimum profile drag. As with conventional sailplanes this should give the tailless another 10% performance increment.

Further improvement of the flapped wing would be possible by using a spanwise variation of flap chord and eliminating the flap chord and deflection discontinuities. The root section could use a 25 percent flap chord and the tip section, a 15 percent flap chord.

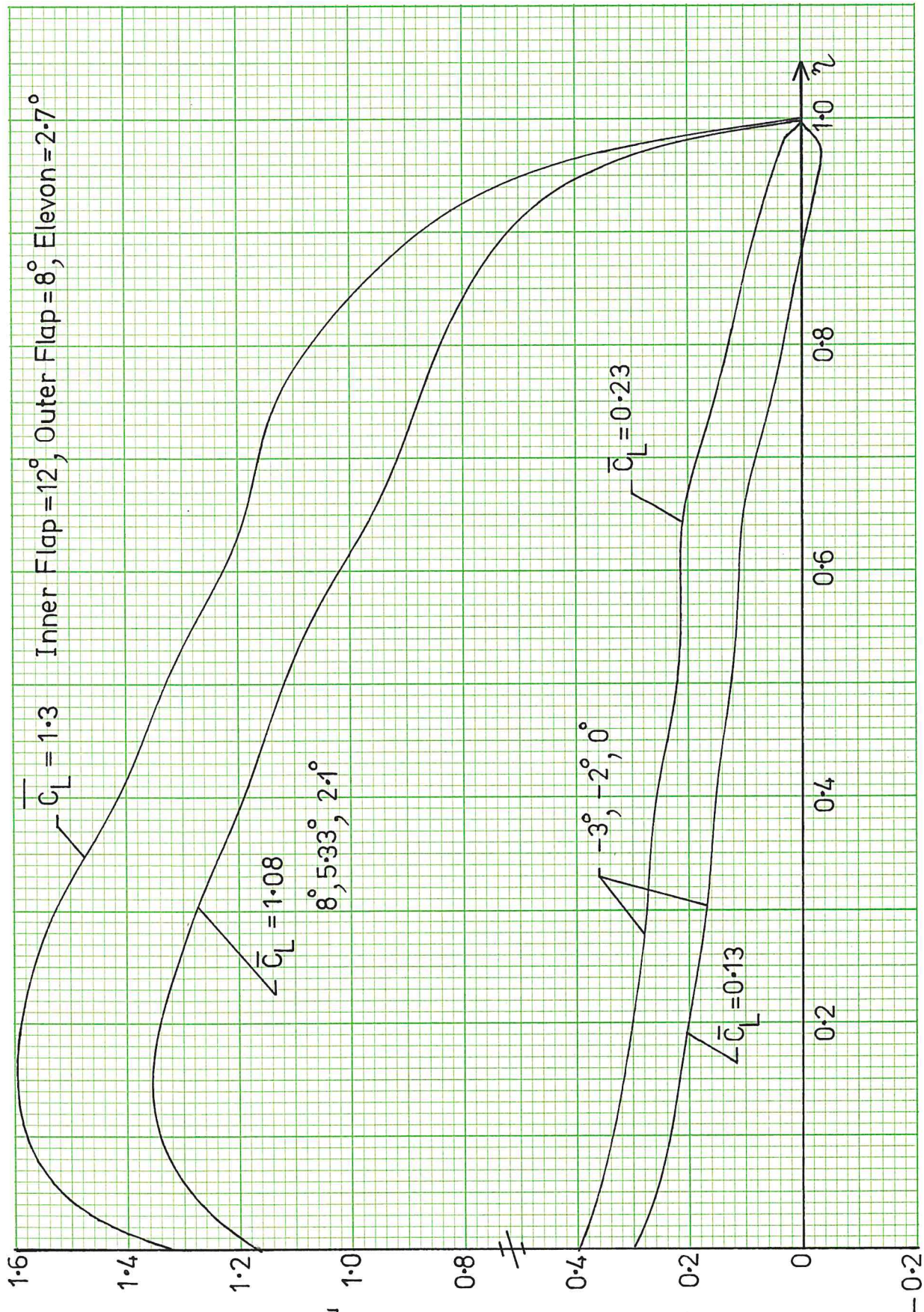

FIG 22. SPANWISE LIFT COEFFICIENT DISTRIBUTIONS FOR FLAPPED PLANFORM

7. LONGITUDINAL DYNAMIC STABILITY AND CONTROL

Reference 43 gives a basic computer program to predict the longitudinal and lateral stability and control of conventional aircraft. The program was firstly modified to predict the characteristics of aircraft with aspect ratios greater than 12. The analysis of the Standard Cirrus sailplane was then carried out and some inflight checks were made on the results. The program was then modified to cope with tailless aircraft.

In this section the longitudinal dynamic stability and control of the rigid sailplane is investigated. A complete analysis and specification of the proposed tailless sailplane, including non-dimensional aerodynamic derivates, is given in section 9.

7.1 Modifications to the Program

a. Lift-curve slope

The program underestimated the lift curve slope for high aspect ratio wings. The values obtained from the Multhopp program in appendix D were used. This is important for the tailless sailplane because it provides a major contribution to the short period damping coefficient.

b. Rate of change of downwash with incidence

The formula,

$$\varepsilon = \frac{2K\, C_{L_W}}{\pi A} \quad ,$$

given in reference 45, gave better agreement with published values of $\frac{d\varepsilon}{d\alpha}$ for sailplanes, than any other formula. The computer program gave a considerable over-estimate.

c. Aircraft response to pitching manoeuvres

Appendix E contains the derivation and solution of the full equations of motion for conventional and tailless aircraft in pitch. Two forms of elevator application have been considered. The instantaneous application of elevator (elevon) allows an investigation of the aircraft "heave" response. The results have been checked against the solution for the Baynes tailless glider (reference 46) and the VC 10 (reference 47). The second solution is for an unchecked exponential elevator (elevon) application. The elevator application rate, K, was determined by considering the time taken to achieve a given climbing pitch angle, during an abrupt "pull up" from cruising flight to thermalling flight. A program was devised and included as a subroutine of the basic program.

d. Force and moment due to pitching

These less familiar terms are important for tailless aircraft and are derived in appendix E. Besides being used in the pitching manoeuvre response equations they are formulated also as aerodynamic derivatives for the dynamic stability equations. The variation of the moment term with aspect ratio, sweep and centre of gravity is shown in figure 23.

e. Moments of inertia

The program predictions of moments of inertia for the conventional and tailless glider were very poor and therefore had to be calculated.

f. Elevator power

The terms a_2 and $(h_c - h_o)$ for the tailless aircraft have been derived in appendix B. $(h_c - h_o)$ was finally determined by using the spanload distribution program given in appendix D.

7.2 Short Period Oscillation

The short period oscillation characteristics, that is the natural frequency and damping, together with the control system dynamics and sensitivity to gusts, define the short term response to control inputs and to gusts, and therefore have a large influence on a pilot's views of the handling qualities of an aircraft. The results of an investigation of the effects of these characteristics is shown in figure 24. Variations of the pitching moment coefficient due to pitching, m_q, between -1.6 and -0.4, and of pitching inertia coefficients between 100 and 175 are investigated for two centre of gravity ranges and for high and low speed. The axes used in figure 24 are the same axes on which pilot opinion ratings are plotted. Therefore direct comparison can be made with opinion ratings contained in references 48 and 49 for example. There appears to be no problem with the slow speed characteristics. The high speed (135 kts), forward centre of gravity characteristics indicate very fast, over sensitive controls, with a risk of pilot induced oscillations. Conventional high performance sailplanes also approach these characteristics when flown at their extreme flight boundaries. However, appendix B illustrates the severe changes in stick travel and force per 'g' that can be expected with large centre of gravity ranges on a tailless sailplane. The high frequency short period oscillation characteristics are therefore best avoided (for the time being at least) by keeping the forward static margin for the tailless aircraft below 8 percent SMC.

Figure 25 compares the short period oscillation characteristics of the Ricochet sailplane, given in drawing TG-GA-01, with the Standard Cirrus sailplane. The speeds for comparison are the same and the centre of gravity ranges are the extremes, being at 21 and 16.5 percent SMC for the tailless. Water ballast has a small effect on the boundaries given in figure 25. By comparison with reference 48 the tailless characteristics appear the better of the two. The exponential characteristics still have a high rating.

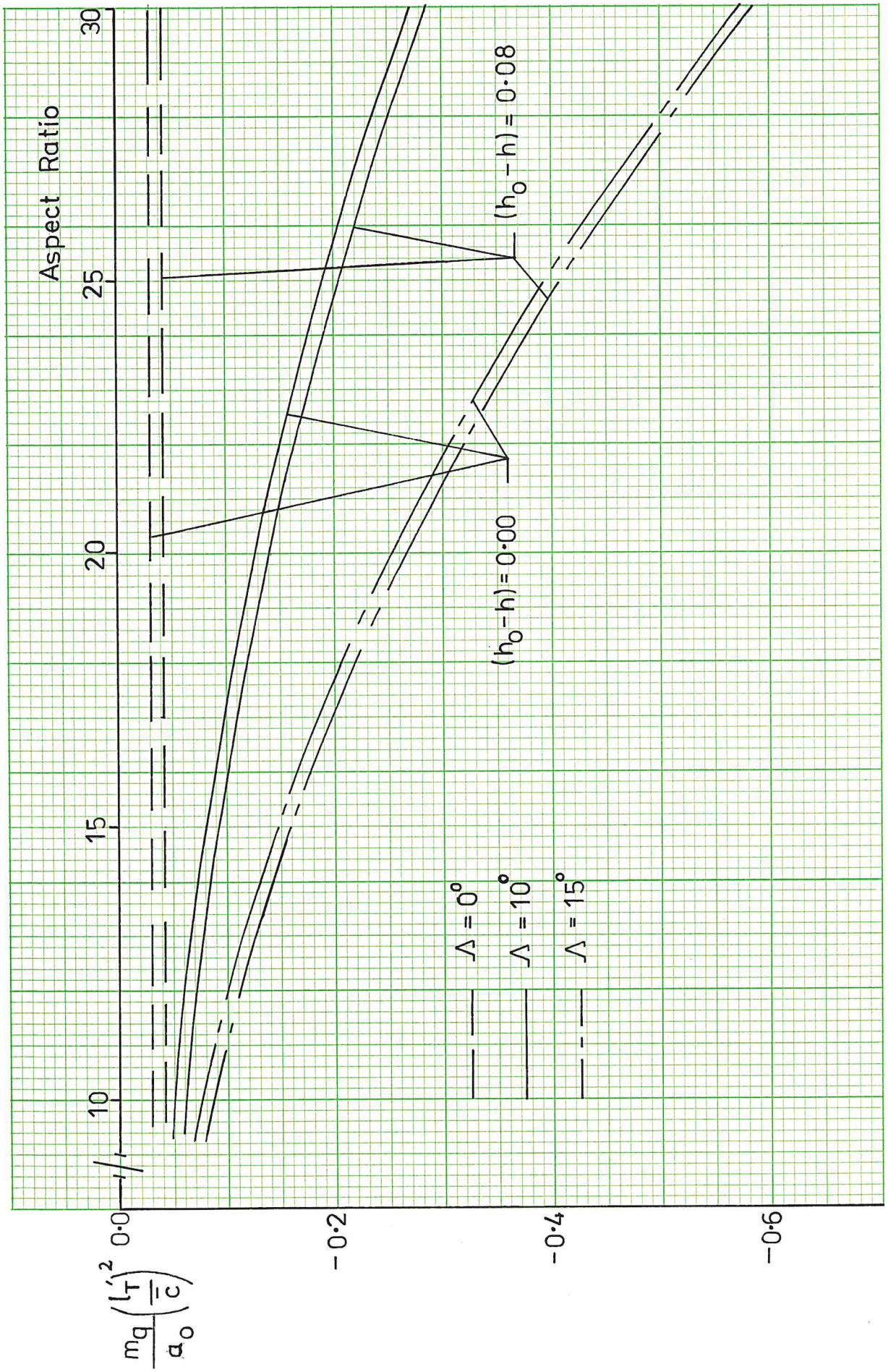

FIG 23. PITCHING MOMENT DERIVATIVE DUE TO PITCH FOR WING ALONE

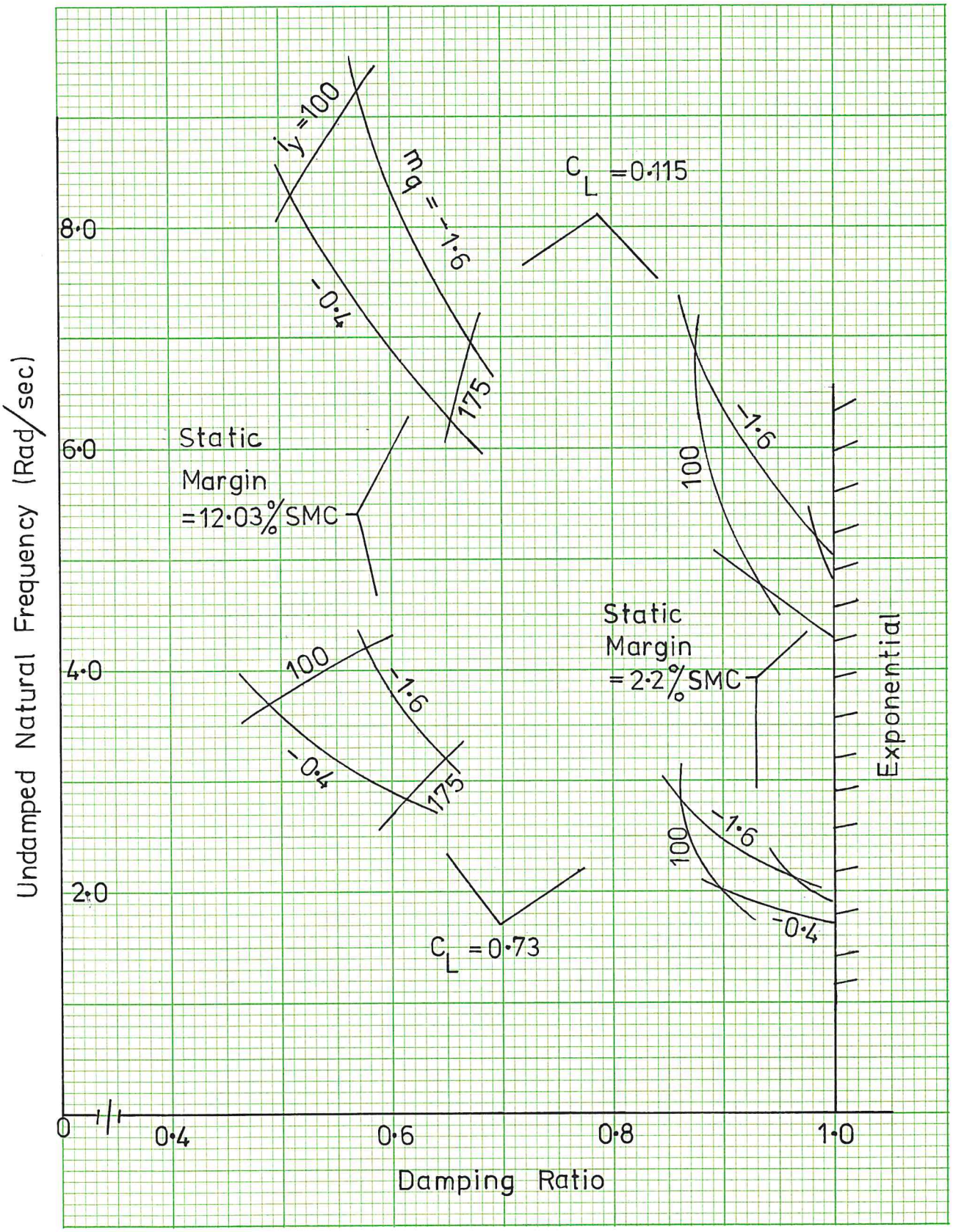

FIG 24. SHORT PERIOD OSCILLATION PARAMETRIC STUDY

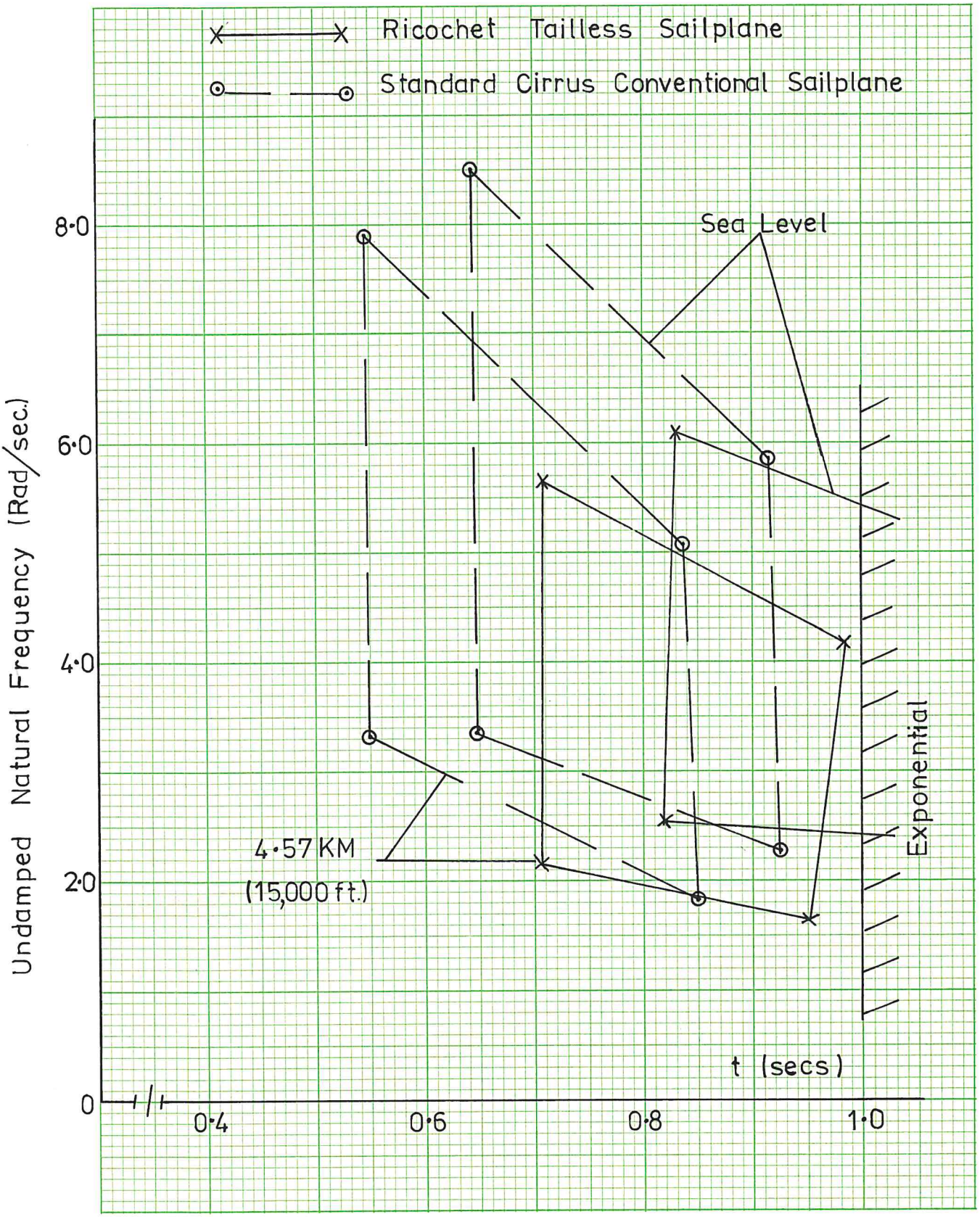

FIG. 25. COMPARISON OF SHORT PERIOD OSCILLATION CHARACTERISTICS OF STANDARD CIRRUS AND RICOCHET SAILPLANES WITHOUT WATER BALLAST.

7.3 Phugoid Motion

The continuous use of the controls by a sailplane pilot would suggest that the phugoid motion is not as critical to pilot opinion as for most other classes of aircraft. The time to double or halve amplitude, rather than damping ratio, is still the most significant handling parameter. A parametric study of the phugoid motion, using the same values as for the short period motion given in figure 24, showed that the pitching inertia had an almost negligible affect and that low values of the static margin and m_q were the most detrimental. The times to double or halve amplitude for all cases considered, remained within acceptable limits.

A comparison of the phugoid characteristics of the Standard Cirrus and Ricochet aircraft is given in figure 26. The shortest time to double amplitude is 17.5 seconds and occurs at slow speed (1.2 V_S), and forward centre of gravity. Reference 48 suggests that the time to double amplitude should be greater than 17 secs and the time to halve amplitude not less than 35 secs for satisfactory handling characteristics. Both these criteria are satisfied.

7.4 Response to Instantaneous Application of Pitch Control

Figure 27 gives a comparison of the normal acceleration increment per unit control deflection for the Standard Cirrus and Ricochet Sailplanes. Although the elevon control is the most effective its full deflection response is limited by its use as an aileron. The most favourable method of pitch control for the flapped tailless aircraft is the inboard flap segment. Optimum dolphin soaring could be achieved by flying on the flaps alone. "Pull ups", to slow speed, are achieved by downward flap deflections which increases the available C_L maximum and allows a further speed reduction. The reverse is true for high speed flight as the flap deflections tend to decrease the wing twist and nose up moment. Figure 28 gives the same comparison at a speed of 118 kts instead of 47.1 kts.

It is apparent that the heave response of the proposed tailless aircraft is negligible.

7.5 Response to Exponential Application of Pitch Control

A sailplane pilot is interested in achieving a certain nose up climbing attitude during a pull up manoeuvre. Figure 29 compares the pitch attitudes obtained per elevator/elevon deflection for the Cirrus and Ricochet at 47 kts and using a response factor, K, of 5.0. The comparison in figure 30 for 118 kts uses a slower response factor of 2.0 as could be expected in practice. Again the elevon control has sufficient reserve in case a loss of efficiency occurs in practice.

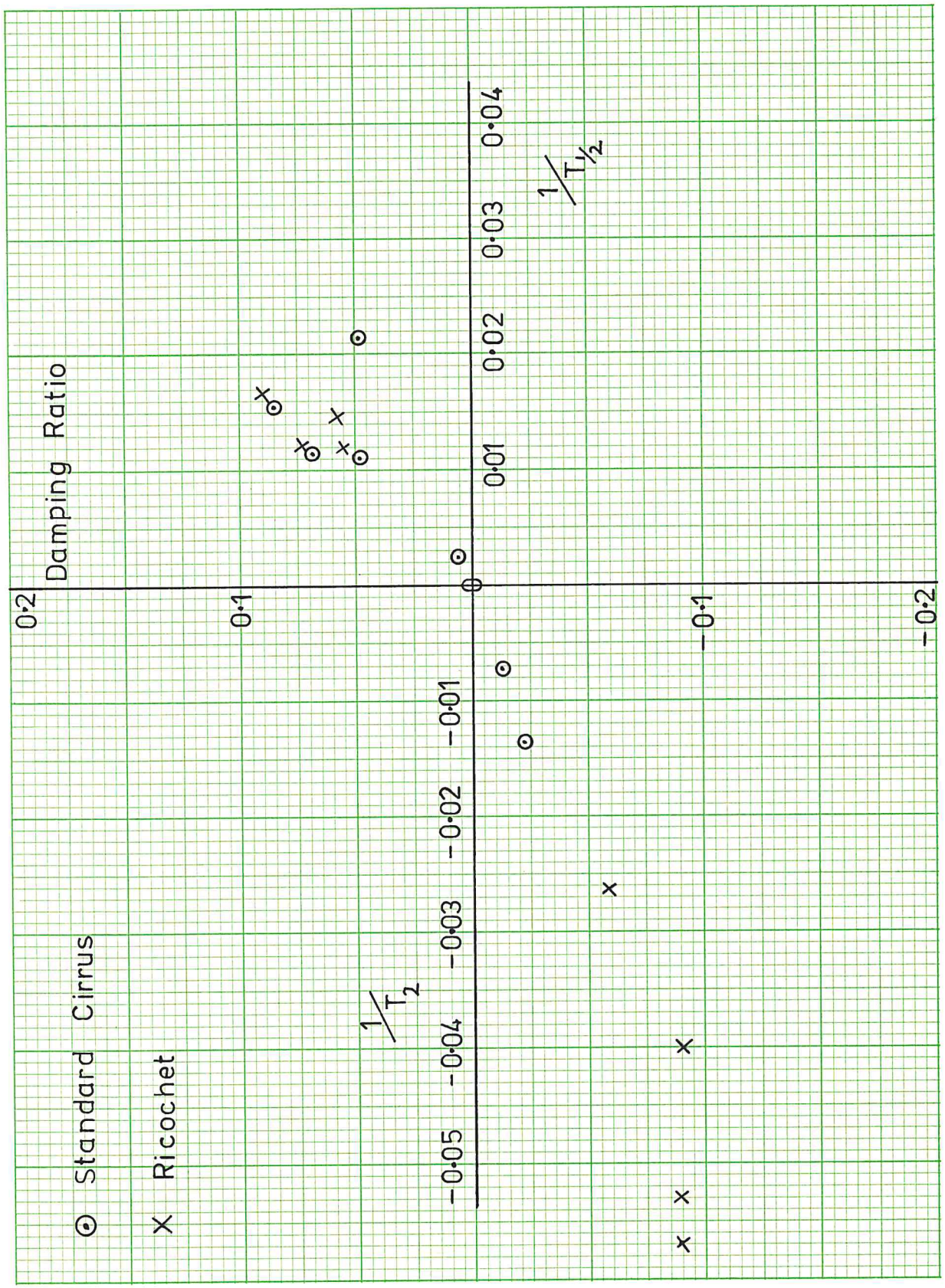

FIG.26. PHUGOID CHARACTERISTICS

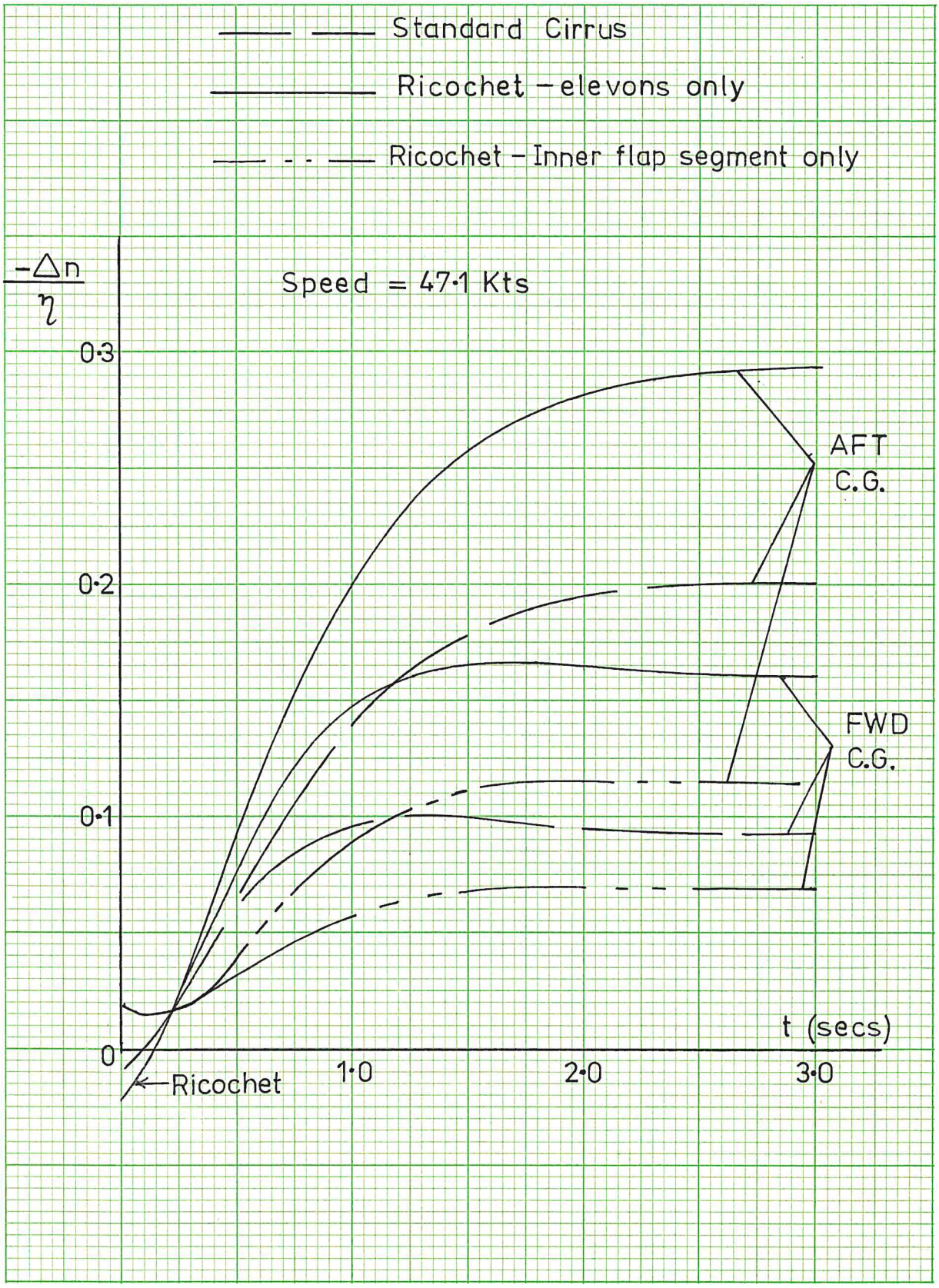

FIG 27. COMPARISON OF RESPONSE TO INSTANTANEOUS APPLICATION OF PITCH CONTROL (No Ballast)

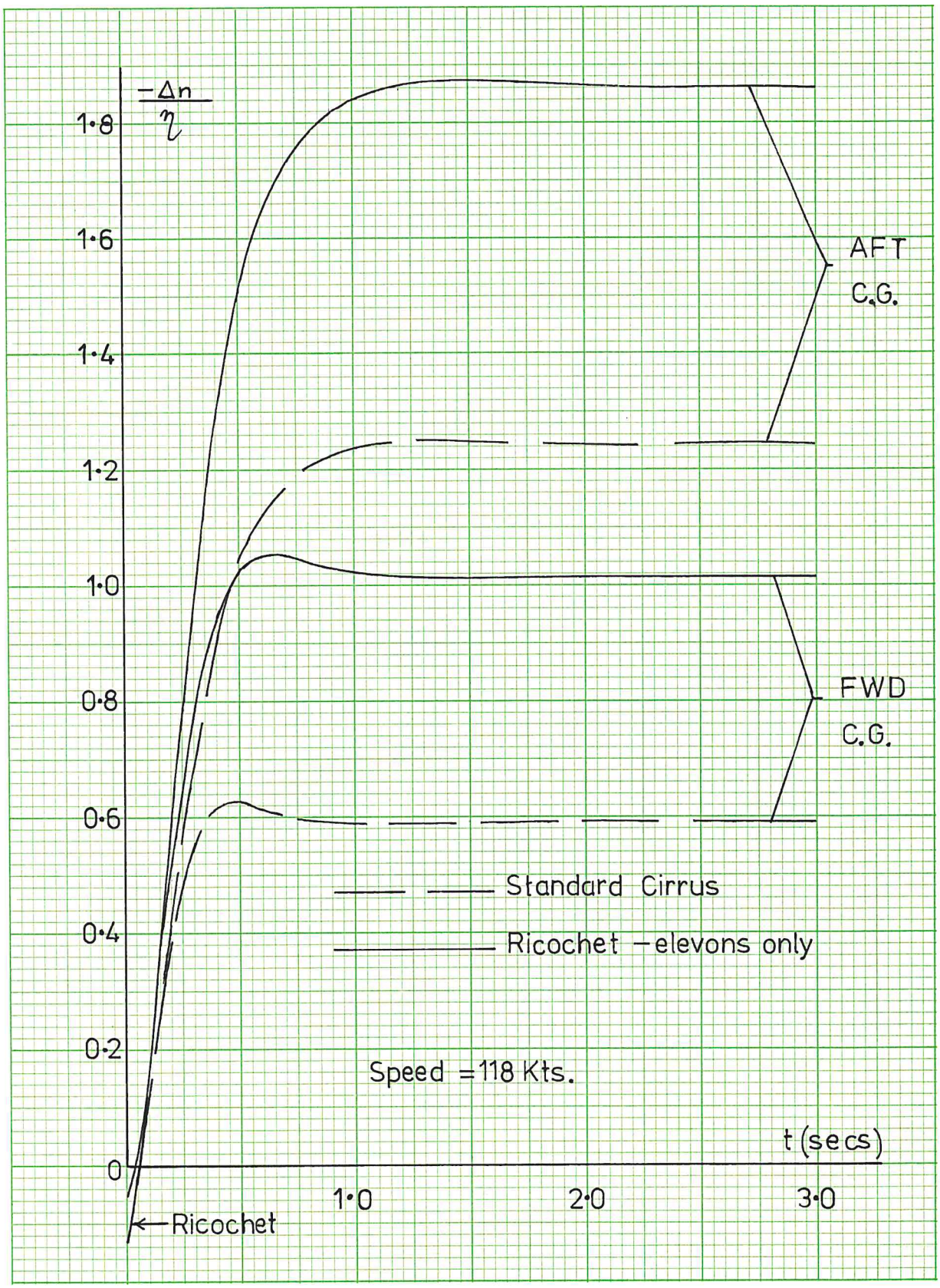

FIG 28. COMPARISON OF RESPONSE TO INSTANTANEOUS APPLICATION OF PITCH CONTROL (No Ballast)

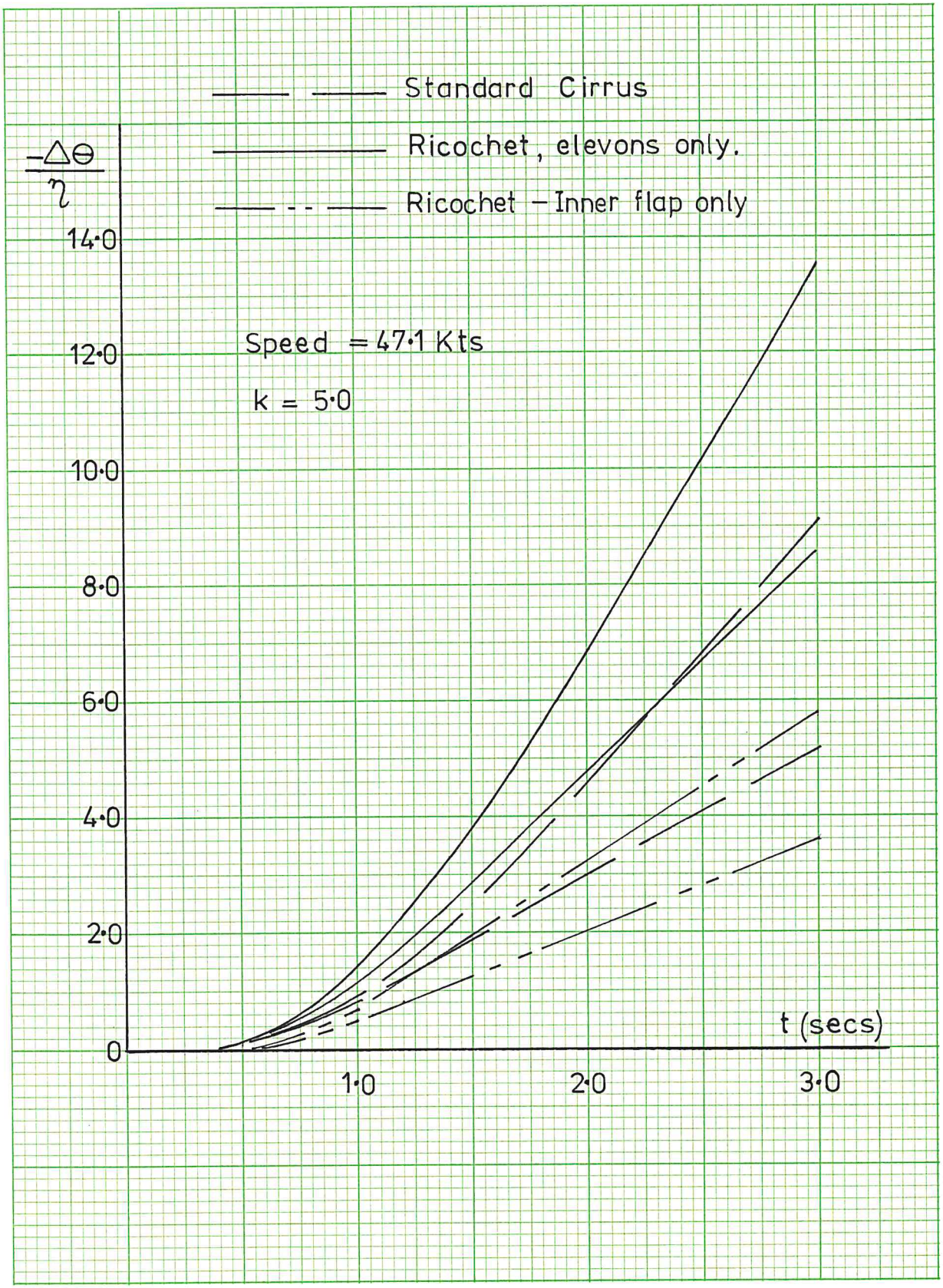

FIG 29. COMPARISON OF RESPONSE TO EXPONENTIAL APPLICATION OF PITCH CONTROL

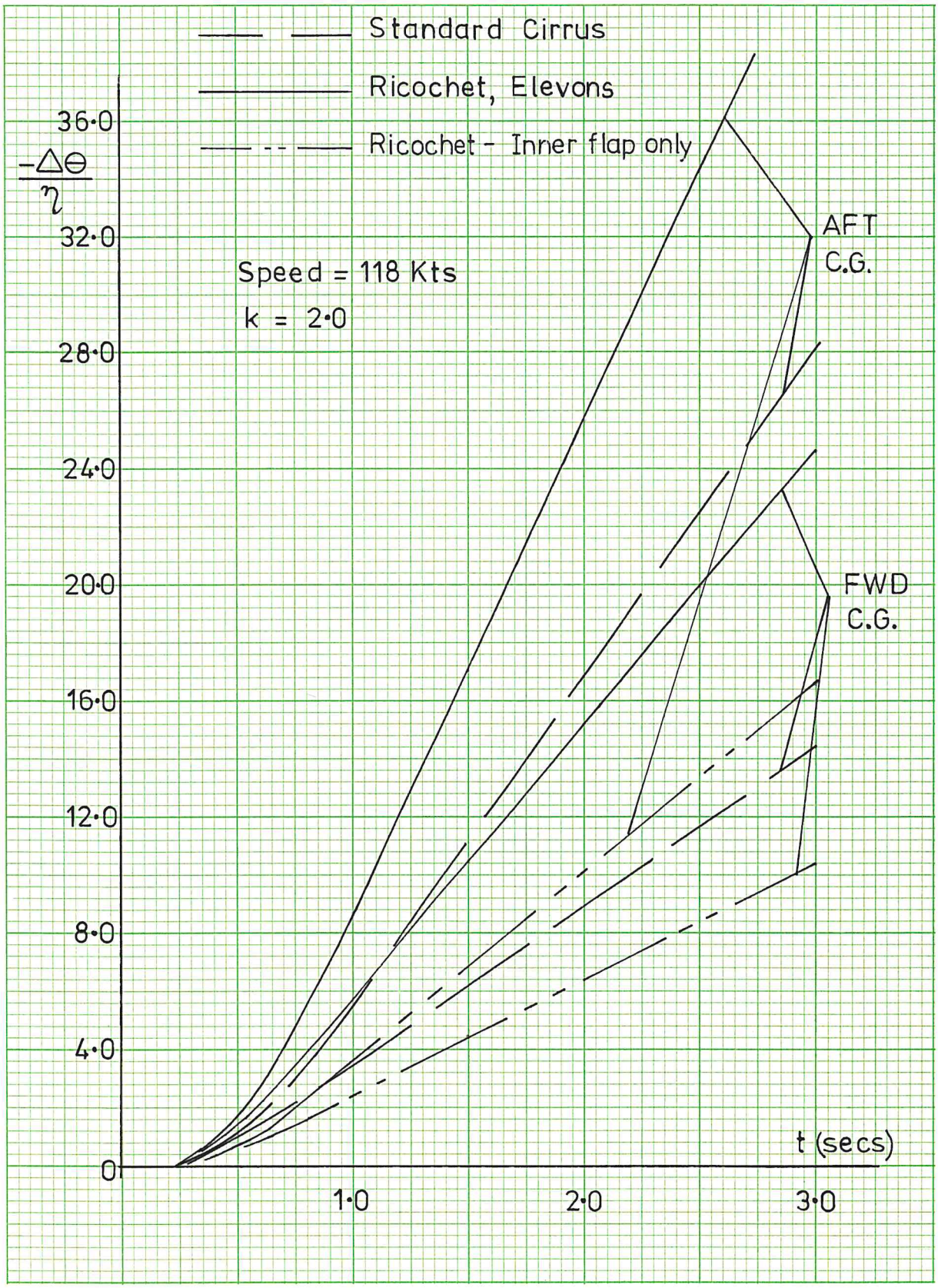

FIG 30. COMPARISON OF RESPONSE TO EXPONENTIAL APPLICATION OF PITCH CONTROL.

8. LATERAL DYNAMIC STABILITY AND CONTROL

Considerable modification of the computer program of reference 43 was required to predict the lateral behaviour of the rigid tailless sailplane. The most common problem was computing errors due to zero values in the input data for empennage and fuselage dimensions. Apart from these, the alterations which can be recalled are listed below. The following formulae are justified by their similar prediction of values for particular sailplanes, published in various OSTIV Congress reports, and the measured behaviour of the Standard Cirrus Sailplane.

8.1 Modifications to the Program

a. Roll damping, l_p

Reference 50 gives a good estimate as

$$l_p = -\frac{a_Z}{12}\,\frac{(1+3\lambda)}{(1+\lambda)}$$

where, $a_Z = \dfrac{a_o}{1+\dfrac{2a_o}{\pi A}}$.

Modifying for sweepback in accordance with reference 51, gives

$$l_p = -\frac{a_Z}{12}\,\frac{(1+3\lambda)}{(1+\lambda)}\left[1 - 0.05\,A\left(\frac{\Lambda}{70}\right)^2\right]$$

b. Aileron Power, l_ξ

Again, from reference 50,

$$l_\xi = \frac{a_Z}{1+\lambda}\,\frac{a_2}{a_1}\left[\frac{(\eta_o^2 - \eta_i^2)}{2} - (1-\lambda)\,\frac{(\eta_o^3 - \eta_i^3)}{3}\right],$$

where η_o and η_i are the non dimensional semispan location of outboard and inboard aileron ends.

The above two corrections reduced the time to roll from +30 degrees to -30 degrees from the 12 secs initially given by the program to the 3 secs measured for the Standard Cirrus.

c. Rolling Moment due to Sideslip, l_v

The wing contribution was calculated from reference 51 as,

$$l_v = -\frac{(\Gamma\, a_{1W}\cos\Lambda + C_L \tan\Lambda)(1+2\lambda)}{6(1+\lambda)}$$

d. Yawing Moment due to Sideslip, n_v

The wing contribution was calculated from reference 51 as,

$$n_v = \left[\frac{C_L^2 \tan \Lambda}{a_1 W} - \Gamma C_L\right]\left[\frac{1 + 2\lambda}{6(1 + \lambda)}\right] \frac{1}{\cos \Lambda} \quad .$$

This parameter is quite important for an aircraft without fin and rudder and illustrates the stabilizing effect of sweepback and destabilizing effect of dihedral. The Ricochet has no built in structural dihedral but a 1g wing bending was calculated as giving 0.7 degrees effective dihedral. Anhedral would give inadequate ground clearance for outlandings.

The body contribution to the yawing moment due to side-slip presented some difficulty. The computer program and the data sheets of reference 5 always predict a destabilizing contribution. Due to the tadpole shapes of conventional sailplanes the predictions were not very good.

The following body contributions to n_v were calculated from reference 5.

-0.01172	for Standard Cirrus
-0.007	for Figure 1
+0.0013	for Figure 19
+0.008	for TG-GA-01 .

The latter value was calculated by the following two methods.

Using the data sheets of reference 5 in reverse such that;

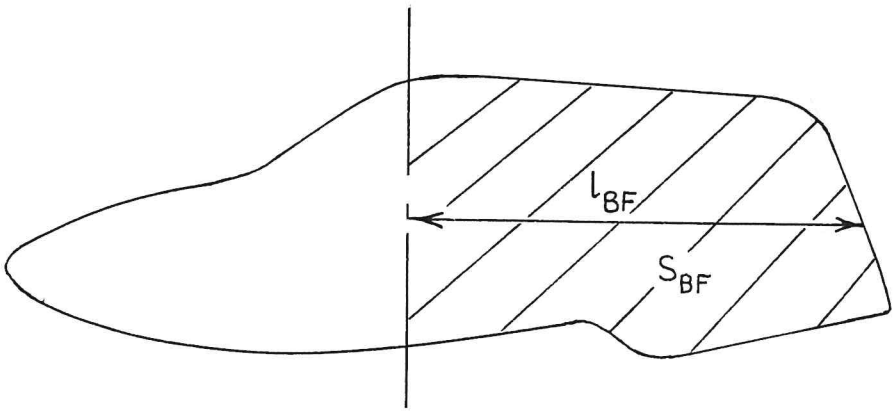

l_{BF} = 1.7 m $\quad$ l_B = 3.4 m $\quad$ S_{BF} = 1.424 m^2 $\quad$ S_B = 2.1 m^2

h = 0.8

$$\frac{h^2}{S_B} = 0.305 \qquad \sqrt{\frac{S_{BF} \cdot l_{BF}}{S_B \; l_B}} = 0.582$$

$$\therefore \quad n_{vB} = -(0.185)\frac{S_B \; l_B}{S \; b} = -0.00858$$

ie $n_{vB} = +0.00858$ in the correct sense.

Considering,

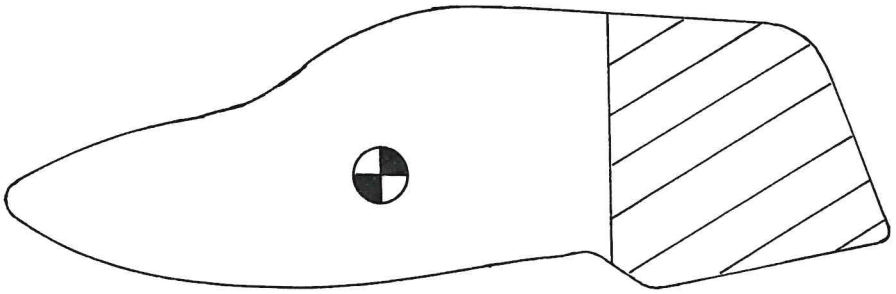

for a body contribution of zero

$$\text{and,} \quad n_{vF} = a_{1F}\frac{S_F \; l_F}{S \; b} = 1.4\,\frac{(0.715)(1.25)}{(10.26)(15)}$$

$$= 0.00813$$

where, $a_{1F} = 1.4$ also estimated from reference 5.

e. Non dimensional Inertias

These were calculated for the actual aircraft and are given in section 9.

f. Response due to Spoilers

The program was modified to give the response due to spoilers alone and due to spoilers and ailerons combined.

8.2 The Lateral Oscillation

The amplitude of bank angle to yaw angle was approximately $\frac{1}{3}$ for the Standard Cirrus and $\frac{1}{4}$ for the Ricochet. An acceptable criterion for predominantly yawing lateral oscillations is that the disturbance must die to one half amplitude by the end of the first cycle. That is the cycles to half amplitude should be less than one. A comparison

of relative values for the Standard Cirrus and Ricochet is given in table 2 for different speeds, height and centre of gravity locations.

Height kM	Speed kts	CYCLES TO HALVE AMPLITUDE			
		Without Ballast		With Ballast	
		Ricochet	Cirrus	Ricochet	Cirrus
0	47.1	0.23	0.37	0.25	0.46
0	47.1	0.22	0.36	0.25	0.44
0	118	0.31	0.57	0.36	0.64
0	118	0.30	0.56	0.36	0.63
4.57	47.1	0.26	0.43	0.33	0.65
4.57	47.1	0.26	0.43	0.32	0.62
4.57	118	0.39	0.72	0.46	0.82
4.57	118	0.38	0.72	0.46	0.80

Table 2

In flight the Standard Cirrus sailplane demonstrates good directional stability allowing the pilot to map read, select optimum flight paths, and etc, without expending much effort on flying. From table 2 the Ricochet appears to have slightly more damping. This is mainly a function of sweep, dihedral and body shape and is considered necessary to guard against any errors in estimating n_v. The Ricochet has no structural dihedral and assumes an aluminium alloy spar giving approximately, 20 cms tip deflection per 'g'.

Another parameter for assessing pilot opinion when lateral roll and yaw coupling occurs is the relationship between the reciprocal of the time to halve amplitude $\frac{1}{T_{\frac{1}{2}}}$ and $\frac{\phi}{v_e}$; where, ϕ is bank angle in degrees and v_e is the equivalent sideslip velocity. This is demonstrated in figure 31.

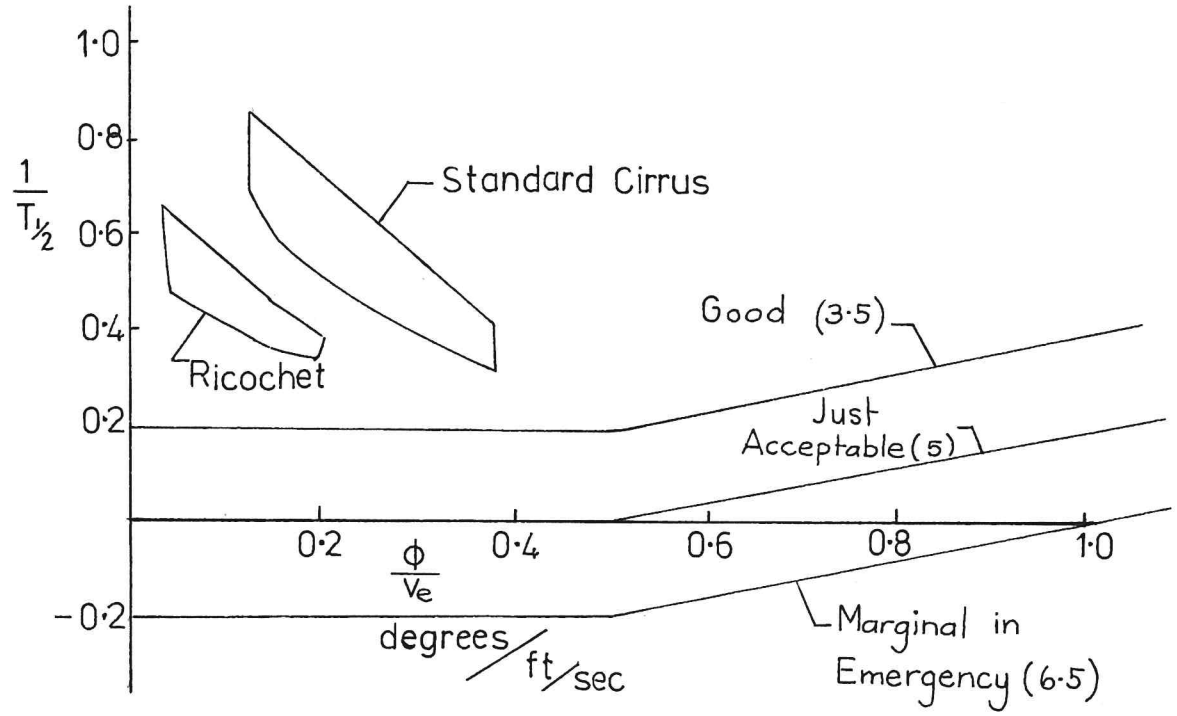

Figure 31

8.3 Spiral Stability

During slow speed thermalling (circling) flight the pilot of a sailplane is actively controlling his aircraft by searching out the stronger cores of lift. A degree of spiral instability is favourable in this flight phase for two major reasons. Firstly, the "holding off" of bank increases the available lift coefficient of the inner wing and allows slower circling speeds, and secondly, the spiral divergence assists the aircraft to seek out the areas of stronger lift by its tendency to bank further as an upwards surge comes through the thermal. In any case the time to double amplitude should not be less than 10 secs for "acceptable" handling qualities.

During the higher speed cruising flight the sailplane has to be more stable, neutral stability being desirable for some speed in the cruising range.

Table 3 gives a comparison of the times to double or halve amplitude for the Cirrus and Ricochet sailplanes.

Height kM	Speed kts	C.G.	TIMES TO DOUBLE OR HALVE AMPLITUDE (secs) Without Ballast		With Ballast	
			Ricochet	Cirrus	Ricochet	Cirrus
0.0	47.1	AFT	-13.6	-11.2	-12.2	-12.0
0.0	47.1	FWD	-13.6	-10.5	-12.2	-11.3
0.0	118	AFT	130.0	128.2	208	-1600
0.0	118	FWD	125.7	127.6	196	179.1
4.57	47.1	AFT	-12.3	-11.0	-14.5	-14.7
4.57	47.1	FWD	-12.3	-10.3	-14.5	-13.8
4.57	118	AFT	159	160	256	222
4.57	118	FWD	153	159	173	225

Table 3

8.4 Lateral Control

It is not surprising that the rudder on the aircraft of figure 1 is only 25% as efficient as the Standard Cirrus. Since the tailless sailplane has less yaw damping than the conventional sailplane a correspondingly lower forcing function is required for the same response. Therefore the tip spoilers of figure 19 were tried next. The yawing control derivative due to full deflection of a top and bottom 30% chord and 5% semispan, tip spoiler is

$$N_S \eta_S = - \frac{A_S C_{DS} l_S}{S b} = - \frac{(0.0914)(1.4)(0.9)(7.5)}{(10.26)(15)}$$

$$= - 0.00561$$

The induced drag contribution is assumed negligible for the moment by providing a suitable aileron deflection to resist any rolling due to the spoiler. The Cirrus yawing derivative due to a 25° rudder deflection at the same speed is

$$N_\xi \xi = - (0.0037) \frac{25}{57.3} = - 0.016$$

Although the spoiler has only one third of the power of the Cirrus rudder, the reduced yaw damping of the tailless provided it with half the response of the Cirrus.

The tip spoiler was abandoned because,

a. a conventional spoiler along the aileron span could give a more favourable roll contribution,

b. a conventional spoiler can more easily be segmented for smoother control response, and

c. tip effects, such as the spoilers effect on the wing tip vortex, reduce the reliability of the calculated response.

Figure 32 gives the response of the Ricochet sailplane (DWG TG-GA-01) to instantaneous application of full spoiler. The predominant response is seen to be in roll, with very little yaw at low speed, and an increased amount at high speed. Unlike the Ricochet aileron response given in figure 33, the yaw, due to spoiler deflection, is favourable, assisting the aircraft into a turn. At slow speed the associated slip is quite small illustrating that the spoiler is likely to be an effective control for executing turns. In fact, at slow speed, its roll response is equivalent to that of the Standard Cirrus, giving approximately 3.7 secs to roll from 30 degrees to -30 degrees, and does not require the normal rudder deflection to overcome adverse yaw.

The spoiler yaw response is due to the profile drag increment of the spoiler and the reduction in induced drag due to the loss of lift. The yawing moments due to these two drag components oppose each other. For take off and landing it is necessary to be able to yaw the sailplane without banking. This can be achieved by using the spoilers for yaw and the ailerons to oppose the roll. The results are given in figure 34 and are compared to the Standard Cirrus response due to full rudder deflection at the same speeds. The wind tunnel tests, given in reference 52, show that the effectiveness of the elevon behind the deflected spoiler is reduced by 50%. Since there are two elevons the total elevon (aileron) efficiency has been reduced by 25%. Thus 95% of full aileron deflection is required at low speed and 60% at high speed to prevent any rolling due to full spoiler deflection. Since the resultant slow speed yaw response is 15% better than the Standard Cirrus the control would appear to be satisfactory.

The Ricochet aileron response (figure 33) is better than the Standard Cirrus response (appendix B), probably due to the increased wing tip (and control) chords of the tailless. The capability exists with the tailless sailplane to give complementary deflections of aileron and spoiler. The results are given in figure 35 and at slow speed provide a roll from 30 degrees bank to -30 degrees bank in 2.2 secs with relatively less adverse yaw than is obtained with conventional ailerons.

For normal flying, the best method of executing turns with the Ricochet will be by spoiler. The response at two speeds, 4.57 km altitude, and full water ballast is given in figure 36. It is still necessary to determine if the use of a spoiler for lateral control degrades the sailplanes cross-country performance any more than conventional ailerons. We can relate the favourable yawing moment due to profile drag of the spoiler to the function of the conventional fin and rudder; the lift reduction being akin to the aileron function. In this way we can compare the power dissipated (DV) by the Ricochet with spoilers, to that dissipated by the Standard Cirrus conventional fin and rudder on any given cross-country flight.

The profile drag coefficient increment due to full spoiler deflection is given by,

$$\Delta C_D = \frac{A_S}{S} C_{DS} = \frac{0.1616}{10.26} (1.4) = 0.022 ,$$

which is over double the zero-lift drag coefficient of the sailplane.

For the Cirrus fin and rudder,

$$\Delta C_D = \frac{1.282}{9.97} (0.08) = 0.0103 , \text{ for full deflection,}$$

and,

$$C_D = (0.0065) \frac{1.282}{9.97} = 0.0008, \text{ for zero deflection}$$

in normal flight.

Approximately 50% of a typical MacReady soaring cross-country flight is spent in circling (thermalling) flight. It is possibly pessimistic to assume that a good competition pilot makes;

2 applications of full rudder every 10 mins
4 " " half " " " "
20 " " quarter " " " " ,

during thermalling flight; ie a major rudder deflection every 20 secs. During cruising flight he might make;

6 applications of a third rudder every 10 mins
10 " " " quarter " " " "

A step application of 1.5 seconds duration, for all deflection types, is not unreasonable. We can also assume that thermalling is conducted at 23 m/sec and cruising at 70 m/sec.

The sea level, rate of power dissipation during a typical 20 minute flight segment using spoilers is,

$$= \frac{(1.5)}{(20)(60)} \frac{(0.022)(1.225)}{(2)} 10.26 \left[(2 + \frac{4}{2} + \frac{20}{4})(23)^3 + (\frac{6}{3} + \frac{10}{4})(70)^3 \right]$$

$$= 285.7$$

For the Standard Cirrus fin and rudder the power dissipation is,

$$= (285.7) \frac{(0.0103)}{(0.022)} + \frac{(0.0008)(1.225)(10.26)}{2} \left[\frac{(23)^3}{2} + \frac{70^3}{2} \right]$$

$$= 133 + 892.8$$

$$= 1026$$

It is apparent that the tailless glider is much better off with spoilers than a conventional sized fin and rudder. The cross-country performance calculations in appendix C assumed the existence of a fin and rudder, as in figure 1, lending a slight amount of pessimism to the results.

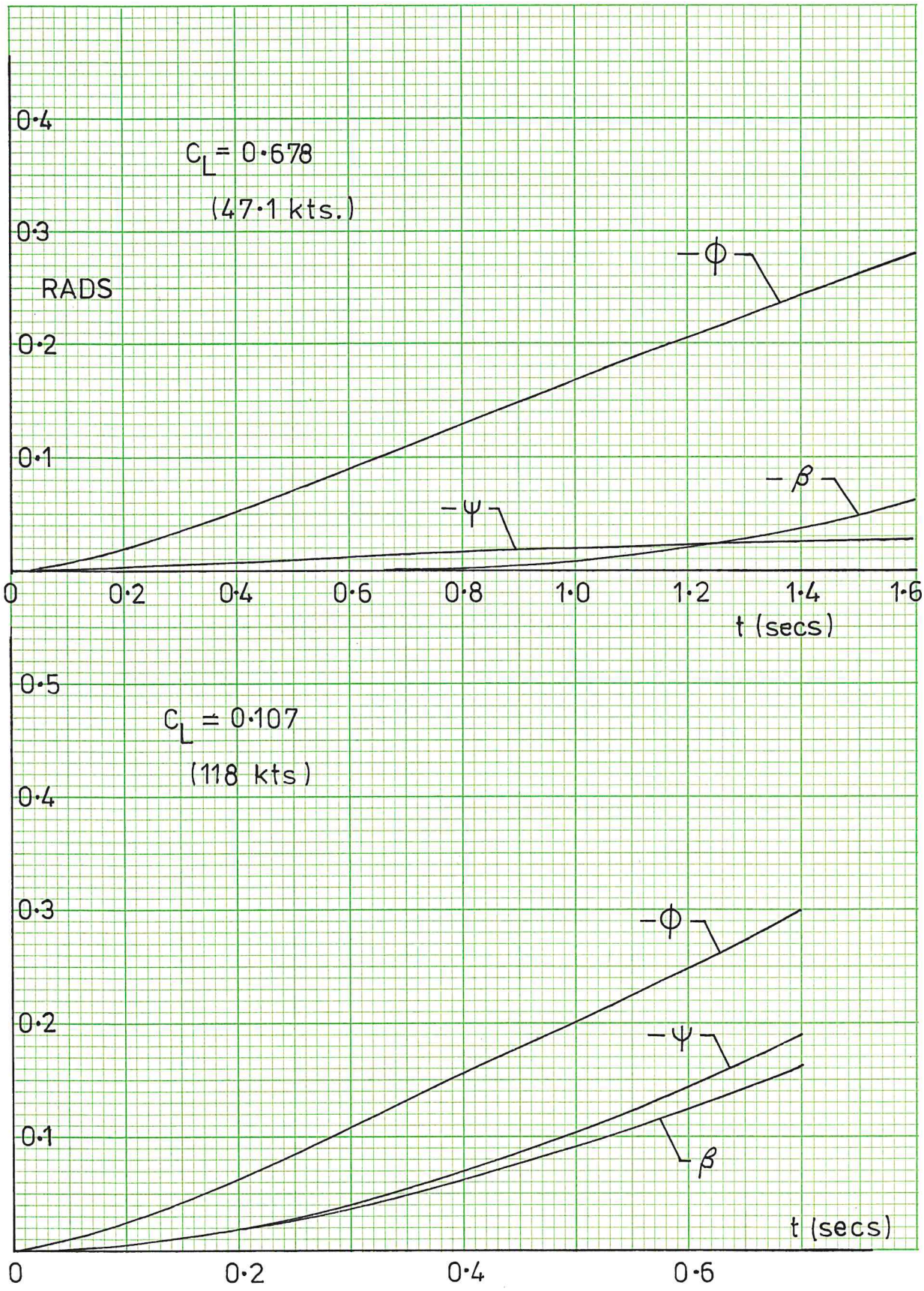

FIG 32 RESPONSE DUE TO INSTANTANEOUS APPLICATION OF FULL SPOILER AT SEA LEVEL, WITHOUT BALLAST.

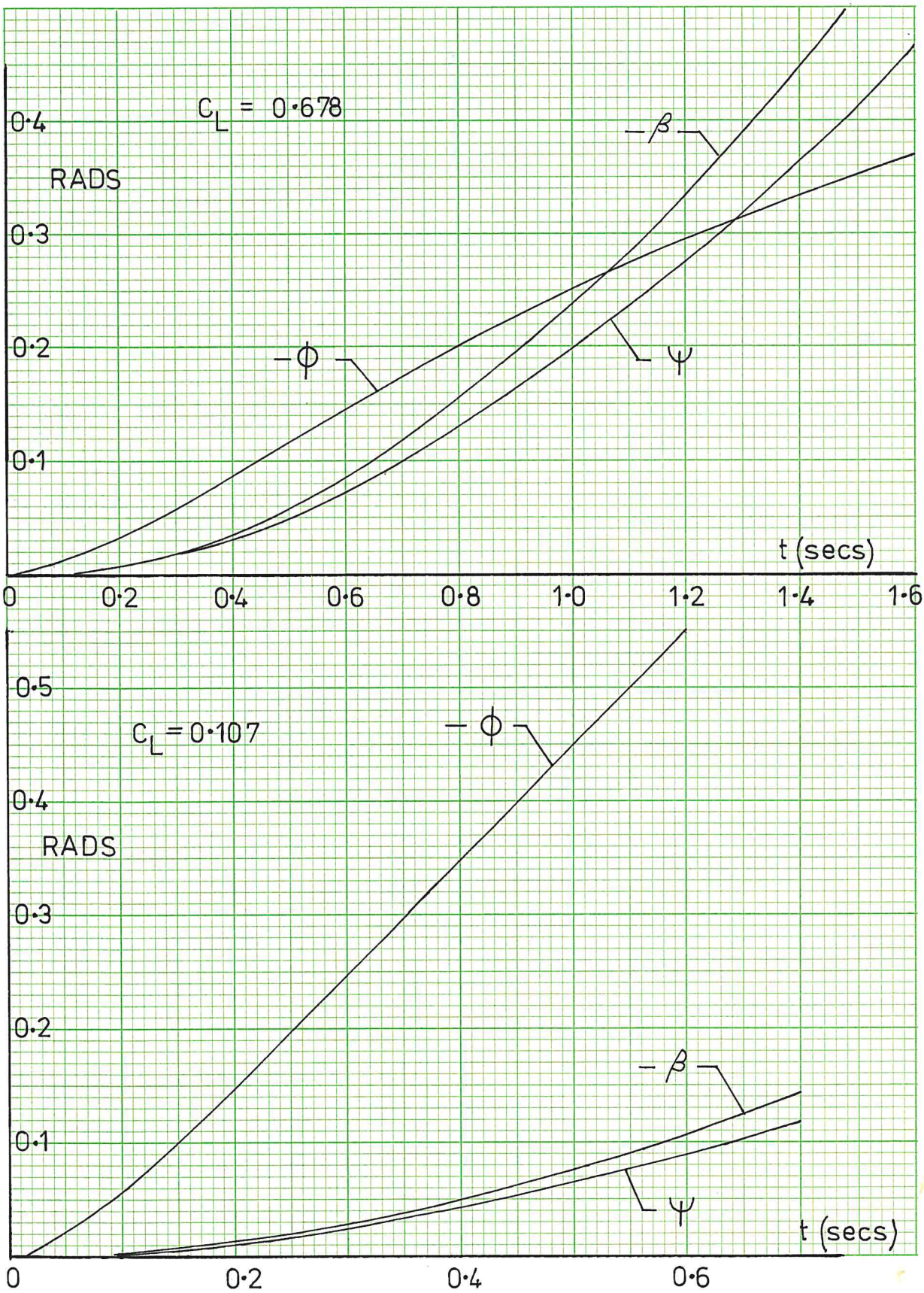

FIG 33 RESPONSE DUE TO INSTANTANEOUS APPLICATION OF FULL AILERON AT SEA LEVEL, WITHOUT BALLAST.

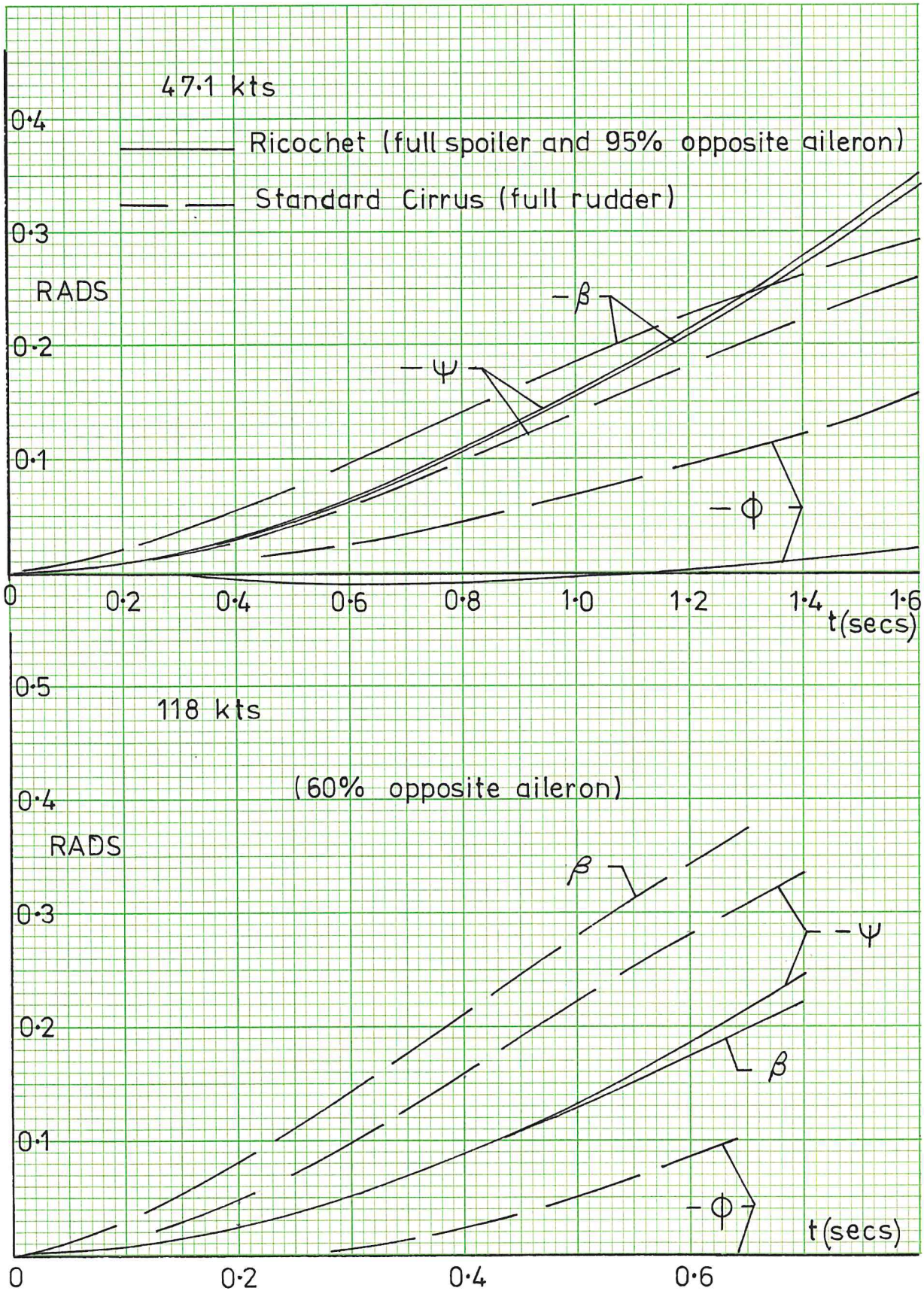

FIG 34 RESPONSE DUE TO INSTANTANEOUS APPLICATION OF FULL SPOILER AND PART DEFLECTION OF OPPOSITE AILERON, NO WATER BALLAST

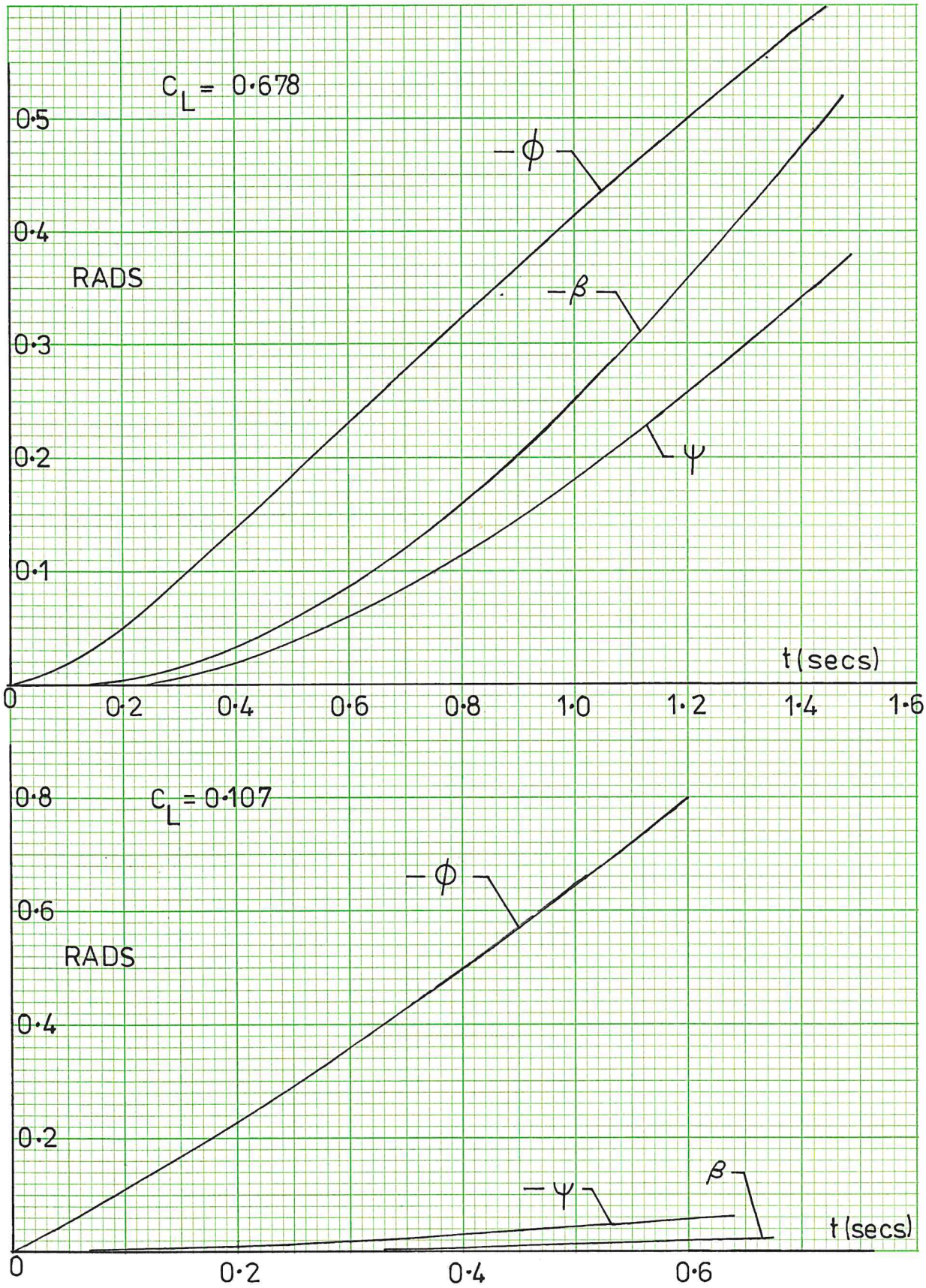

FIG 35 RESPONSE DUE TO INSTANTANEOUS APPLICATION OF FULL SPOILER AND FULL AILERON AT SEA LEVEL, NO WATER BALLAST

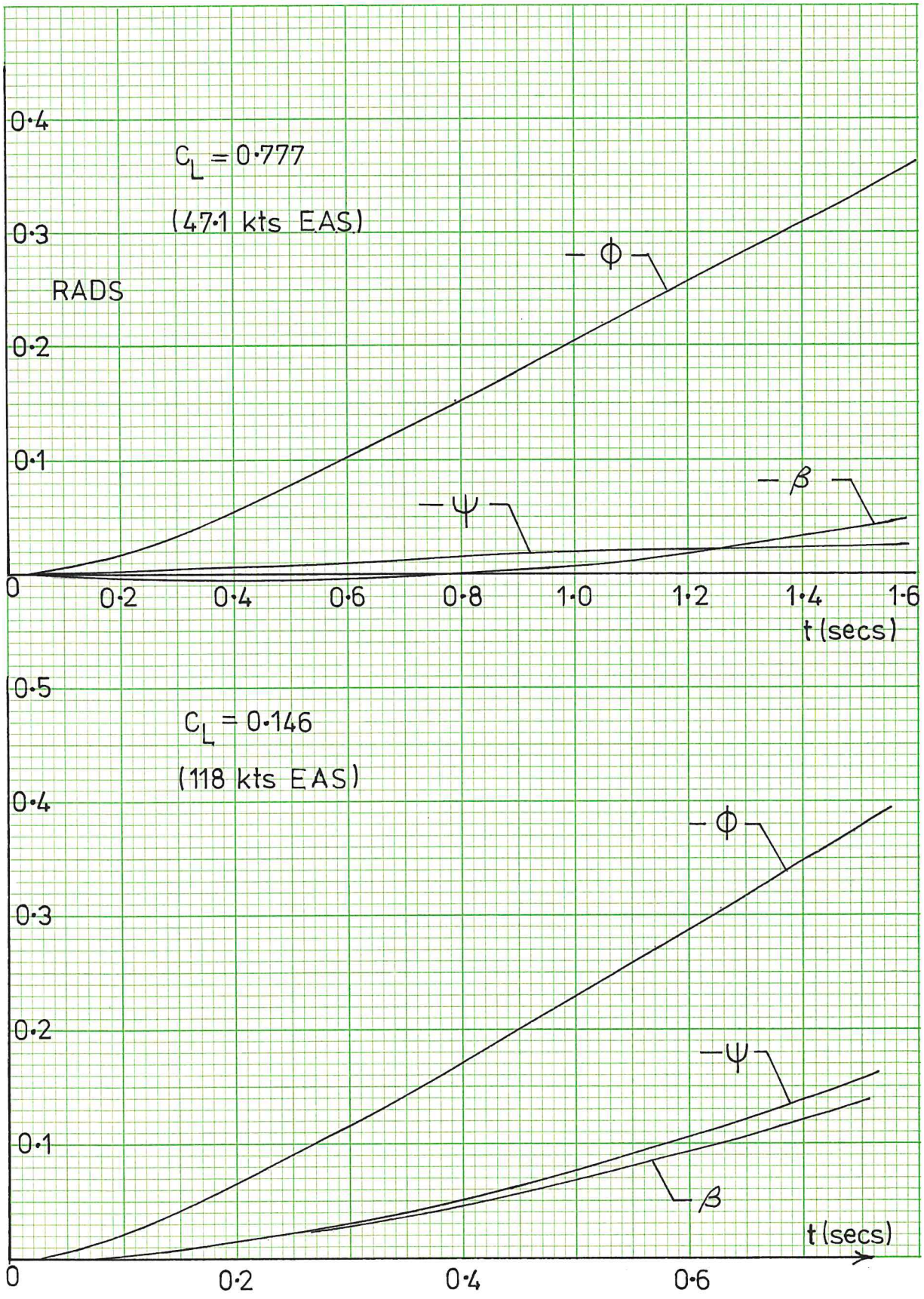

FIG 36 RESPONSE DUE TO INSTANTANEOUS APPLICATION OF FULL SPOILER AT 4·57 KM HEIGHT, FULL BALLAST

9. SUMMARY ANALYSIS OF THE RICOCHET SAIPLANE

This section contains information about the Ricochet sailplane which has not been divulged in the discussion so far. Comparisons can be made with appendix A for the Standard Cirrus. This is only intended to be a precis of the results for the rigid aircraft solution so far. This list of particulars help define the aircraft considered.

9.1 Ricochet Particulars

WINGS

Span (b)	15 m (49.2 ft)
Area (S)	10.26 m^2 (110.45 ft^2)
Aspect Ratio (A)	21.93
Wing Root Chord (c_r)	0.73 m (2.395 ft)
Wing Tip Chord (c_t)	0.50 m (1.641 ft)
Wing Crank Chord (c_m)	0.73 m (2.395 ft)
Standard Mean Chord ($\bar{c}$)	0.683 m (2.24 ft)
Mean Aerodynamic Chord ($\bar{\bar{c}}$)	0.689 m (2.26 ft)
Taper Ratio (λ)	0.685
$\frac{1}{4}$ Chord Sweep (Λ)	13 degrees
Dihedral (Γ)	0.0 degrees
Aero. Twist Root/Tip (Θ_a)	5.0 degrees
Aerofoil Section	Eppler

ELEVONS

Type	Plain
Span	2.625 m (8.61 ft)
Area (each)	0.283 m^2 (2.88 ft^2)
Percentage Chord	17.5
Maximum Deflection Up	26.67 degrees
Maximum Deflection Down	13.33 degrees

SPOILERS

Type	triple segmented, Simple Hinge
Span	2.625 m (8.61 ft)
Area	0.161 m^2 (1.74 ft^2)
Percentage Chord	10.0
Maximum Deflection Up	85.0 degrees

FLAPS

Inboard Segment	
Span	2.625 m (8.61 ft)
Area (each)	0.335 m^2 (3.61 ft^2)
Percentage Chord	17.5
Maximum Deflection Up	10 degrees
Maximum Deflection Down	80 degrees
Lift Curve Slope (a_2)	0.70
Centre of Pressure (h_c)	-0.134

Outboard Segment	
Span	1.875 m (6.15 ft)
Area	0.24 m^2 (2.58 ft^2)
Percentage Chord	0.175
Maximum Deflection Up	6.7 degrees
Maximum Deflection Down	56.7 degrees

FUSELAGE

Overall Length	3.4 m (11.16 ft)
Maximum Width	0.585 m (1.92 ft)
Maximum Height	0.82 m (2.69 ft)

WEIGHTS

Wings (both)	99.8 kg (220 lb)
Fuselage	55.33 kg (122 lb)
Empty Weight	155.1 kg (342 lb)
Instruments	6.8 kg (15 lb)
Batteries	2.27 kg (5 lb)
Equipped Weight (W_E)	164 kg (362 lb)
Maximum Pilot Weight (with above equipment (W_P)	113.4 kg (250 lb)
Maximum Water Ballast	90.7 kg (200 lb)
Maximum All Up Weight	368.3 kg (812 lb)
Nominal Weight Used for Stability and Control Calculations	
Without Ballast	254.9 kg (562 lb)
With Ballast	345.6 kg (762 lb)

INERTIAS

Taken about aircraft centre of gravity at all up weights of 254.9 kg (562 lb) without ballast and 345.6 kg (762 lb) with ballast.

Forward Centre of Gravity	Without Ballast	With Ballast
Rolling (I_X)	1751 kg m^2 (1290 sl.ft^2)	2421 kg m^2 (1783.6 sl.ft^2)
Pitching (I_Y)	194.1 kg m^2 (143 sl.ft^2)	195 kg m^2 (145 sl.ft^2)
Yawing (I_Z)	1832 kg m^2 (1350 sl.ft^2)	2616 kg m^2 (1927 sl.ft^2)
Aft Centre of Gravity		
Rolling (I_X)	1751 kg m^2 (1290 sl.ft^2)	2421 kg m^2 (1784 sl.ft^2)
Pitching (I_Y)	168.3 kg m^2 (124 sl.ft^2)	171 kg m^2 (126 sl.ft^2)
Yawing (I_Z)	1832 kg m^2 (1350 sl.ft^2)	2592 kg m^2 (1910 sl.ft^2)

CENTRES OF GRAVITY

Forward (percentage standard mean chord)	16.5 % SMC
Aft (percentage standard mean chord)	21% SMC

SPEEDS

Stalling Speed (V_S) at W = 254.9 kg (IAS)	39.2 kts
Stalling Speed (V_S) at W = 345.6 kg (IAS)	45.6 kts
1.2 V_S at W = 254.9 kg (IAS)	47.1 kts
1.2 V_S at W = 345.6 kg (IAS)	54.8 kts
Design Diving Speed	125 kts

9.2 Gliding and Turning Performance

Figure 37 gives the Ricochet straight glide performance for a nominal pilot weight of (200 lb), with and without water ballast. The best, straight line fit to the C_D versus C_L^2 curve is given by;

$$C_D = 0.0076 + 1.28 \frac{C_L^2}{\pi A}$$

that is;

$$C_D = 0.0076 + \left(\frac{1.05}{\pi A} + 0.00333\right) C_L^2$$

Figure 38 gives the turning performance at the same wing loadings. The effect of water ballast on turn radius and sink rate is readily apparent.

9.3 Aerodynamic Stability and Control Derivatives

The stability and control chracteristics have been analysed at the boundaries of the sailplane operating envelope. Centres of gravity, fully forward and fully aft have been combined with speeds of 1.2 times stalling speed, maximum placard speed, with heights at sea level and 4.57 km (15000 ft), and with and without water ballast.

Two typical sets of the derivatives for the rigid aircraft are given below.

	c.g. forward	c.g. aft
Weight	345.6 kg	254.9 kg
Height	0.0 km	4.57 km
Speed (TAS)	118 kts	55 kts
Centre of Gravity	16.5%	21.0 %
Aircraft Lift Curve Slope	5.68	5.68
Static Margin	6.28% SMC	1.79%
Manoeuvre Margin	9.7% SMC	4.8%

Longitudinal, non dimensional, Stability Derivatives

x_u	-0.0093	-0.0191
x_w	0.0595	0.3264
x_q	0.0	0.0
Z_u	-0.1452	-0.7972
Z_w	-2.845	-2.85
Z_q	-0.8883	-0.761
m_u	0.0	0.0
m_w	-0.1718	-0.051

m_q	-1.254	-1.311
$m_{\dot{w}}$	0.0	0.0
$\hat{t}$	0.451	1.145
μ_1	50.13	58.86
i_y	1.89	2.2
Pitching Damping Ratio	1.814	1.74
Natural Damped Frequency	2.37	1.177
Longitudinal Control Derivatives		
Elevon Lift Curve Slope (a_2)	0.82	0.82
Elevon Centre of Pressure location (h_c)	1.04	1.04
Inner Flap Lift Curve Slope (a_2)	0.7	0.7
Inner Flap Centre of Pressure location	-0.134	-0.134
Lateral, non dimensional, Stability Derivatives		
l_v	-0.0171	-0.0196
n_v	0.0079	0.0116
y_v	-0.0829	-0.0829
l_r	0.0422	0.2316
n_r	-0.028	-0.0269
l_p	-0.7206	-0.7212
n_p	-0.0199	-0.1094
Lateral Control Derivatives		
Elevon Rolling Derivative l_ξ	-0.2598	-0.2173
Elevon Yawing Derivative n_ξ	0.0057	0.0263
Spoiler Rolling Derivative (For full deflection)	-0.0394	-0.0423
Spoiler Yawing Derivative (For full deflection)	-0.0056	-0.0056
μ_2	3.667	4.306
i_x	0.1246	0.1222
i_z	0.1345	0.1278
i_{xz}	0.0	0.0003

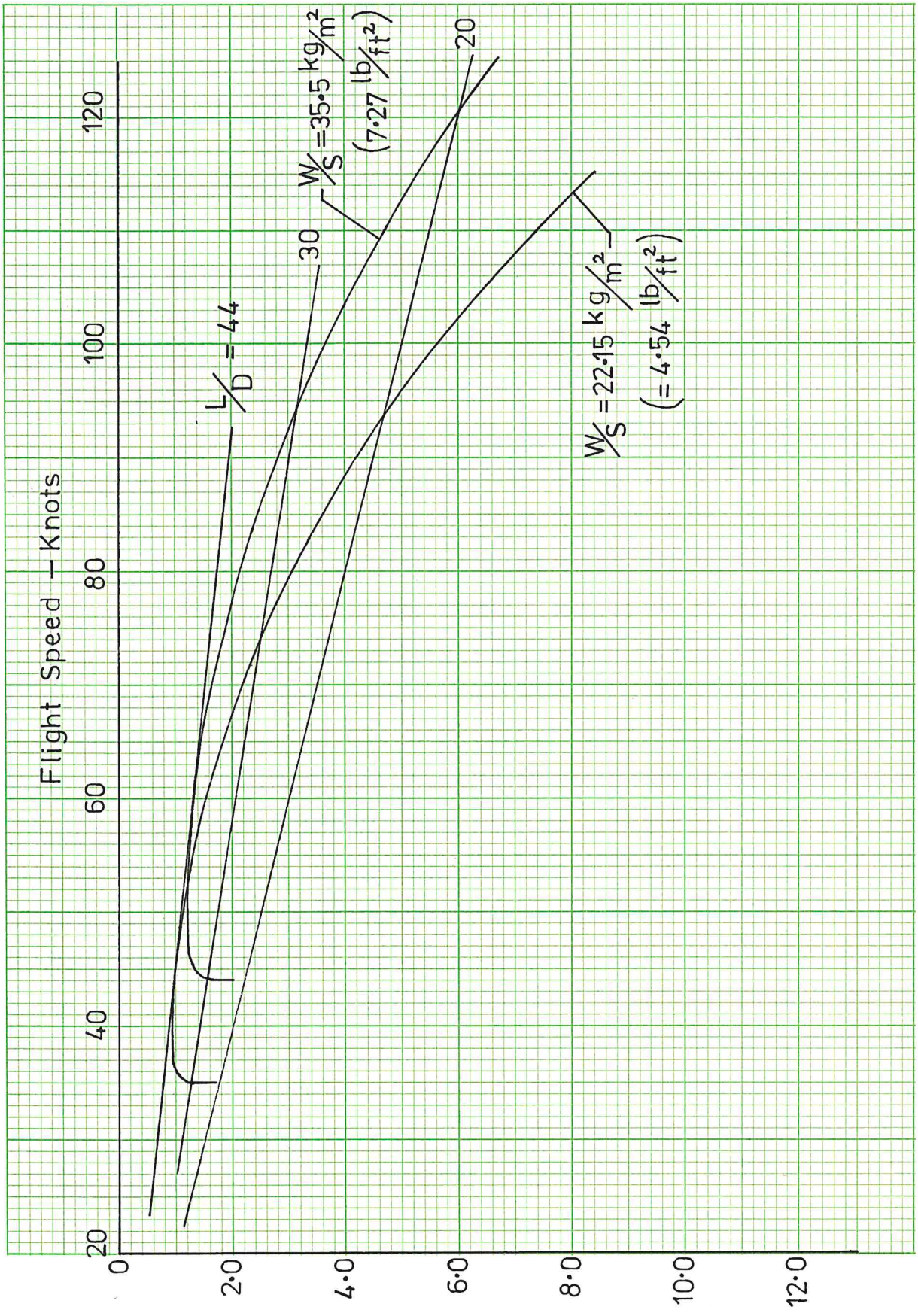

FIG 37 RICOCHET GLIDE PERFORMANCE

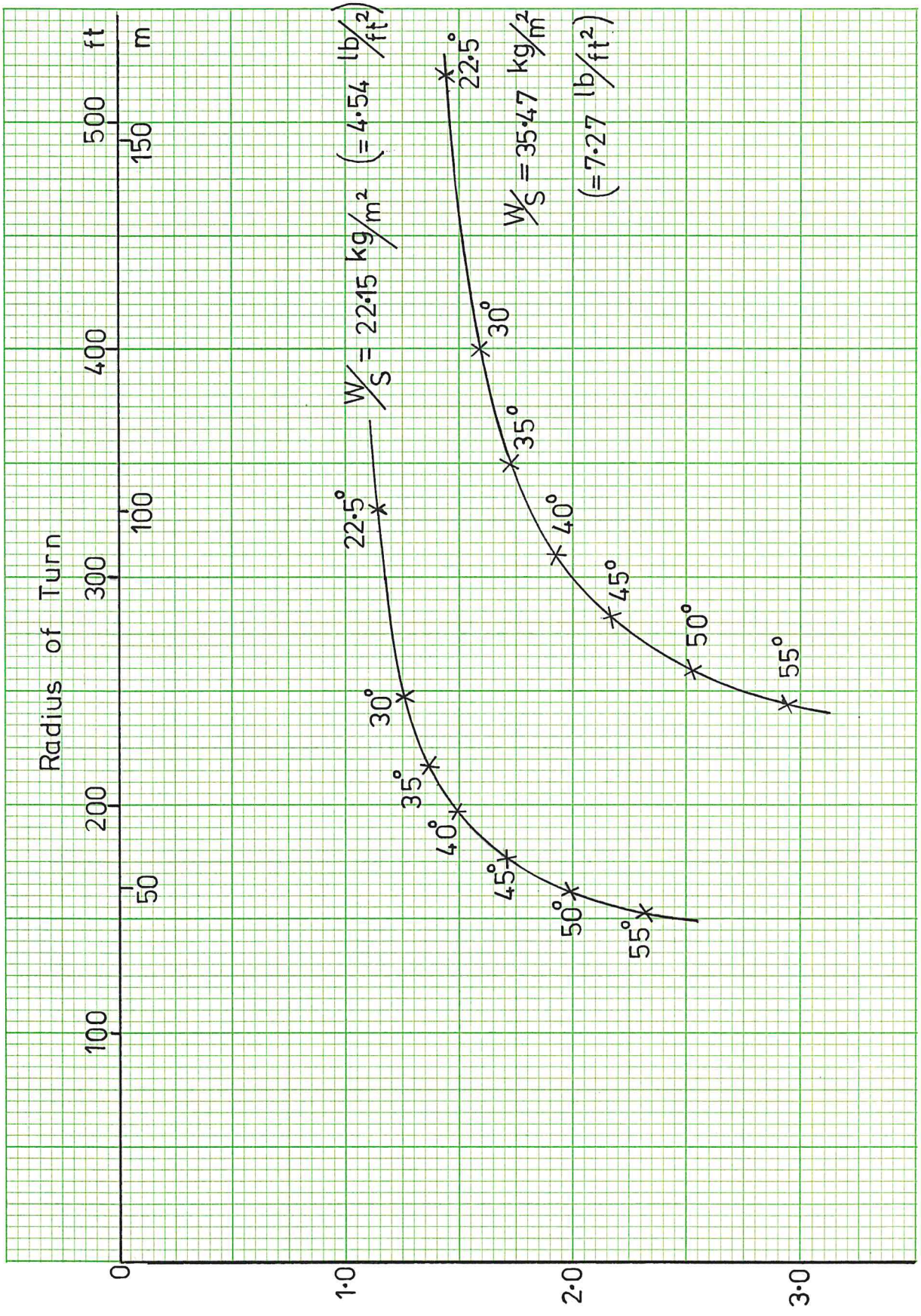

FIG 38 RICOCHET TURN PERFORMANCE.

10. THE NON-RIGID STRUCTURE

Apart from the effective dihedral due to 1g wing bending the aircraft has so far been considered rigid. The possible effects of structural flexibility have already been illustrated on the design study flow chart. Some of these are now considered in a little more detail.

Appendix F derives the most critical spanwise load distributions for the preliminary stressing given in appendix G. The resultant wing structure is shown in drawings TG-W-01 to TG-W-04, from which the wing stiffnesses can be determined. Formulae for the wing torsional flexibility will be required and will now be derived.

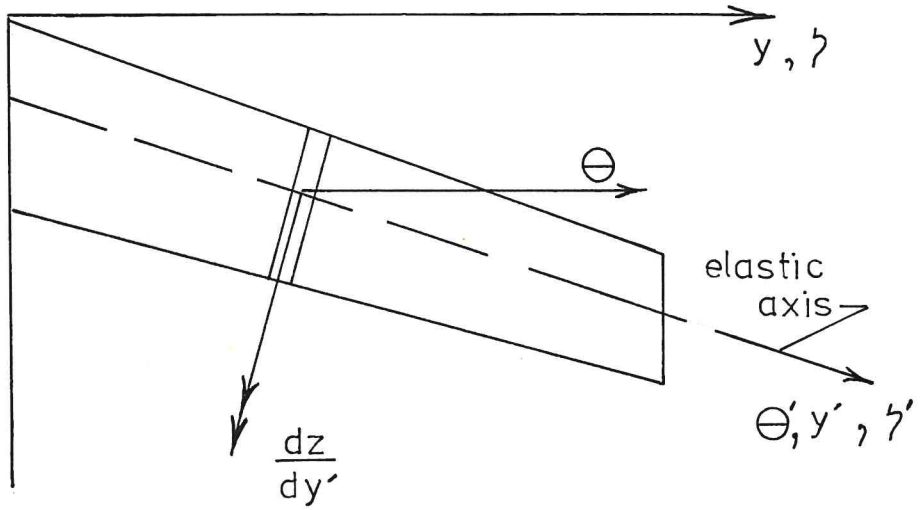

Twist of a Three Cell, symmetric box.

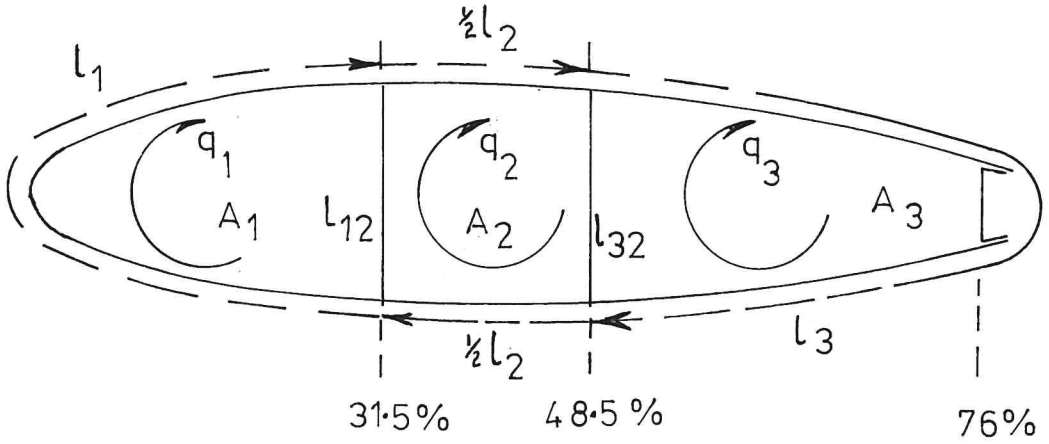

$$T = 2q_1 A_1 + 2q_2 A_2 + 2q_3 A_3$$

θ' is the local twist about the wing flexural axis and is assumed the same for all cells.

ie $$\frac{1}{A_1}\oint_1 \frac{q}{t}\,dp = \frac{1}{A_2}\oint_2 \frac{q}{t}\,dp = \frac{1}{A_3}\oint_3 \frac{q}{t}\,dp$$

Defining $l'_{12} = \frac{l_{12}}{t_{12}}$ $\qquad l'_1 = \frac{l_1}{t_1}$ etc,

gives;

$$q_1 = K_1 q_2$$

$$q_3 = K_3 q_2$$

$$q_2 = \frac{T}{2A_2 + 2A_1 K_1 + 2A_3 K_3}$$

and,

$$\frac{d\theta'}{dy'} = \frac{1}{2G A_1}\left[K_1 (l_1' + l_{12}') - l_{12}'\right] q_2$$

where, $$K_1 = \frac{A_3 \frac{l'_{12}}{l'_3 + l'_{32}} - A_1 \frac{l'_{32}}{l'_3 + l'_{32}} + A_1 \frac{l'_2 + l'_{12} + l'_{23}}{l'_{23}} + A_2 \frac{l'_{12}}{l'_{23}}}{A_3 \frac{l'_1 + l'_{12}}{l'_3 + l'_{32}} + A_1 \frac{l'_{12}}{l'_{23}} + A_2 \frac{l'_1 + l'_{12}}{l'_{23}}}$$

and, $$K_3 = \frac{l'_2 + l'_{12} + l'_{23}}{l'_{23}} - K_1 \frac{l'_{12}}{l'_{23}} - \frac{A_2}{A_1}\left(K_1 \left(\frac{l'_1 + l'_{12}}{l'_{23}}\right) - \frac{l'_{12}}{l'_{23}}\right)$$

For a constant wing chord of 0.73 m, and $t_1 = t_2 = t_3 = t_{12} = t_{32} =$ 0.5 mm, $t_2 = 2.0$ mm, we obtain,

$$A_1 = 0.0193 \text{ m}^2, \quad A_2 = 0.0131 \text{ m}^2, \quad A_3 = 0.0176 \text{ m}^2$$

and, $K_1 = 0.4317$, $K_3 = 0.4129$

giving, $q_2 = 17.42\,T$ N/m

$$\frac{d\theta'}{dy'} = \frac{6.26}{10^6} T \text{ rads/m}$$ where, y' is measured along the wing flexural axis.

Twist of Outer Wing

The 'I' spar contribution to torque is negligible. The tapered section of wing is therefore considered as a single cell box. Hence,

$$q = \frac{T}{2A} \qquad \text{and} \qquad \frac{d\theta'}{dy'} = \frac{1}{2GA} \oint \frac{q}{t}\, dp$$

and $$A = (0.75)(0.13)\, C^2 = (0.0975)\, C^2$$

$$p = (2(.75) + 0.05 + 0.08)\, C = 1.63\, C$$

$$t = \text{const} = 0.5 \text{ mm}$$

giving,

$$\frac{d\theta'}{dy'} = \frac{3.14}{10^6} \left(\frac{T}{C^3}\right) \text{ rads/m}$$

when T is in N/m and C in metres.

Structural wing twist θ' due to torque represents an aerodynamic twist θ_T, given by,

$$\theta_T = \theta' \cos\Lambda .$$

$$= \frac{b \cos\Lambda}{2} \int_0^1 \frac{d\theta'}{dy'}\, d\eta$$

$$= \frac{b \cos\Lambda}{2} \int_0^1 \frac{2.44}{10^6} \frac{T}{C^3}\, d\eta \qquad \text{for the untapered section}$$

$$= \frac{b \cos\Lambda}{2} \int_0^1 \frac{3.14}{10^6} \frac{T}{C^3}\, d\eta \qquad \text{for the tapered section.}$$

10.1 Variation of Wing Twist with Speed

Pure bending of the wing along its elastic axis does not involve structural twisting but does produce an aerodynamic twist. The local aerodynamic twist due to bending, θ_B, is given by,

$$\theta_B = -\frac{dz}{dy'} \sin\Lambda \; ; \qquad \text{nose up}$$

when $\frac{dz}{dy'}$ is the local wing slope along the elastic axis with z deflection positive upwards.

Since,

$$\frac{dz}{dy'} = -\int_0^{\rho y'} \frac{M}{EI}\, dy' = -\frac{b}{2\cos\Lambda}\int_0^{\rho\eta} \frac{M}{EI}\, d\eta$$

we have,

$$\Theta_B = \frac{b}{2}\tan\Lambda \int_0^{\rho\eta} \frac{M}{EI}\, d\eta \ .$$

(M and I are determined along the elastic axis).

The nett aerodynamic twist, Θ_a, is given by;

$$\Theta_a = \Theta_T + \Theta_B$$

The spanwise variation of Θ_T is calculated in table 4 for $C_L = 1.0$ and table 5 for $C_L = 0.2$. An aircraft mass of 277.3 kg, composed of maximum cockpit load and no water ballast, has been used in these calculations. The corresponding spanwise variations of Θ_B is calculated in table 6 and the nett aerodynamic twist is plotted on figure 39. The resultant 0.2 degrees of washout, at both speeds, is the worst case for the aircraft. A reduction in cockpit load, or the addition of water ballast will reduce the wing bending and associated washout. A greater nose up torque is also obtained by the addition of water ballast, further reducing the washout. The aircraft with full water ballast has a nett washout of 0.12 degrees at $C_L = 1.0$ and 0.11 degrees at $C_L = 0.2$.

Further rearwards shift of the twist axis on the wing to reduce the nett twist is possible but is probably not justified at this stage.

10.2 Symmetric Gust and Manoeuvre Stability

A symmetrical upgust or positive 'g' manoeuvre produces a wing bending deformation corresponding to the increment in additional lift distribution. The effective aerodynamic washout due to upwards wing bending produces a further nose up moment and increase in load factor. This situation is unstable but not necessarily dangerous because, in the gust case, their exists a nose down moment due to the aircraft aerodynamic centre being aft of the centre of gravity, and in the manoeuvre case the response time constant is being controlled by the pilot, implying that corrective action is likely to be possible for a sensible wing structure before a dangerous situation develops. This depends on the amount of wing twist caused by the gust or manoeuvre. As already illustrated the washout due to bending is partially offset by the wash-in due to torque.

The manoeuvre case is distinctive by the elevon deflection. However, since the elevon centre of pressure almost coincides with the local wing elastic axis we can ignore the local torque, due to control deflection, and attribute the initial nose up rotation of the

	Torque, T, n=1 C_L=1.0, W=277.3						
η	Lift	Wing Mass	C_{mac}	T N-m	$\frac{T}{C^3}$ N/m^2	$\int_0^{\rho^1} \frac{T}{C^3} d\eta$	Θ_T degrees
0	139.1	19.3	-39.1	119.3	306.7	0	0
0.1	120.5	16.5	-31.6	105.4	271	28.75	0.029
0.2	102.4	13.9	-24.6	91.7	235.7	54.0	0.055
0.3	84.9	11.5	-18.4	78.0	200.5	75.75	0.077
0.4	68.4	9.3	-12.6	65.1	167.3	94.25	0.096
0.5	52.5	7.3	-7.7	52.1	134	109.25	0.112
0.6	37.8	5.3	-4.3	38.8	99.7	120.75	0.123
0.7	23.9	3.5	-1.5	25.9	85.2	130.4	0.171
0.8	13.3	2.0	-0.4	14.9	64.1	137.9	0.181
0.9	4.65	0.8	+0.4	5.85	33.8	142.7	0.188
1.0	0	0	0	0	0	144.6	0.190

Table 4

	Torque T, n=1.0, C_L=0.2, W=277.3						
η	Lift	Wing Mass	C_{mac}	T N-m	$\frac{T}{c^3}$ N/m2	$\int_0^{\eta} \frac{T}{c^3} d\eta$	θ_T degrees
0	139	19.3	-195.5	-37.2	-95.6	0	0
0.1	116.2	16.5	-158	-25.3	-65.0	-7.8	-0.008
0.2	93.8	13.9	-123	-15.3	-39.3	-12.95	-0.013
0.3	73.1	11.5	-92	-7.4	-19.0	-15.85	-0.016
0.4	54.3	9.3	-63	+0.6	+1.5	-16.79	-0.017
0.5	37.4	7.3	-38.5	6.2	15.9	-15.9	-0.016
0.6	22.1	5.3	-21.5	5.9	15.2	-14.4	-0.015
0.7	10.9	3.5	-7.5	6.9	22.7	-12.6	-0.013
0.8	4.0	2.0	-2.0	4.0	17.2	-10.7	-0.011
0.9	1.0	0.8	+2.0	3.8	21.9	-8.7	-0.009
1.0	0	0	0	0	0	-7.7	-0.008

Table 5

		C_L=1.0, W=277.3, n=1			C_L=0.2, W=277.3, n=1		
η	I Cm^4	M N-m	$\int_0^{\rho 1} \frac{M}{EI} d\eta$ x 10^4	Θ_B degrees	M N-m	$\int_0^{\rho 1} \frac{M}{EI} d\eta$ x 10^4	Θ_B degrees
0	562.2	2903	0	0	1951	0	0
0.1	491.3	2229	6.623	-0.066	1392	4.32	-0.043
0.2	421.2	1687	12.53	-0.124	929	7.86	-0.078
0.3	319.5	1220	17.91	-0.178	553	10.53	-0.104
0.4	225.7	848	23.0	-0.228	293	12.63	-0.125
0.5	187.6	553	27.69	-0.275	121	14.0	-0.139
0.6	103.4	318	31.9	-0.316	18	14.6	-0.145
0.7	85.1	160	36.7	-0.364	-22	14.5	-0.144
0.8	70.1	52	38.8	-0.385	-27	14.0	-0.139
0.9	6.75	11	40.3	-0.40	-16	12.9	-0.128
1.0	6.75	0	41.0	-0.407	0	11.4	-0.113

Table 6

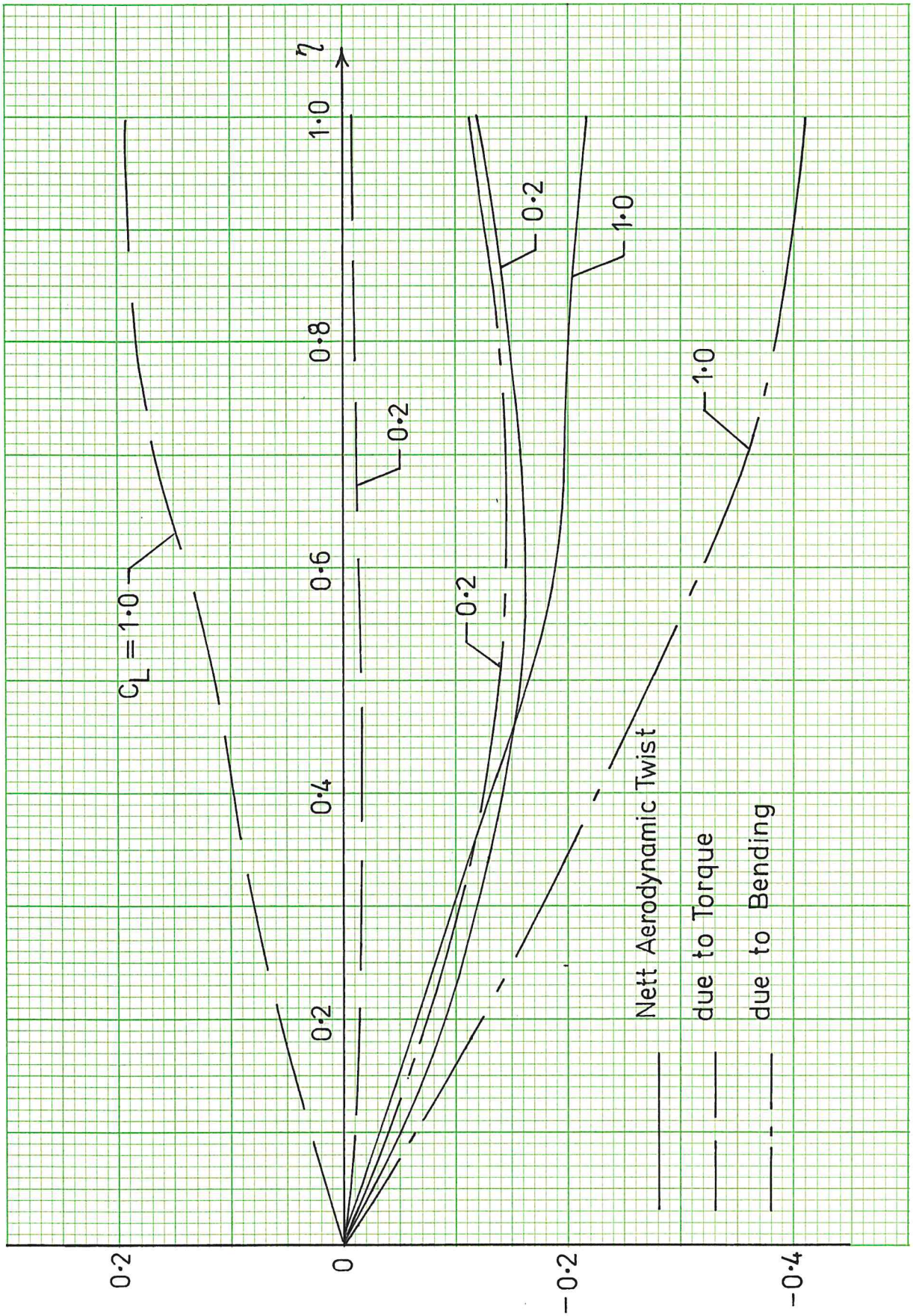

FIG 39 AERODYNAMIC WING TWIST AT C_L = 1·0 AND 0·2

aircraft to the change in spanwise loading. In a high 'g' manoeuvre this change in spanwise loading is likely to be of secondary importance to the additional spanwise loading due to incidence. The latter will cause the wing bending and associated washout as in the gust case. The preliminary investigation will therefore combine the gust and manoeuvre response by considering the nett wing deformation due to a change in incidence.

Figure 40 gives the nett change in aerodynamic twist along the wing due to a unit change in load factor. The components of this twist due to bending and torque are also illustrated on the figure. The resultant 0.2 degrees washout per positive 'g' increment is quite small. Even at aft centre of gravity the nose down moment from a lift increment due to upgust, acting behind the aircraft centre of gravity, is greater than nose up moment due to the increased wing washout. Hence a stable response is assured. In the manoeuvre case 0.2 degrees twist per 'g' is equivalent to 1.5 degrees per g of control deflection and is likely to manifest itself more as an increase in control sensitivity than an instability. However the local torque due to elevon deflection and the change in spanwise distribution, which have been neglected in the above, act in a sense to reduce the calculated wing twist and no problem is anticipated.

10.3 Coupling of Lontiduinal Dynamic Oscillations and Wing Distortions

If the aircraft encountered a disturbance, causing the wing to vibrate in bending, an oscillatory pitching moment due to Θ_B would be applied to the aircraft. This will not be resisted by an in-phase Θ_T. In fact Θ_T is likely to be in the same sense as Θ_B as in the case of classical torsional flexural flutter. For normal flight speeds the vibration is likely to be damped. However, the possibility exists for the wing bending frequency to be close enough to a rigid aircraft longitudinal oscillation frequency, causing dynamic resonance to occur. The coupling is most likely, as it is in this case, between the short period pitching oscillation and the wing bending vibration.

Appendix H is used to derive the formulae for the aircraft natural frequencies in bending and torsion. The solution assumes a uniform wing of constant mass per unit length, m and constant moment of inertia I. It is given by,

$$Pl = \left(\frac{\omega}{\sqrt{\frac{EI}{m}}}\right)^{\frac{1}{2}}$$ where l is the semispan and, ω the natural frequency in bending

$= 2.029$ for $m = 7.25$ kg/m

$= 2.098$ for $m = 13.3$ kg/m.

for the fundamental mode, and

$= 4.839$ to 4.926 for the second mode.

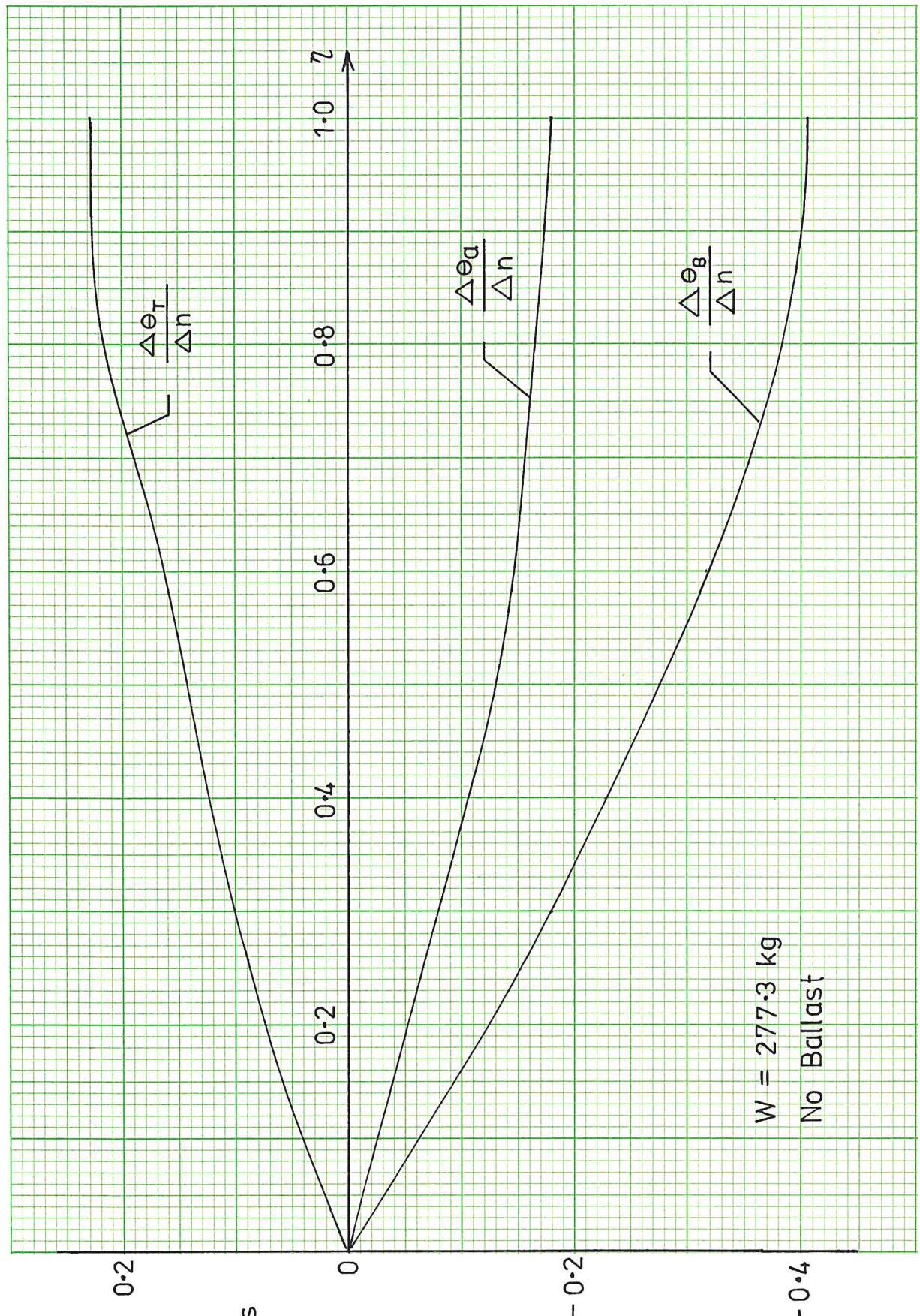

FIG 40 CHANGE IN AERODYNAMIC TWIST PER UNIT CHANGE IN LOAD FACTOR.

The aircraft modes of distortion and other parameters for the Ricochet sailplane required for the solution, are given in the appendix.

Table 7 gives the natural frequencies for wings of different uniform stiffnesses, with and without water ballast.

Pl	m (kg/m)	EI ($N - m^2$)	ω rad/sec
2.029	7.25	289.6×10^3	14.63
2.098	13.3	289.6×10^3	11.55
2.029	7.25	144.8×10^3	10.35
2.098	13.3	144.8×10^3	8.16
2.029	7.25	72.4×10^3	7.32
2.098	13.3	72.4×10^3	5.77
4.839	7.25	144.8×10^3	58.8
4.926	13.3	144.8×10^3	45.01

Table 7

The value of EI = 144.8×10^3 $N - m^2$ corresponds to the Ricochet wing stiffness at approximately 45% semispan. The other two values occur at approximately 20% and 65% semispan.

The range of undamped short period oscillation frequencies is,

0 to 6.1 rads/sec without ballast

0 to 5.6 rads/sec with ballast.

The range of damped short period oscillation frequencies is,

0 to 4.0 rads/sec without ballast

0 to 4.3 rads/sec with ballast.

It is not obvious that coupling will be avoided. Work has been initiated on the flexible aircraft dynamics.

It can be seen from table 7 that the first overtone frequency is not likely to cause any problems with the rigid body dynamics. The proximity of the wing fundamental torsional frequency is worth checking. The estimate given in appendix H, is 53 rads/sec, which coincides with the first overtone in bending. The mode shape of the latter is likely to preclude any coupling.

10.4 Flutter, Divergence and Elevon Reversal

a. Flutter

From BCAR section E, the critical flutter speed in knots

EAS, is given by

$$V_{CF} = \sqrt{\frac{m_\Theta}{\rho_o \frac{b}{2} c^2} \frac{(1 - 0.37K)(1 - 0.1r)}{(1.6)(g - 0.1)(1.3 - h)} (0.95 + \frac{1.3}{\sigma_w})}$$

where, m_Θ = wing torsional stiffness between root and 0.7 semispan

$$= \frac{10^6}{43.5} \text{ lb.ft/radian}$$

b = wing span in ft

= 49.2 ft

c = SMC

= 2.244 ft

K = taper ratio

= 0.9 for rectangular tapered

g = percentage chord location of inertia axis

= 0.45

h = percentage chord location of flexural axis

= 0.4

r = stiffness ratio

$$= \frac{5}{A^2} \frac{^1\Phi}{m_\Theta}$$

= 0.006

$^1\Phi$ = wing flexural stiffness between wing root and 0.7 semispan

$$= \frac{10^6}{72.2} \text{ lb.ft/radian}$$

A is aspect ratio

= 22

σ_w = wing relative density

$$= \frac{\text{wing density}}{\text{air density}}$$

= 11.62

$$\text{wing density} = \frac{\text{Total weight of wing}}{\text{wing area x C}}$$

$$= 0.89 \text{ lb/ft}^3$$

Giving, $V_{CF} = 392$ kts

This can only be regarded as a rough estimate because although the sweep only has a small effect, the body freedom effect is unknown.

b. Divergence

The Broadbent criterion to cover the case of divergence is:-

$$U \geq 0.0004 \frac{V_D^2 \, C^2 \frac{b}{2}}{\cos^{\frac{1}{2}} \Lambda} (a_1 \, e)$$

where, U is the strain energy in lb.ft/radian for a torsional deflection about the centreline of the box varying linearly from zero at the wing centreline to one radian at the tip.

V_D is the design diving speed.

$= 211$ f.p.s.EAS

$C = 2.244$ ft

$\Lambda = 13^\circ$

$a_1 = 5.6$

e is the fraction of chord that the flexural axis is behind the aerodynamic axis

$= 0.15$

We therefore require

$$U \geq 1877 \text{ lb.ft/radian}$$

The wing torsional stiffness is given by

$$U = \frac{2G}{b} \int_0^{1.0} \frac{2 A^2 t}{P} d\eta$$

$$= 120 \times 10^3 \text{ lb.ft/radian}$$

and satisfies the condition.

c. Elevon Reversal

Use of the Av.P 970 aileron reversal criterion suggests

that;

$$V_R = \left(\frac{4 m_\Theta}{\rho_o \, b \, c^2} \, \frac{a_2}{a_1 \, m} \right)^{\frac{1}{2}}$$

where, V_R is the aileron reversal speed f.p.s. EAS

m_Θ is antisymmetrical torsional stiffness at the mid aileron section

$= \frac{10^6}{68}$ lb.ft/radian

a_2 = 2.3 per radian

a_1 = 5.6 per radian

m = slope of curve of nose down moment coefficient against aileron angle at constant incidence.

= 0.5

Hence, V_R = 286 f.p.s. EAS

= 170 kts.

The Broadbent criterion is perhaps more comprehensive and suggests

$$U \geq 0.00035 \, \frac{V_D^2 \, c^2 \, b}{\cos^{\frac{1}{2}} \Lambda_{2}} \cdot \frac{a_1 \, m}{a_2}$$

ie $U \geq 2380$ lb.ft/radian

which is satisfied.

11. CONCLUSIONS

For a given span, the conventional sailplane is likely to reach its performance plateau by 1980. The only avenues of development for further performance gains are variable geometry conventional sailplanes or tailless sailplanes. Prototypes of the conventional chord concept have been built in Great Britain and South Africa, and of the variable span concept in Germany. None of these aircraft have shown any performance gains and they are all prohibitively expensive.

A review of the tailless sailplane, designed for high performance, has been initiated in this thesis. It has been found that the demands of high performance are not in conflict with those of stability and control. A certain amount of additional care will be required to determine the longitudinal balance and aerodynamic derivatives, but these should only be temporary in nature. The greatest demands on aircraft layout occur during the take off and landing phases. Increase in wing dihedral to provide adequate wing tip to ground clearance gives a reduction in dutch roll stability and an increase in spiral stability. The increase in spiral stability has a considerable affect on sailplane cross-country performance due to the reduction in climbing lift coefficient with negative inboard elevon deflections. This problem is associated with the undercarriage layout. To reduce the 'pitch-over' tendency caused by hitting a bump on ground roll the aircraft should be low to the ground and/or have a long wheel base straddling the centre of gravity. The long wheel base prevents rotation of the aircraft by the elevons and therefore requires a high wing angle of attack for take off. This in turn reduces the wing tip clearance.

The swept wing water ballast tanks do pose a problem for a 35% wing loading increment.

With a metal wing, and the structural layout offered by low Reynolds number aerofoil sections, the problems of flexibility have a reasonable chance of solution. Although the sailplane layout given in this thesis has theoretically different short period oscillation and wing bending frequencies the possibility of dynamic coupling cannot be ruled out. A sophisticated theoretical analysis will not provide absolute responses during a coupled vibration but it could estimate the likely damping.

The lack of satisfactory aerofoil sections is understandable and with the existing tools this problem should only be temporary. The tailless sailplane is likely to achieve a 10% cross-country performance increment over the conventional sailplane of equal span.

LIST OF REFERENCES

1.	PAUL F. BIKLE	Polars of Eight. Soaring, June 1972
2.	W.M. FOLEY	Recent Standard Cirrus Performance Measurements. Motorless Flight Research, 1972 NASA CR 2315
3.	F.G. IRVING	Computer Analysis of the Performance of 15 m Sailplanes Using Thermals with Parabolic Velocity Distributions. OSTIV Publication XI.
4.	H.C.N. GOODHART	A note on the Measurement of the Induced Drag Factor (K) of a Glider. Technical Soaring Vol.1, No.4
5.		E.S.D.U. (R.Ae.S.) Data Sheets
6.	I.H. ABBOT AND A.E. VON DOENHOFF	Theory of Wing Sections. Dover Publications
7.	PROF. DR.ING. F.X. WORTMANN	Zur Optimierung von Klappenprofilen. Swiss Aero Revue 2/1969
8.	PROF. F.X. WORTMANN	Symmetrical Airfoils Optimized for Small Flap Deflection. Swiss Aero Revue 3/1973
9.		The Worlds Sailplanes Vol.II.
10.	PROF. F.X. WORTMANN	Einige Laminarprofile für Segelflugzeuge. OSTIV Congress Argentina 1963
11.		
12.	PROF. F.X. WORTMANN	Drag Reduction in Sailplanes. Soaring, June 1966
13.	PROF. F.X. WORTMANN	Airfoils with High Lift-Drag Ratio at a Reynolds Number of about one million. Soaring, Nov. 1973
14.	A. RASPET	Boundary Layer Studies on the Phoenix Sailplane. OSTIV Congress, Colognee Germany 1960

15. DR. R. EPPLER — Direkte Berechnung von Tragflügelprofilen aus der Druckverteilung. Ingenieur-Archiv, 25 Band, I.Heft 1957

16. PROF. F.X. WORTMANN — A critical Review of the Physical Aspects of Airfoil Design at Low Mach Numbers. Proceedings of the First International Symposium on the Technology and Science of Motorless Flight. M.I.T. Cambridge Mass. U.S.A. 1972

17. DR. S.J. MILEY — An Analysis of the Design of Airfoil Sections for Low Reynolds Numbers. A dissertation submitted to the Mississippi State University January 1972

18. ANN AND LORNE WELCH — Soaring Pilot.

19. DEREK PIGGOT — Gliding.

20. FRED WEINHOLTZ — The Theory of Modern Cross-Country Gliding.

21. H.C.N. GOODHART — Glider Performance: A New Approach. Swiss Aero Revue Jan. 1966

22. DIPL.-ING. O. NIEHUSS — On Optimization of Glider Cross-Country Flight Using Thermals. Swiss Aero Revue Dec. 1963

23. C.D. CONE JR. — An Index for Predicting Flight Reliability of Sailplanes in Thermal Soaring. Swiss Aero Revue May 1964

24. PROF. DR. PIERO MORELLI — The Gliding Characteristics of Sailplanes as Affected by the Strength and Direction of the Wind. Swiss Aero Revue April 1965

25. D. MACKINNON — Thermaling Flight Optimization. Swiss Aero Revue Dec. 1968

26. F.G. IRVING — The Effect of Errors in Inter-Thermal Speed on the Average Cross-Country Speed. Technical Soaring Vol. III Spring 1974 No.2

27. F.G. IRVING — Cloud Street Flying. Technical Soaring Vol. III Winter 1973 No.1

28. JOZSEF GEDEON — Dynamic Analysis of Dophin-Style Thermal Cross-Country Flight. Technical Soaring Vol.III Winter 1973 No.1

29. RISTO ARHO — Optimal Dolphin Soaring as a Variational Problem. Technical Soaring Vol. III Winter 1973 No.1

30. D.J. MARSDEN — Circling Performance of Sailplanes. OSTIV Publication XI 1970

31. F.G. IRVING — Computer Analysis of the Performance of 15 m Sailplanes Using Thermals with Parabolic Velocity Distributions. OSTIV Publication XI 1970

32. F.G. IRVING — Computer Analysis of the Performance of 15 m Sailplanes. Motorless Flight Research 1972 NASA CR. 2315

33. R. EPPLER — When Should We Use Water Ballast Motorless Flight Research NASA CR 2315

34. D. ALTHAUS — Wind-Tunnel Measurements on Bodies and Wing-Body Combinations. Motorless Flight Research NASA CR 2315 1972

35. S.P. HARRIS, J. TROCH, H. HARRIS — Computer Programs for the Evaluation of Spanwise and Chordwise Loadings on a Wing of arbitrary Planform in Subcritical Flow. Cranfield Institute of Technology Minor Thesis 1971

36. B. THWAITES — Incompressible Aerodynamics. Oxford 1960

37. D. KÜCHEMANN — A simple method for calculating the Span and Chordwise Loadings on thin Swept Wings. R.A.E. Report Aero. 2392

38. D. KÜCHEMANN — A simple method of Calculating the Spanwise and Chordwise Loading on Straight and Swept Wings of any given Aspect Ratio at Supersonic Speeds. R. & M 2935

39. J. WEBER, D.A. KIRBY, D.J. KETTLE — An Extension of Multhopp's Method of Calculating the Spanwise Loading of Wing-Fuselage Combinations. R & M No. 2872

40. J. WEBER, G. BREBNER — Low Speed Tests on a 45° Swept Back Wing. R & M 2882

41. H. MULTHOPP — A Simple Method of Caculating the Spanwise Lift Distribution over Wings of Arbitrary Shape.

42. R. BUTLER, W. SCHUEMANN — Wing Twist, How Great the Penalty. NASA CR 2315

43. C.G.B. MITCHELL — A Computer Program to Predict the Stability and Control of Projected Aircraft.

44. T. CZAYKOWSKI — Loading Conditions of Tailed Aircraft in Longitudinal Manoeuvres. R & M 3001

45. J.T. BAUMAN — Effect of Stabilizer Lift on Sailplane Performance. Technical Soaring Vol. 1 No.4

46. K.G. WILKINSON, J.A.H. SHEPPERD — The Longitudinal Response of Tailless Aircraft RAE Report Aero 2060 July 1945

47. A.G. BARNES, D.E.A. HOUGHTON, C. COLCLOUGH — A Simulator Study of Direct Lift Control British Aircraft Corporation Report No. Ae 312

48. F. O'HARA — Handling Criteria. J. RAeS Vol. 71 1967

49. J.F. MARTIN — The Standard Sailplane - Parametric Studies. Canadian Symposium for Recreational Aircraft Carleton University, Ottawa 23-25 June 1975

50. H. ROBERTS — Rolling Performance of Aircraft Aircraft Engineering June 1948

51. A.W. BABISTER — Aircraft Stability and Control. Pergamon Press

52. — Wind Tunnel Tests on Inboard Fin and Drag Rudders on a Tailless Glider. RAE TN 1639 May 1945